SYNTHESES OF NEW MULTIFUNCTIONAL DONOR ACCEPTOR TYPE POLYMERS FOR ELECTROCHROMIC AND ORGANIC SOLAR CELL APPLICATIONS

A THESIS SUBMITTED TO
THE GRADUATE SCHOOL OF NATURAL AND APPLIED SCIENCES
OF
MIDDLE EAST TECHNICAL UNIVERSITY

BY

ŞERİFE ÖZDEMİR HACIOĞLU

IN PARTIAL FULFILLMENT OF THE REQUIREMENTS
FOR
THE DEGREE OF DOCTOR OF PHILOSOPHY
IN
CHEMISTRY

SEPTEMBER 2016

Approval of the thesis:

SYNTHESES OF NEW MULTIFUNCTIONAL DONOR ACCEPTOR TYPE POLYMERS FOR ELECTROCHROMIC AND ORGANIC SOLAR CELL APPLICATIONS

submitted by **ŞERİFE ÖZDEMİR HACIOĞLU** in partial fulfillment of the requirements for the degree of **Doctor of Philosophy in Chemistry Department, Middle East Technical University** by,

Prof. Dr.Gülbin Dural Ünver _____
Dean, Graduate School of **Natural and Applied Sciences**

Prof. Dr. Cihangir Tanyeli _____
Head of Department, **Chemistry**

Prof. Dr. Levent Toppare _____
Supervisor, **Chemistry Dept., METU**

Prof. Dr. Özdemir Doğan _____
Co-Supervisor, **Chemistry Dept., METU**

Examining Committee Members:

Prof. Dr. Teoman Tinçer _____
Chemistry Dept., METU

Prof. Dr. Levent Toppare _____
Chemistry Dept., METU

Assoc. Prof. Dr. Yasemin Arslan Udum _____
Advanced Technologies, Gazi University

Prof. Dr. Mustafa Güllü _____
Chemistry Dept., Ankara University

Assist. Prof. Dr. Görkem Günbaş _____
Chemistry Dept., METU

Date: 02/09/2016

I hereby declare that all information in this document has been obtained and presented in accordance with academic rules and ethical conduct. I also declare that, as required by these rules and conduct, I have fully cited and referenced all material and results that are not original to this work.

Name, Last name: Şerife Özdemir Hacıoğlu

Signature :

ABSTRACT

SYNTHESES OF NEW MULTIFUNCTIONAL DONOR ACCEPTOR TYPE POLYMERS FOR ELECTROCHROMIC AND ORGANIC SOLAR CELL APPLICATIONS

Özdemir Hacıoğlu, Şerife

PhD,Chemistry Department

Supervisor: Prof. Dr. Levent Toppare

September 2016, 151 pages

Combining donor and acceptor moieties in the polymerbackbone enhances D–A interactions and helps in developing themost efficient polymers for various applications. Besides obtaining low bandgap polymers, the D–A approach is also useful in producingpolymers with improved optical, mechanical and electronic properties.Changing both or either of the donor/acceptor groups is aneffective method to design these alternating systems.For this purpose different acceptors units such as; benzothiodiazole, benzotriazole, quinoxaline and benzimidazole were coupled with different donor units but the desired properties could not be combined up to now. In this thesis firstly it is aimed to design a new acceptor unit which is the combination of benzotriazole and quinoxaline units (triazoloquinoxaline unit). After synthesis of this new acceptor unit, it was coupled with donor units and electrochemical and spectroelectrochemical characterization were performed. Furthermore affect of π bridge on electrochemical behaviors were also investigated via synthesizing benzotriazole and triphenylamine bearing random copolymers. Cyclic Voltammetry (CV) and UV–Vis-NIR spectrohotometer were used to

investigate electrochemical behaviors of the the monomers and conducting polymers.Finally while triazoloquinoxaline derivatives were used for electrochromic device applications, triphenylamine bearing copolymers were used for organic solar cell applications as donor materials.

Keywords: Electrochromism, organic solar cell, electrochromic device , benzotriazole,triphenylamine

ÖZ

ORGANİK GÜNEŞ PİLİ VE ELEKTROKROMİK UYGULAMALAR İÇİN ÇOK FONKSİYONLU DONÖR- AKSEPTÖR TİPİ KONJÜGE POLİMERLERİN SENTEZLENMESİ

Özdemir Hacıoğlu, Şerife

Doktora, Kimya Bölümü

Tez Yöneticisi: Prof. Dr. Levent Toppare

Eylül 2016, 151 sayfa

Donör ve akseptör ünitelerinin polimer zincirinde sıralanması D-A etkileşimini güçlendirirken değişik uygulamalar için çok fonksiyonlu polimer sentezini kolaylaştırmaktadır. Donör-Akseptör yaklaşımı düşük bant aralığına sahip polimer sentezini kolaylaştırırken aynı zamanda elde edilen polimerin optik, elektronik ve mekanik özelliklerini iyileştirmektedir. Bu amaçla literatürde benzotiyadiazol, benzotriazol, kinoksalin ve benzimidazol gibi alıcı gruplar farklı verici moleküller ile monomer yapısında birleştirilmiştir. Bu çalışmada, ilk olarak benzotriazol ve kinoksalin ünitelerini içeren yeni bir akseptör grup sentezi amaçlanmıştır. Bu yeni akseptör ünitesi değişik donör gruplarla kenetlenme reaksiyonu ile birleştirilmiştir ve elektrokimyasal özellikleri incelenmiştir. Ayrıca π-köprüsü kullanımının elektrokimyasal özelliklere etkisi, trifenilamin ve benzotriazol içeren

rasgelekopolimerlerin sentezi ile incelenmiştir. Dönüşümlü voltametri ve UV-Vis-NIR spektrofotometre kullanılarak electrokimyasal ve spektroelektrokimyasal özellikler incelenmiştir. Son olarak triazolokinoksalin türevleri electrokromik cihazlarda aktif tabaka olarak ve trifenilamin içeren kopolimerler ise organik güneş pillerinde donör grup olarak aktif tabakada kullanılmıştır.

Anahtar kelimeler: Electrokromizm organik güneş pilleri, elecktrokromik cihaz, benzotriazol, trifenilamin

To my husband Fırat and my baby Elif Duru

ACKNOWLEDGEMENTS

I would like to express my sincere thanks to mysupervisor Prof. Dr. Levent Toppare for his invaluable guidance, support, suggestions and advice for the completion of my thesis and for everything.

I would like to thank to my co-supervisor Prof. Dr. Özdemir Doğan for his guidance and support.

Many thanks to Assoc. Prof. Dr Ali Çırpan, Assoc. Prof. Dr. Yasemin Arslan Udum and Assist. Prof. Dr. Görkem Günbaş for listening and helping me in many ways.

I would like to thank to Derya Baran, Merve Şendur and Ayda Nurioğlu for their helps during electrochemical characterization, Abidin Balan for helping me to the organic synthesis, Gönül Hızalan and Ece Aktaş for the helps during organic solar cell fabrication and characterization. Many thanks to Seza Göker for her helps during polymer synthesis.

I want to special thank to Naime Akbaşoğlu not only for her help about the organic synthesis but also being a true friend. Our friendships started at the beginning of Ms. studies and I wish she will be in my life everytime.

I would like to thank the friends I have, Gönül, Merve, Seda, Ebru, Çağla, Seza, Melis, Janset, Ece, Mustafa, Buket for their kind friendships and happy coffee breaks. Special thanks go to Merve, Seda and Duygu for their nice collaboration in D-149 and also Ebru for her help and encourangement during writing this thesis.

I would like to thank to Saniye Söylemez for her valuable discussions and friendship.

Many thanks to Sema Demirci Uzun for her true and nice friendship and also for her valuable discussions during orgnic synthesis.

I would like thank to all Toppare Research Group, Çırpan Resarch Group and Günbaş Resarch Group members for their valuable colloborattions, cooperation and kind friendships.

I would like to thank Dr. Abidin Balan and Dr. Derya Baran for their helps, stimulating conversations besides their friendships and also their helps during writing the first articles.

I would like to thank TUBITAK 2211 (Scholarship Program for PhD students) fellowship for financial support

I would like to thank my familyfor believing in me and giving me endless support.

Finally, my special thanks goes to my lovely husband Fırat Hacıoğluand our baby Elif Duru Hacıoğlu. Words fail to express my eternal gratitude to Fıratfor his continuous support, love and patience to my long working hours. Without him none of this work could be accomplished. After our baby Elif Duru born, she became the meaning of my life. Life does not mean anything without her smile, smell and love.

TABLE OF CONTENTS

ABSTRACT v

ÖZ vii

ACKNOWLEDGEMENTS x

TABLE OF CONTENT xii

LIST OF TABLES xvii

LIST OF FIGURES xviii

LIST OF SCHEMES xxiv

LIST OF ABBREVIATIONS xxv

CHAPTERS

1. INTRODUCTION 1

1.1. Conducting polymers 1

1.3. Conduction Mechanism 4

1.3.1. Charge Carriers 4

1.3.2 Doping 6

1.4. Synthesis of conjugated polymers 7

1.4.1 Chemical synthesis of conjugated polymers 7

1.4.1.1 Suzuki Coupling 8

1.4.1.2 Stille Coupling 9

1.4.2. Oxidative Chemical Polymerization 10

1.4.3. Electrochemical Polymerization 11

1.5. Characterization of Conducting Polymers 14

1.6. Application Areas of Conducting Polymers 14

1.6.1. Organic Solar Cell 14

1.6.1.1. Working Principle of Solar Cell 15

1.6.1.2. Solar cell architectures 18
1.6.1.3. Characterization of organic solar cells 19
1.6.2. Electrochromic Devices 20
1.6.2.1. Electrochromism 20
1.6.2.2. Electrochromism in conjugated polymers 22
1.6.2.3. Electrochromic Device Architecture 24
1.6.2.4. Electrochromic device performance parameters 25
1.7. Building blocks for fuctional polymers 27
1.7.1. Triphenylamine (TPA) bearing polymers 28
1.7.1.1. A novel electrochromic polymer containing triphenylamine derivative and pyrrole 30
1.7.1.2. Triphenylamine-based multielectrochromic material and its neutral green electrochromic devices 31
1.7.1.3. Synthesis and characterization of photoelectronic polymers containing triphenylamine moiety 33
1.7.1.4. Toward the Development of New Textile/Plastic Electrochromic Cells Using Triphenylamine-Based Copolymers 34
1.7.1.5. Electrochemical synthesis and electrochromic properties of new conjugated polycarbazoles from di(carbazol-9-yl)-substituted triphenylamine and N-phenylcarbazole derivatives 36
1.7.2. Triazoloquinoxaline bearing polymers 38
1.7.2.1. Triazoloquinoxaline and Fluorene bearing polymers for organic solar cells 39
1.7.2.2. Design and synthesis of triazoloquinoxaline polymers with positioning alkyl or alkoxyl chains for organic photovoltaics cells [60] 40
2. EXPERIMENTAL 43
2.1. Materials and Methods 43

2.1.1. Organic Solar Cell Device Fabrication and Characterization 44

2.2. Synthetic procedures 45

2.2.1. Synthesis of 2-dodecylbenzotriazole 45

2.2.2. Synthesis of 4,7-dibromo-2-dodecylbenzotriazole 46

2.2.3. Synthesis of 4,7-dibromo-2-dodecyl-5,6-dinitro-2H-benzo[d][1,2,3]triazole 47

2.2.4. Synthesis of 2-dodecyl-5,6-dinitro-4,7-di(thiophen-2-yl)-2H-benzo[d][1,2,3]triazole 48

2.2.5. Synthesis of 2-dodecyl-6,7-diphenyl-4,9-di(thiophen-2-yl)-2H-[1,2,3]triazolo[4,5-g]quinoxaline 49

2.2.6. Synthesis of 2-dodecyl-4,6,7,9-tetra(thiophen-2-yl)-2H-[1,2,3]triazolo[4,5-g]quinoxaline 50

2.2.7. Synthesis of 6,7-bis(4-tert-butylphenyl)-2-dodecyl-4,9-di(thiophen-2-yl)-2H-[1,2,3]triazolo[4,5-g]quinoxaline 51

2.2.9. Synthesis of 2-dodecyl-4,7-di(thiophen-2-yl)-2H-benzo[d][1,2,3]triazole 52

2.2.10. Synthesis of 4,7-bis(5-bromothiophen-2-yl)-2-dodecyl-2Hbenzo[d][1,2,3]triazole 53

2.2.11. Synthesis of Poly4-(5-(2-dodecyl-7-methyl-2H-benzo[d][1,2,3]triazol-4-yl)thiophen-2-yl)-N-(4-(5-methylthiophen-2-yl)phenyl)-N-phenylaniline (PTPB1) 55

2.2.12. Synthesis of Poly4'-(2-dodecyl-7-methyl-2H-benzo[d][1,2,3]triazol-4-yl)-N-(4'-methyl-[1,1'-biphenyl]-4-yl)-N-phenyl-[1,1'-biphenyl]-4-amine (PTPB2) 57

2.2.13. Synthesis of Poly4-(5'-(2-dodecyl-7-(5-methylthiophen-2-yl)-2H-benzo[d][1,2,3]triazol-4-yl)-[2,2'-bithiophen]-5-yl)-N-(4-(5-methylthiophen-2-yl)phenyl)-N-phenylaniline (PTPB3) 59

2.2.14. Synthesis of Poly4-(5-(2-dodecyl-7-methyl-2H-benzo[d][1,2,3]triazol-4-yl)thiophen-2-yl)-N-(4-(5-methylthiophen-2-yl)phenyl)-N-phenylaniline (PBTP1) 60

2.2.15. Synthesis of Poly4-(5'-(2-dodecyl-7-(5-methylthiophen-2-yl)-2H-benzo[d][1,2,3]triazol-4-yl)-[2,2'-bithiophen]-5-yl)-N-(4-(5-methylthiophen-2-yl)phenyl)-N-phenylaniline (PBTP2) 62

3. RESULTS AND DISCUSSION 65

3.1. A promising combination of benzotriazole and quinoxaline units: A new acceptor moiety toward synthesis of multipurpose donor–acceptor type polymers 65

3.1.1. Synthesis 66

3.1.2. Electrochemistry 67

3.1.3. Electronic and optical studies 71

3.1.4. Electrochromic switching studies 75

3.2. Synthesis and electrochromic properties of triphenylamine containing copolymers: Effect of π-bridge on electrochemical properties 77

3.2.1 Synthesis 77

3.2.2. Electrochemical Properties 78

3.2.3. Spectroelectrochemical Properties 81

3.2.4. Electrochromic contrast and switching studies 85

3.3. Construction and characterization of triazoloquinoxaline derivative P2 /PEDOT based dual type electrochromicdevice (ECD) 87

3.3.1. The construction of an electrochromic device (ECD) 87

3.3.2. Spectroelectrochemistry 89

3.3.3. Kinetic studies 90

3.3.4. Open Circuit Memory Studies for P2/PEDOT ECD 91

3.3.5. The long term stability of P2/PEDOT ECD 93

3.4.1. Electrochemistry 95
3.4.2. Spectroelectrochemistry 98
3.4.3. Electrochromic contrast and switching studies 101
3.4.4. Photovoltaic Properties 103
4. CONCLUSION 109
REFERENCES 113
APPENDIX A 117
NMR DATA 117
CURRICULUM VITAE 141

LIST OF TABLES

TABLES

Table 1. 1. Electrochemical and optical behaviors of PNB, PNT and PNF..... 34
Table 1. 2. Optical, Electrochemical, and Colorimetric Data of Copolymers. 36
Table 1. 3. Electrochemical and optical results for triazoloquinoxaline based polymers. 39
Table 1. 4. Electrochemical and optical results for triazoloquinoxaline based polymers. 42

Table 3. 1. Summary of electrochemical and spectroelectrochemical properties of P1, P2 and P3. 70

Table 3. 2. Summary of kinetic and optic studies of P1, P2 and P3. 76
Table 3. 3. Summary of electrochemical and spectroelectrochemical properties of PTPB1, PTPB2 and PTPB3. 81
Table 3. 4. Summary of kinetic studies of polymers..... 86
Table 3. 5. Summary of optical and kinetic results for P2/PEDOT ECD. 91
Table 3. 6. Summary of electrochemical properties of PBTP1 and PBTP2. 96
Table 3. 7. Summary of spectroelectrochemical properties of PBTP1 andPBTP2.. 101
Table 3. 8. Summary of kinetic studies of PBTP1 and PBTP2..... 102
Table 3. 9. Photovoltaic properties of bulk heterojunction OSCs based on PBTP1/PBTP2: $PC_{71}BM$..... 106

LIST OF FIGURES

FIGURES

Figure 1. 1. Structures of common conducting polymers. 2
Figure 1. 2. Generation of bands in polyacetylene. 4
Figure 1. 3. Formation of polaron, bipolaron, and soliton pair on a trans-polyacetylene chain via doping process. 5
Figure 1. 4.P-type doping of PTh. 7
Figure 1. 5. Energy bands in the mid gap. 7
Figure 1. 6. An overview of transition metal catalyzed polycondensation reaction. ... 8
Figure 1. 7. Suzuki Coupling. 9
Figure 1. 8. Stille Coupling. 10
Figure 1. 9. Chemical polymerization with $FeCl_3$. 11
Figure 1. 10. Electropolymerization mechanism of thiophene. 12
Figure 1. 11. Schematic device structure for bulk heterojunction solar cells. 16
Figure 1. 12. Working principle of organic solar cell. 17
Figure 1. 13. (a) Bilayer device configuration (b) Bulk heterojunction device configuration. 18
Figure 1. 14. Current-voltage curve under illumination and in dark. 20
Figure 1. 15. The three common viologen redox states (dication, radical cation, neutral states). 21
Figure 1. 16. Allowed transitions for neutral, polaron and bipolaron states with illustration of electronic, absorption spectral changes of a conjugated polymer upon oxidation. 23
Figure 1. 17. Examples of commercial applications of ECDs a s smart windows. 24
Figure 1. 18. Schematic illustration of dual type sandwich structured electrochromic device configurations. 25
Figure 1. 19. Chemical structures of widely used donor units during the design of conjugated polymers. 27
Figure 1. 20. Chemical structures of widely used acceptor units during the design of conjugated polymers. 28

Figure 1. 21. (a) Structure of TPA and (b) possible position of TPA unit in the polymer chain. 29
Figure 1. 22. Structure of DPTPA and corresponding colors for electrochemically synthesized polymer [45]. 31
Figure 1. 23. Structure of PTEPA and corresponding colors for electrochemically synthesized polymer [46]. 32
Figure 1. 24. Structures of TPA bearing polymers PNB, PNT and PNF [48]. 33
Figure 1. 25. Structures of 4-butyltriphenylamine (BuTPA) bearing polymers and corresponding colors for different states [49]. 35
Figure 1. 26. Structures of polymers (P(PhCz-2Cz)) and (P(TPA-2Cz)) and corresponding colors for different states [50]. 37
Figure 1. 27. Structures of triazoloquinoxaline and fluorene based polymers [57-59]. 40
Figure 1. 28. Structures of triazoloquinoxaline and benzodithiophene based polymers [60]. 41

Figure 2. 1. . Synthesis of 2-dodecylbenzotriazole 45
Figure 2. 2. Synthesis of 4,7-dibromo-2-dodecylbenzotriazole 46
Figure 2. 3. Synthesis of 4,7-dibromo-2-dodecyl-5,6-dinitro-2H-benzo[d][1,2,3]triazole 47
Figure 2. 4. Synthesis of 2-dodecyl-5,6-dinitro-4,7-di(thiophen-2-yl)-2H-benzo[d][1,2,3]triazole 48
Figure 2. 5.Synthesis of 2-dodecyl-6,7-diphenyl-4,9-di(thiophen-2-yl)-2H-[1,2,3]triazolo[4,5-g]quinoxaline 49
Figure 2. 6. Synthesis of 2-dodecyl-4,6,7,9-tetra(thiophen-2-yl)-2H-[1,2,3]triazolo[4,5-g]quinoxaline 50
Figure 2. 7. Synthesis of 6,7-bis(4-tert-butylphenyl)-2-dodecyl-4,9-di(thiophen-2-yl)-2H-[1,2,3]triazolo[4,5-g]quinoxaline 51
Figure 2. 8. Synthesis of 2-dodecyl-4,7-di(thiophen-2-yl)-2H-benzo[d][1,2,3]triazole 52

Figure 2. 9. Synthesis of 4,7-bis(5-bromothiophen-2-yl)-2-dodecyl-2Hbenzo[d][1,2,3]triazole 53
Figure 2. 10. Synthesis of Poly4-(5-(2-dodecyl-7-methyl-2H-benzo[d][1,2,3]triazol-4-yl)thiophen-2-yl)-N-(4-(5-methylthiophen-2-yl)phenyl)-N-phenylaniline (PTPB1) 55
Figure 2. 11. Synthesis of Poly4'-(2-dodecyl-7-methyl-2H-benzo[d][1,2,3]triazol-4-yl)-N-(4'-methyl-[1,1'-biphenyl]-4-yl)-N-phenyl-[1,1'-biphenyl]-4-amine 57
Figure 2. 12. Synthesis of Poly4-(5'-(2-dodecyl-7-(5-methylthiophen-2-yl)-2H-benzo[d][1,2,3]triazol-4-yl)-[2,2'-bithiophen]-5-yl)-N-(4-(5-methylthiophen-2-yl)phenyl)-N-phenylaniline (PTPB3) 59
Figure 2. 13. Synthesis of Poly4-(5-(2-dodecyl-7-methyl-2H-benzo[d][1,2,3]triazol-4-yl)thiophen-2-yl)-N-(4-(5-methylthiophen-2-yl)phenyl)-N-phenylaniline (PBTP1) 60
Figure 2. 14. Synthesis of Poly4-(5'-(2-dodecyl-7-(5-methylthiophen-2-yl)-2H-benzo[d][1,2,3]triazol-4-yl)-[2,2'-bithiophen]-5-yl)-N-(4-(5-methylthiophen-2-yl)phenyl)-N-phenylaniline (PBTP2) 62

Figure 3. 1. Electrochemical polymerizations of (a) M1 (b) M2 (c) M3 at 100mVs^{1-} in 0.1M $TBAPF_6/CH_2Cl_2$/ACN on ITO electrodes. 70
Figure 3. 2. Single scan cyclic voltammograms of P1, P2 and P3 films using ACN as the solvent and 0.1 M $TBAPF_6$ as the supporting electrolyte at a scan rate of 100 mV s^{-1} and reduction peaks. 71
Figure 3. 3. P-type doping spectra for P1 (a), P2 (b) and P3 (c) in 0.1 M 0.1 M $TBAPF_6$ /ACN supporting electrolyte/ solvent system 73
Figure 3. 4. N-type doping spectra for P1 (a), P2 (b) and P3 (c). 74
Figure 3. 5. Absorption spectra of monomers in solution (a) and thin film form (b). 74
Figure 3. 6. Structures of the polymers and their colors under different applied potentials. 75
Figure 3. 7. Optical contrasts and switching times of (a) P1, (b) P2 and (c) P3 at different wavelengths. 76
Figure 3. 8. Structures of PTPB1, PTPB2 and PTPB3. 79

Figure 3. 9. Single scan cyclic voltammograms of a) PTPB1, b) PTPB2 and c) PTPB3 films using ACN as the solventand 0.1 M $TBAPF_6$ as the supporting electrolyte at a scan rate of 100 mV s^{-1}. 80
Figure 3. 10. Electronic absorption spectra of a) PTPB1 switching between 0.9 V and 1.8 V, b) PTPB2 between 0.5 V and 1.5 V, c) PTPB3 between 0.4 V and 1.5 V in 0.1 M $TBAPF_6$/ACN solution. 83
Figure 3. 11. Structures of the polymers and their colors at their neutral and oxidized states. 84
Figure 3. 12. Optical contrasts and switching times monitored at different wavelengths for (a) PTPB1 and (b) PTPB3 in 0.1 M $TBAPF_6$/ACN solution. 85
Figure 3. 13. Colors for P2/PEDOT based ECD at two extreme states. 90
Figure 3. 14. Electronic absorption spectra of the P2/PEDOT ECDbetween +1.3 V and -1.3 V. 90
Figure 3. 15. Optical contrasts and switching times P2/PEDOT ECD at 590 nm. 91
Figure 3. 16. Open circuit memory of P2/PEDOT ECD monitored by single wavelength absorption spectroscopy at +1.3V and -1.3V. 92
Figure 3. 17. Stability tests for P2/PEDOT ECD after 500 cycles 93
Figure 3. 18. Single scan cyclic voltammograms of (a) PBTP1 and (b) PBTP2 in a monomer free 0.1 M $TBAPF_6$/ACN solution. 96
Figure 3. 19. Scan rate dependence of (a) PBTP1 and (b) PBTP2 films in a 0.1 M $TBAPF_6$ /ACN solution. 97
Figure 3. 20. Electronic absorption spectra of (a) PBTP1 and (b) PBTP2 in 0.1 M $TBAPF_6$/ACN solution. 99
Figure 3. 21. Structures of the polymers and corresponding colors at their neutral and oxidized/reduced states. 100
Figure 3. 22. Optical transmittance changes (a) for PBTP1 at 480 nm, 780 nm, 1300 nm and (b) for PBTP2 at 475 nm, 700 nm, 1100 nm in 0.1 M ACN/$TBAPF_6$ solution. 102
Figure 3. 23. Schematic representation of device configuration. 103
Figure 3. 24. Energy levels of polymers, ITO, PEDOT:PSS, PC71BM, LiF and Al 104

Figure 3. 25. J–V curves of bulk heterojunction OSCs based on PBTP1/PBTP2:$PC_{71}BM$. 105
Figure 3. 26. IPCE curves of the best performance solar cells. 107

Figure A. 1. ^{1}H-NMR spectrum of 2-Dodecyl-2H-benzo[d][1,2,3] triazole..... 117
Figure A. 2. ^{13}C-NMR spectrum of 2-Dodecyl-2H-benzo[d][1,2,3] triazole. 118
Figure A. 3. ^{1}H-NMR spectrum of 4,7-dibromo-2-dodecyl-2H-benzo[d][1,2,3]triazole. 119
Figure A. 4. ^{13}C-NMR spectrum of 4,7-dibromo-2-dodecyl-2H-benzo[d][1,2,3]triazole. 120
Figure A. 5. ^{1}H-NMR spectrum of tributyl(thiophen-2-yl)stannane. 121
Figure A. 6. ^{13}C-NMR spectrum of tributyl(thiophen-2-yl)stannane..... 122
Figure A. 7. ^{1}H-NMR spectrum of 2-dodecyl-4,7-di(thiophen-2-yl)-2H-benzo[d][1,2,3]triazole. 123
Figure A. 8. ^{13}C-NMR spectrum of 2-dodecyl-4,7-di(thiophen-2-yl)-2H-benzo[d][1,2,3]triazole. 124
Figure A. 9. ^{1}H-NMR spectrum of 4,7-bis(5-bromothiophen-2-yl)-2-dodecyl-2Hbenzo[d][1,2,3]triazole. 125
Figure A. 10. ^{13}C-NMR spectrum of 4,7-bis(5-bromothiophen-2-yl)-2-dodecyl-2Hbenzo[d][1,2,3]triazole. 126
Figure A. 11. ^{1}H-NMR spectrum of 4,7-dibromo-2-dodecyl-5,6-dinitro-2H-benzo[d][1,2,3]triazole. 127
Figure A. 12. ^{13}C-NMR spectrum of 4,7-dibromo-2-dodecyl-5,6-dinitro-2H-benzo[d][1,2,3]triazole. 128
Figure A. 13. ^{1}H-NMR spectrum of 2-dodecyl-5,6-dinitro-4,7-di(thiophen-2-yl)-2Hbenzo[d][1,2,3]triazole. 129
Figure A. 14. ^{13}C-NMR spectrum of 2-dodecyl-5,6-dinitro-4,7-di(thiophen-2-yl)-2Hbenzo[d][1,2,3]triazole. 130
Figure A. 15. ^{1}H-NMR spectrum of 2-dodecyl-6,7-diphenyl-4,9-di(thiophen-2-yl)-2H- [1,2,3]triazolo[4,5-g]quinoxaline (M1). 131
Figure A. 16. ^{13}C-NMR spectrum of 2-dodecyl-6,7-diphenyl-4,9-di(thiophen-2-yl)-2H-[1,2,3]triazolo[4,5-g]quinoxaline (M1). 132

Figure A. 17. ^{1}H-NMR spectrum of 2-dodecyl-4,6,7,9-tetra(thiophen-2-yl)-2H-[1,2,3] triazolo[4,5-g]quinoxaline (M2). 133
Figure A. 18. ^{13}C-NMR spectrum of 2-dodecyl-4,6,7,9-tetra(thiophen-2-yl)-2H-[1,2,3]triazolo[4,5-g]quinoxaline (M2). 134
Figure A. 19. ^{1}H-NMR spectrum of 6,7-bis(4-tert-butylphenyl)-2-dodecyl-4,9-di(thiophen-2-yl)-2H-[1,2,3]triazolo[4,5-g]quinoxaline (M3). 135
Figure A. 20. ^{13}C-NMR spectrum of 6,7-bis(4-tert-butylphenyl)-2-dodecyl-4,9-di(thiophen-2-yl)-2H-[1,2,3]triazolo[4,5-g]quinoxaline (M3). 136
Figure A. 21. ^{1}H-NMR spectrum of Poly4-(5-(2-dodecyl-7-methyl-2H-benzo[d][1,2,3]triazol-4-yl)thiophen-2-yl)-N-(4-(5-methylthiophen-2-yl)phenyl)-N-phenylaniline (PTPB1). 137
Figure A. 22. ^{1}H-NMR spectrum of Poly4-(5'-(2-dodecyl-7-(5-methylthiophen-2-yl)-2H-benzo[d][1,2,3]triazol-4-yl)-[2,2'-bithiophen]-5-yl)-N-(4-(5-methylthiophen-2-yl)phenyl)-N-phenylaniline (PTPB3). 138
Figure A. 23. ^{1}H-NMR spectrum of resynthesized Poly4-(5-(2-dodecyl-7-methyl-2H-benzo[d][1,2,3]triazol-4-yl)thiophen-2-yl)-N-(4-(5-methylthiophen-2-yl)phenyl)-N-phenylaniline (PBTP1). 139
Figure A. 24. ^{1}H-NMR spectrum of resynthesized Poly4-(5'-(2-dodecyl-7-(5-methylthiophen-2-yl)-2H-benzo[d][1,2,3]triazol-4-yl)-[2,2'-bithiophen]-5-yl)-N-(4-(5-methylthiophen-2-yl)phenyl)-N-phenylaniline (PBTP2). 140

LIST OF SCHEMES

SCHEMES

Scheme 3. 1. Schematic illustration for the combination of benzotriazole and quinoxaline units to get new and stronger acceptor unit. 65
Scheme 3. 2. Synthetic route for the monomers. 67
Scheme 3. 3. Electrochemical polymerization of the monomers. 68
Scheme 3. 4. Synthetic route for the polymers. 78
Scheme 3. 5. Schematic illustration of colors and structures for resulting polymers. 87
Scheme 3. 6. Schematic illustration for the electrochromic device construction. 88
Scheme 3. 7. Schematic representation of the P2/PEDOT ECD. 89
Scheme 3. 8. Synthetic route for the polymers. 94

LIST OF ABBREVIATIONS

CP	Conducting polymers
PA	Polyacetylene
PPy	Polypyrrole
HOMO	Highest occupied molecular orbital
LUMO	Lowest unoccupied molecular orbital
D	Donor
A	Acceptor
OSC	Organic solar cell
OFET	Organicfield effect transistor
BHJ	Bulk heterojunction
SCLC	Space charge limiting current
ITO	Indium tin oxide
PEDOT	Poly (3,4-ethylenedioxythiophene)
PSS	Polystyrene sulfonate
ECD	Electrochromic device
V_{OC}	Open circuit voltage
J_{SC}	Short circuit current
FF	Fill factor
PCE	Power conversion efficiency
AM	Air mass
IPCE	Incident photon to current efficiency
E_g	Bandgap
BLA	Bond length alternation
BTz	Benzotriazole
PC60BM	[6,6]-phenyl C_{61} butyric acid methyl ester
PC70BM	[6,6]-phenyl C_{71} butyric acid methyl ester

$TBAF_6$	Tetrabutylammoniumhexafluorophosphate
TPA	Tripheylamine
TQ	Triazoloquinoxaline
TLC	Thin layer chromatography
TMS	Trimethylsilane
NMR	Nuclear magnetic resonance
HRMS	High resolution mass spectroscopy
CV	Cyclicvoltammetry
GPC	Gelpermeation chromatography
AFM	Atomic force microscopy
TEM	Transmission electron microscopy

CHAPTER 1

INTRODUCTION

1.1. Conducting polymers

Interest in conducting polymers as a new class of electronic materials started with the synthesis of polyaniline as a blue-black colored shiny powder via anodic oxidation of aniline by Letheby and coworkers in 1862[1].However the popularity of conducting polymers increased significantlywith the breakthrough of the discovery of polyacetylene (PA) which is the simplest conjugated polymer with -CH=CH- repeating unit. Altough the first synthesis of PA was performed in 1955, because of its irrespective preparation method, air sensitivity and infusibility, it didnotdraw much attention until 1977 [2].

During the study, PA was synthesized by Shirakawa and coworkers as bright silvery films instead of black powder as a result of accidental insertion of a thousand times more Ziegler-Natta catalystinto reaction. Then, three famous scientists Shirakawa, Heeger, and Mac Diarmid discovered the properties of newly synthesized silvery film PA. They measured the conductivity of PA film by four-probe method which was exposed to bromine vapor. Results are really interesting because they reported that conductivity of PA film was increased by 10 million times. As a result, it was concluded that PA could be transferred from insulator to a semiconductorupon doping process [3].Forachieving conductivity, π-conjugation is the first prerequisite and doping is the addition of chemicals which provide free movement of electrons.

Due to this investigation, Heeger, Shirakawa and MacDiarmid were awarded with the Nobel Prize in 2000 ‘for the discovery and development of conductive polymers[4].

However insolubility and air sensitivity of PA make it impossible to characterize and use in different application fields. To solve these problems, researchers focused on more stable and processable conjugated polymers such as; polythiophene, polyfluorene, polypyrrole, polyaniline, and polycarbazole.(Figure 1.1) In addition, these polymers could be functionalized easily to make them applicable in many fields such aselectrochromic devices(ECDs)[5], organic solar cells (OSCs)[6], organic light emitting diodes (OLEDs)[7], organic field effect transistors (OFETs)[8] and biosensors[9].

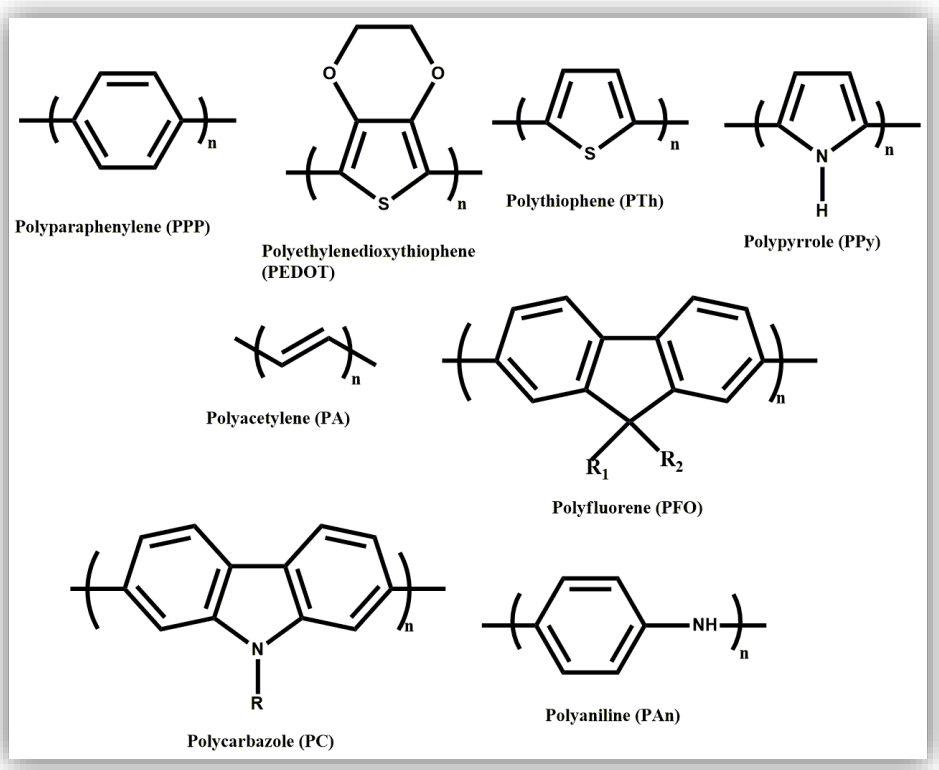

Figure 1. 1. Structures of common conducting polymers.

1.2. Band Theory

Band gap could be defined as the energy difference between valence band (VB) (highest occupied molecular orbital (HOMO)) and conduction band (CB) (lowest unoccupied molecular orbital (LUMO)). Band theory has been used to describe the properties of insulators, metals, and semiconductors in terms of band structures.
Band gap of metals are zero and they can conduct electricity due to partially filled valance and conduction bands. By the way,for insulators and semiconductors valence band is fully occupied and conduction band is fully empty. The band gap (the difference between valance and conduction band) is wide for insulators duringband gap of semiconductors is narrow.While semiconductors have a band gap between 0.5 to 3.0 eV, insulators have band gaps greater than 3.0 eV.

Since band structures of conducting polymers could be changed by removal or addition of electron (doping process), they generally counted as semiconductors [10]. Generation of a band structure during conjugation increases from ethylene to polyacetylene was represented in
Figure 1.2.From ethylene to polyacetylene, while the number of repeating unit increases, the discrete energy levels turn tothe continuum of the states which results in the formation of band structures [11]. As a result during the conjugation length increases, the energy difference between the valence band and the conduction band decreases.

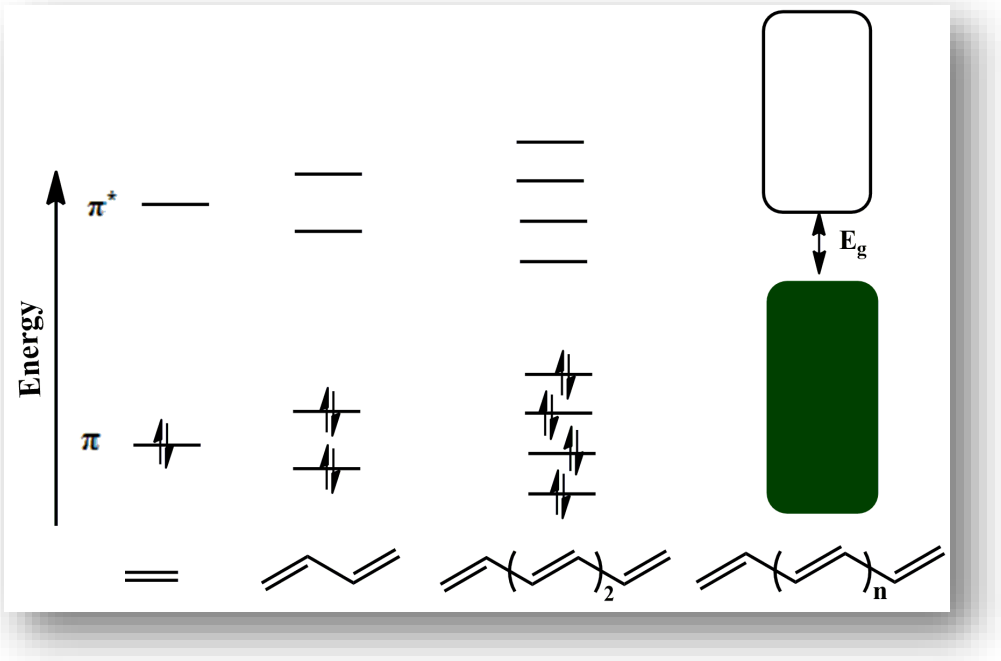

Figure 1. 2. Generation of bands in polyacetylene.

1.3. Conduction Mechanism

1.3.1. Charge Carriers

Since conjugated polymers do not have any charge carriers in their neutral states, the formation of charge carriers could be achieved via oxidation and reduction processes. This process is called as doping process and could be performed by oxidizing and reducing agents.Oxidation/reduction processes are quite easy for conducting polymers in other words, π- electrons can be easily removed/inserted to form charge carriers without affecting sigma bonds due totheir small ionization potentials and large electron affinities [12]. These charge carriers like polarons, bipolarons, solitons, free carriers etc. could be defined according to the ground state degeneracy states of conducting polymers [13].

The famous conducting polymer PA has degenerate ground states with isoenergetic regions, hence during doping process solution formation was observed for the

systemas illustrated in Figure 1.3. After insertion of an electron to the conduction band, a radical anion (polaron) is created (Figure 1.3b). During the formation of polarons, newenergy states from the bottom of the conduction band and the topof the valence band were injected into the band gap. Further reduction via addition of an extra electron on CP results the formation of a bipolaron with dimerization of two polarons.

While a polaron as a charge carrier has both spin (1/2) and charge (±1 e), bipolaron is spinless. As summarized in Figure 1.3d, formation of two spinless solitons lower their energy of bipolarons but this case is valid only for conjugated polymers with a degenerate ground states suach as;PA. In other words, soliton formation could not be observed for conjugated polymers with nondegenerate ground states, like polypyrrole, polythiophene, and polyaniline [14].

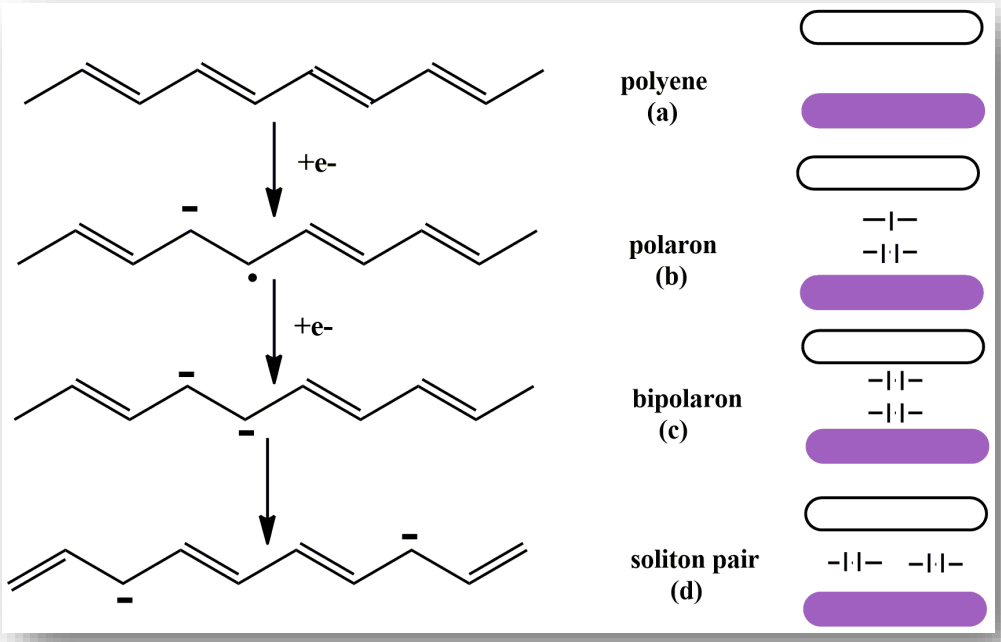

Figure 1. 3. Formation of polaron, bipolaron, and soliton pair on a trans-polyacetylene chain via doping process.

1.3.2. Doping

Doping could be defined as the insertion of charges to the polymer backbone via redox processes. By this techniquethe electrical conductivity of a polymer can be controlled over a range from insulating to conducting states. Doping couldbe achieved with either adding or removing an electron from the polymer chain. Those were called as p-type doping and n-type doping,respectively.(Figure 1.4)

During doping and dedoping processes, in order to stabilize the oxidized/reduced states, counter ions should be involved into the medium. These dopants could be inserted via chemically or electrochemically which also determine the type of doping process either chemical or electrochemical doping[15].

During chemical doping, doping process are performed by electron acceptors and donors such as; iodine(electron acceptor) and $(Na^{+})(C_{10}H_{8})^{-}$ (electron donor)[10]. Although chemical doping is an efficient method and has some certain advantages, difficulty in controlling results inhomogeneous doping leves. After invention of electrochemical doping these common problems were solved. During electrochemical doping, redox processes can be achieved by electrochemically applying appropriate voltages. Since all processes are performed in an electrolyte solution, generated charges can be neutralized by the counter ions[15].To explain clearly, electrochemical doping of PPy can be illustrated by the following equations.

(a) p-type electrochemical doping

$(PPy)_n + [Li^{+} (BF_4^{-})]_{soln} \rightarrow [(PPy)^{+y} (BF_4^{-})_y]_n +$ Li (electrode)

(b) n-type electrochemical doping

$(PPy)n +$Li (electrode) $\rightarrow [(Li^{+})_y (PPy)^{-y}]_n + [Li^{+} (BF_4^{-})]_{soln}$

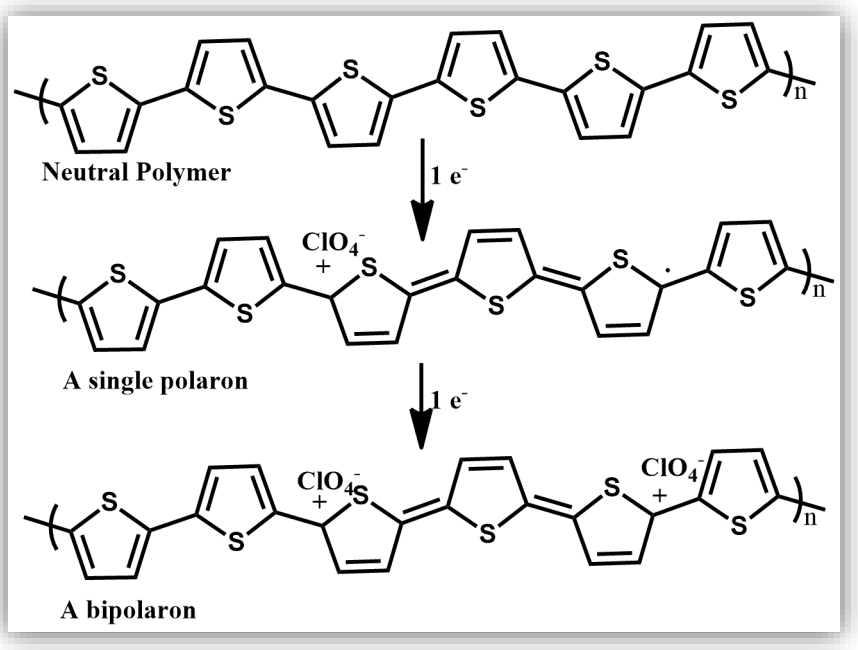

Figure 1. 4.P-type doping of PTh.

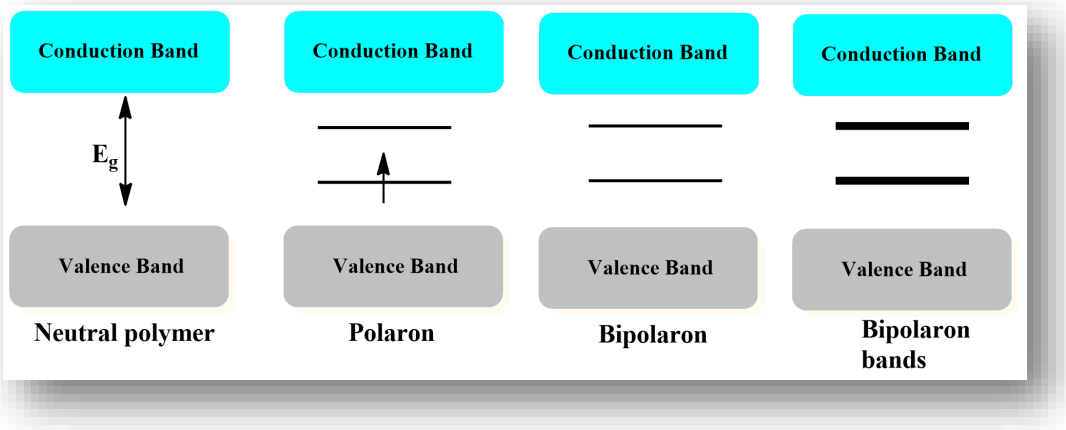

Figure 1. 5. Energy bands in the mid gap.

1.4. Synthesis of conjugated polymers

1.4.1. Chemical synthesis of conjugated polymers

For efficient conjugated polymer syntheses, most widely used method is polycondensation reaction catalyzed with transition-metals. Stille coupling and

Suzuki coupling reactions are the two significant examples for transition metal catalyzed polycondensation reactions and general mechanism for corresponding coupling reactions is summarized in Figure 1.6.

During polycondensation reactions the molecular weight of the target polymer is very cruial for the applicability of the resulting polymers. For that reason reactivity of monomers, solvent, end groups and the stoichiometry of monomers should be arranged to get the polymers with desired molecular weights and purity [16].

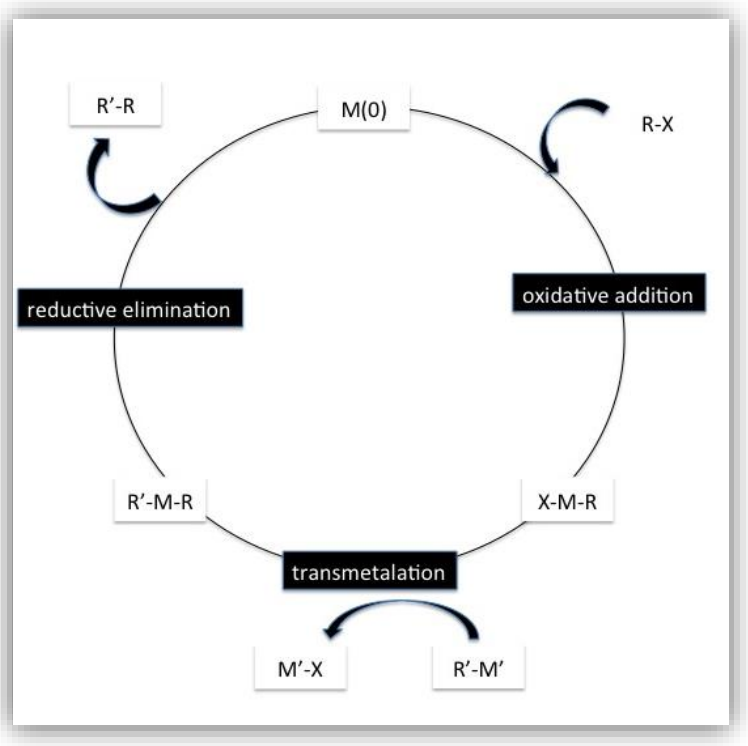

Figure 1. 6. An overview of transition metal catalyzed polycondensation reaction.

1.4.1.1. Suzuki Coupling

Suzuki coupling is widely used for the formation selective of C-C bonds with coupling reactions of boronic acid/ester and the halogen substituted alkenyls. Pd(0) catalyst is used for Suzuki coupling reaction which starts the cross coupling reaction

with the synthesis of an aryl halide. Thenreductive elimination and transmetallation complete the coupling reaction as depicted in Figure 1.6 [17].While nontoxic side products and reagents compared to Stille coupling are the main advantages of Suzuki coupling and makes it preferable, difficulty in purification of monomers containing boronic acid is the main drawback which affects the molecular weight of resulting polymers significantly.

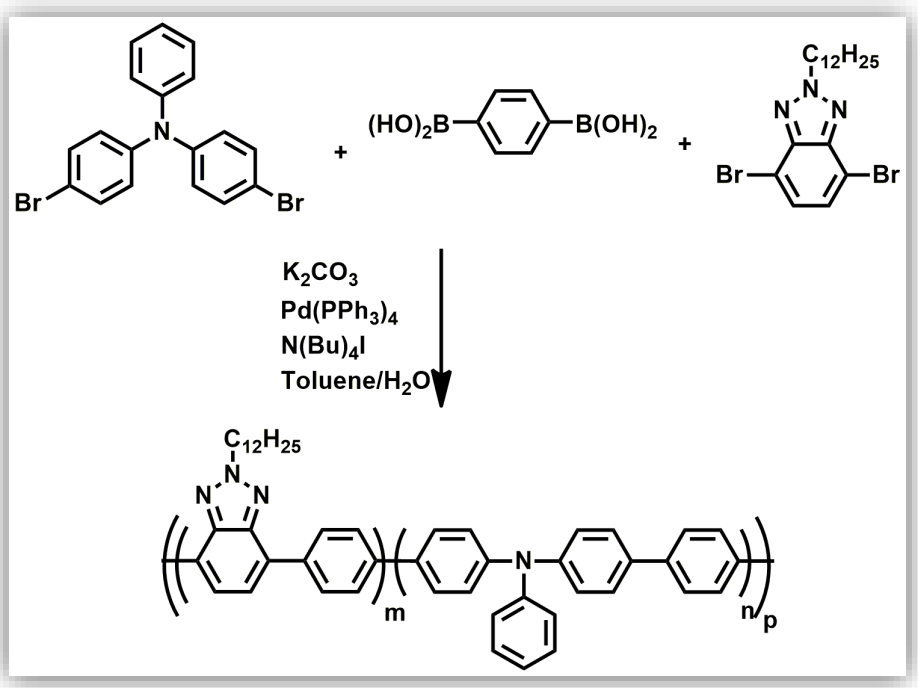

Figure 1. 7. Suzuki Coupling.

1.4.1.2.Stille Coupling

The Stille coupling is one of the most efficient coupling reactions which uses stannanes and halides to form C-C bonds. Via stille coupling alternating and random copolymers could be synthesized with high yields. Similar to the Suzuki coupling, oxidative addition of Pd from the aryl halide, transmetallation, and reductive elimination form the mechanism of this efficient technique.

While stille coupling has numerous advantages such as; milder reaction conditions and lower oxygen sensitivity, toxicity of stannylated monomers and its side products are the main disadvantages of this technique [16].

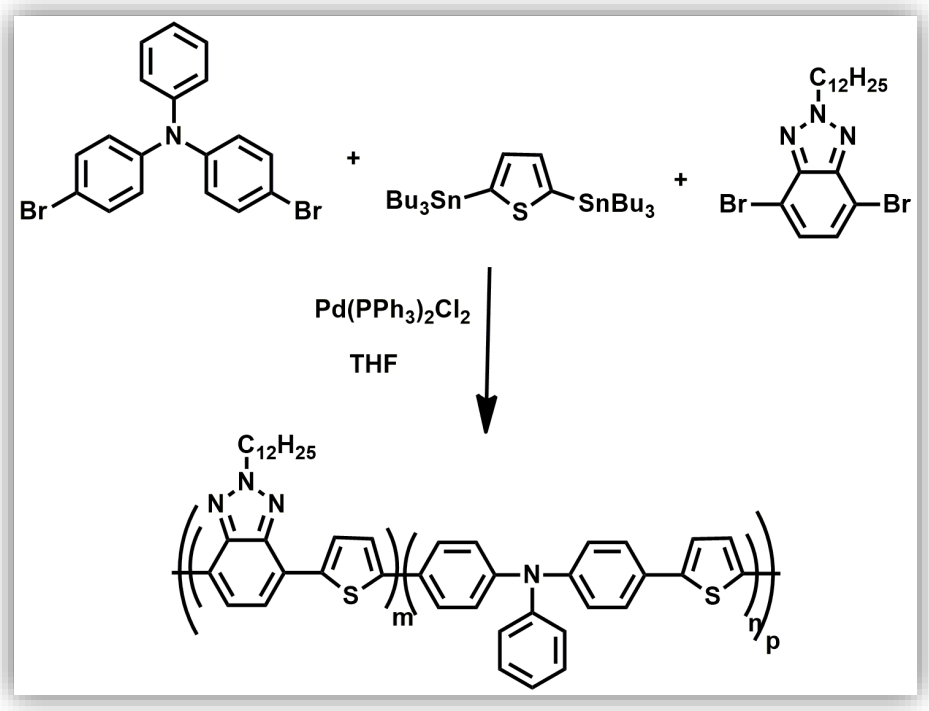

Figure 1. 8. Stille Coupling.

1.4.2. Oxidative Chemical Polymerization

Oxidative chemical polymerization is widely used for polymerization of heterocyclic compounds. During polymerization anhydrous Lewis acid like $MoCl_5$, $FeCl_3$, $RuCl_3$ were used as catalysts and as a consquence funtional polymers with high molecular weight and high conductivity could be achieved. In addition resulting polymers are very similar to electrochemically synthesized polymers which makes possible to comparison[18].

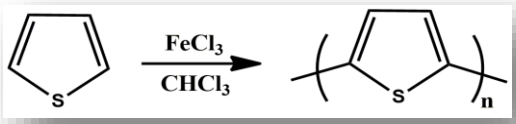

Figure 1. 9. Chemical polymerization with $FeCl_3$.

1.4.3. Electrochemical Polymerization

Compared with other widely used chemical polymerizations, it is a fact that electropolymerization technique could not used in industrial production however; this polymerization technique is very crucial for fundamental studies due to some certain advantages suc as [19];

- ✓ A small amount of monomer is sufficient for electrochemical polymerization.
- ✓ Electropolymerization could be performed via in-situ growing process which provides time saving because whole electrochemical and spectroelectrochemical analyses can be completed rapidly.
- ✓ During electropolymerization, conducting polymers are coated onto the electrode surface and this electrode could be used for further analysis directly.
- ✓ The film thickness could be calculated with the charge under the area of voltammogam. In addition thickness could be controlled with the number repeating cycles.

Besides these certain advantages, the main drawback of electrochemical polymerization is the small amount and low solubility of resulting polymers. Due to solubility problem, characterization of electrochemically synthesized polymers is quite difficult. The mechanism proposed for the electropolymerization of thiophene is illustrated in Figure 1.10. It is also valid for other heterocycles such as; furan, pyrrole with the same steps. The oxidation of the monomer to form radical cation is the initial step and it is an electrochemical process(E). After sufficient amount of

radical cationsare produced near the electrode surface, the second step takes place which is the coupling of the two radical cations. Then achemical step (C)takes place to convert the radical cations into dimers, with the loss of two protons recovering aromaticity. When oxidation potentials of resulting dimer and monomer are compared, the former has a lower oxidation potential than the latter one because of extended conjugation. Therefore in the next step, dimer oxidizes andthe produced radical cation undergoes coupling to form oligomers.

Finallyelectrochemical polymerization takes place with defined electrochemical (E) and chemical (C) steps until polymers are produced ontothe electrode surface [20].

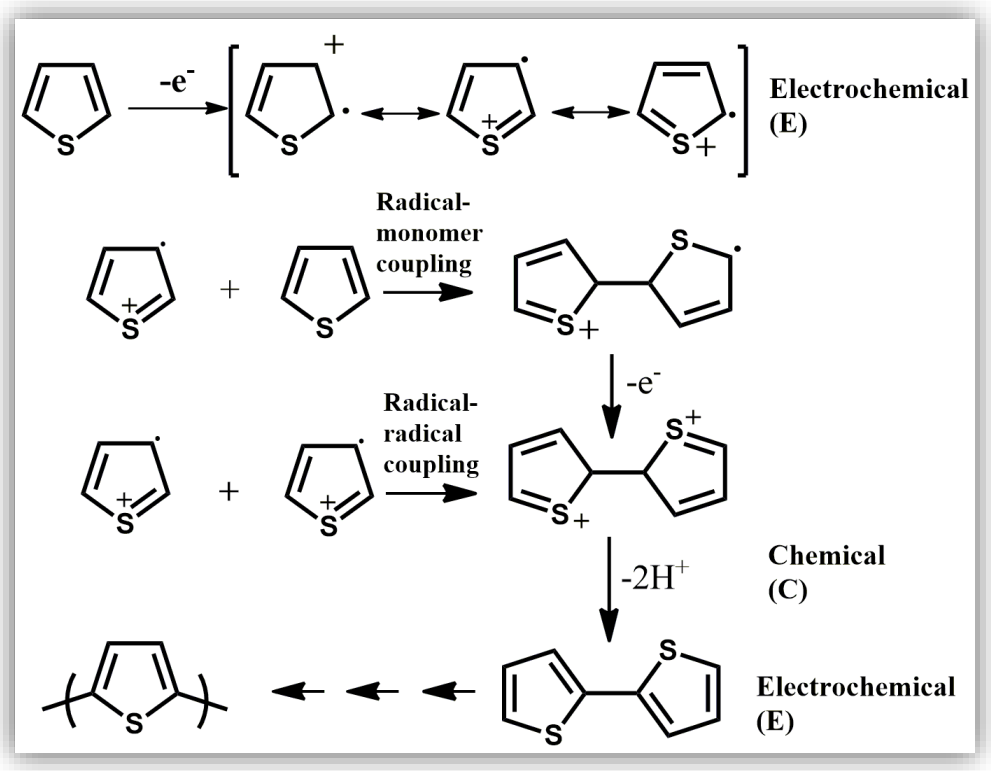

Figure 1. 10. Electropolymerization mechanism of thiophene.

Electrochemical polymerization is carried out either potentiostatically or galvanostatically. Constant potential is applied to the material during potentiodynamic techniquesand also during experiment repetitive potential waveform is recorded. Cyclic voltametry is widely used potentiodynamic technique for

electropolymerization. Qualitative information about the redox processes were obtained via galvanostatic techniques. In addition, via CV both electropolymerization and the electrochemical characterization of the resulting polymer films can be explored [21].

For an efficient electrochemical polymer synthesis and characterization, there are some key parameters such as; solvent/electrolyte types, concentration of monomer and electrodes which significantly affect the properties of the resulting polymers. For electropolymerization and electrochemical characterizations solvent choice is very vital, the proper solvent should has high dielectric constant in order to satisfy ionic conductivity of the electrolytic medium. In addition the solvent should not undergo any electrochemicalprocess in the working potential range hence, it should have high resistance against decomposition. Acetonitrile, propylene carbonate, nitromethane are commonly preferred solvents which have high dielectric constants.

Supporting electrolyte has two important roles during electrochemical polymerization, firstly it ensures electrical conductivity in solution, and secondly it dopes the polymer via acting as a counter ion. Electropolymerization is performed in the presence of small anions such as ClO_4^-, PF_6^-, and BF_4^- associated with lithium/sodium or tetraalkylamonium cations. Hence, the nature of the anion and cation couple significantly affect both electrochemical behavior and morphology of resulting conducting polymers[22]. In literature it is stated that while anion of supporting electrolyte affects the electrodeposition process, the cation on the other hand affects the charge-discharge process because discharge process not only comprises the anion expulsion, but also the temporary incorporation of cations [20].

During electropolymerization, after the monomer is dissolved in a proper solvent and supporting electrolyte couple, potential is applied for oxidation of monomer on a working electrode surface. Indium–tin oxide (ITO) coated glass, platinum, gold and glassy carbonare examples for widely used working electrodes (anodes) for electrochemical studies.

1.5. Characterization of Conducting Polymers

Conducting polymers could be synthesized either chemically or electrochemically. After succesful synthesis and purification processes, the possible application fields for resulting polymers are investigated. For these researches, some crucial parameters such as; molecular weight, HOMO-LUMO energy levels, band gaps, optical contrast and switching time should be explored carefully. Cyclic voltammetry, spectroelectrochemistry, kinetic studies, gel permeation chromatography and NMR spectroscopy were widely used or these vital characterizations. Redox properties and corresponding HOMO-LUMO energy levels are generally detected from cyclic voltammetry studies. Spectroelectrochemical studies were peformed in order to investigate vital informations such as the band gap (E_g), λ_{max}, and polaron and bipolaron formation upon stepwise oxidation. During studies, in situ stepwise oxidation of polymer is performed and results are recorded with both electrochemical and spectroscopic techniques. Optical contrast and switching times are other important parameters which allow the applicability of these materials in electrochromic devices. Percent transmittance changes and switching times are determined via kinetic studiesby sweeping the applied potentials between two extreme states (the neutral and oxidized states).Besides electrochemical and spectroelectrochemical behaviors, molecular weight of resulting polymers affects application fields significantly so the number average, weight average molecular weights and polydispersity index of the polymer could be determined via gel permeation chromatography.

1.6. Application Areas of Conducting Polymers

1.6.1. Organic solar cell

The requirement to investigate inexpensive renewable energy sources apprises ofmost of the researchers to focus on efficient, low-cost photovoltaic devices. The main drawbacks of fossil fuels are their harmful emission, noise manifacture, and undesired by-products. Hence, in order to produce energy from light via cheap and

easy methods, the polymer-based (organic) photovoltaics studies were constructed and their popularity increased dramatically [23].

Photovoltaics convert light into electrical energy and this process could be performed using either inorganic or organic materials. Recentlymost part of the photovoltaics market comprises of silicon solar cells but certain drawbacks of silicon cell technology such as high prices force researchers to focus on alternatives. Therefore, organic solar cells are developed as an alternative to inorganic solar cells. After their discovery, the popularity of solution-processable organic solar cells (OSCs) increased significantly due to their various advantages such as low cost, light weight, ease of fabrication by large-scale, possibility of flexible device production and tunable properties via small modifications. Besides various advantages, organic solar cells also have some drawbacks such as; low stability and poor performance.[24,25].

1.6.1.1. Working principle of solar cell

Schematic device structure for bulk heterojunction solar cellwas depicted in Figure 1.11. Generally organic solar cells have a planar-layeredstructure, light-absorbing active layer is sandwiched between two different electrodes. While semi-transparent electrodes like indium–tin-oxide (ITO) forms the anode contact, a thin metal layer like aluminium electrode is generally used as the cathode. In addition, calcium, magnesium, gold are alternatives that could be used instead of Al electrode[26].

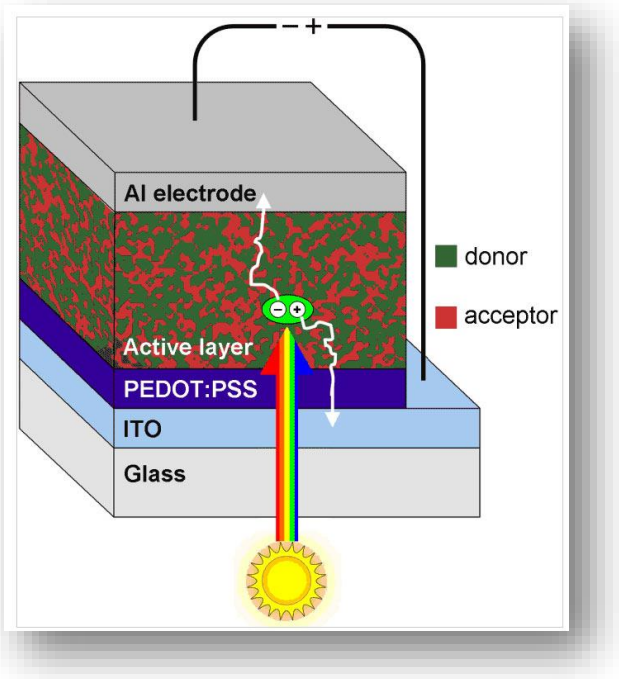

Figure 1. 11. Schematic device structure for bulk heterojunction solar cells.

Absorption of photon takes place by photoactive materialand after absorption, an electron is excited from conjugated polmers'HOMO to LUMO energy levels. In the second step, exciton (a bound electron-hole pair with strong coulombic attraction) is generated. Exciton can travel to a certain distance called asexciton diffusion length (5-20 nm) before recombination process. Exciton diffuses to the donor-acceptor interface which consists of heterojunction blend of organic materials (donor and acceptor) and then from LUMO of the donor to LUMO of the acceptor material photoinduced charge transfer occurs. Charge transfer occurs only if the energy difference between the HOMO (donor) and the LUMO (acceptor) equals to exciton binding energy. Photoinduced charged transfer process followed by generation of geminate pairs; electrons on acceptor and holes on donor. Finally newly generated free charges transported to the appropriate electrodes (holes to anode through PEDOT:PSS and electrons to cathode through PCBM) for charge extraction.

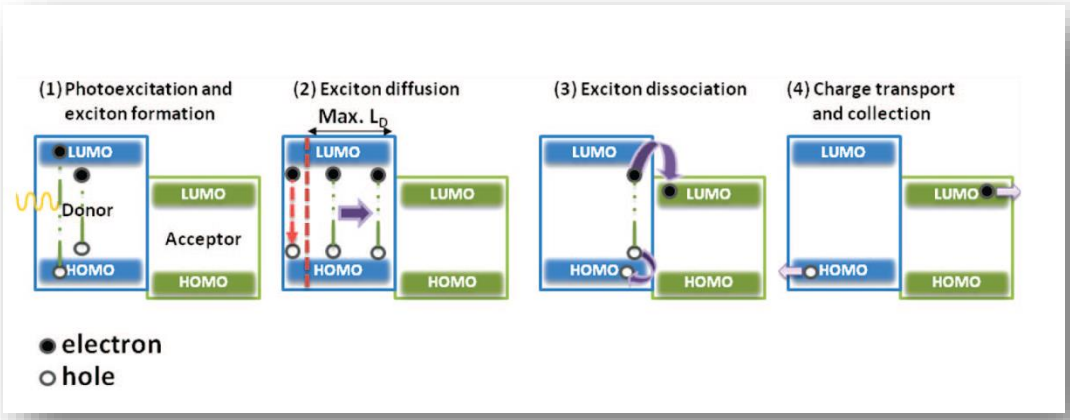

Figure 1. 12. Working principle of organic solar cell.

Working principles of organic solar cells could be summarized with five steps as illustrated in Figure 1.12for photoinduced charge transfer [27,28] .

- absorption of light and exciton generation
- diffusion of exciton to the interface between the donor and acceptor materials
- exciton dissociation
- charge transport to the electrodes (anode and cathode)
- collection of charge on the electrodes

To produce an efficient organic solar cell, HOMO and LUMO energy levels of donor materials (conjugated polymers or small molecules for OSCs) and work functions of anode/cathode which affect charge transport mainly is crucial. Conjugated polymers' HOMO should match with work function of anode, at the same time its LUMO should match with work function of cathode to create ohmic contact. For this purpose, in literature different kinds of anodes, cathodes and active layers were combined. [26, 28,29].Light-induced charge generation contains different steps and if energy levels and work functions are not suitable, undesired recombinations can take place and as a result generated charges can be lost. Hence for the efficiency of OSCs, recombination is the main limiting factor [30].

1.6.1.2. Solar cell architectures

The early examples of organic solar cells was constructed with bilayer heterojunction device architecture. As illustrated in Figure 1.13(a), in this configuration p-type and n-type materials in the active layer coated separately which increase the thickness of active layer. While the thickness of active layer is approximately 100 nm, the exciton diffusion length is nearly 10-20 nm. Hence, the area between the donor and acceptor interface that excitons could be generated is very small. In addition this drawback increase the possibility of recombination of excitons after the generation and decrease the efficiency ofresulting organic solar cells [31].

In order to minimize the drawbacks of bilayer device architecture, bulk heterojunction (BHJ) type OSCs were constructed by Yu et al. by blending donor and acceptor materials in the active layer. Blending two materials results an interpenetrating network with a large D-A interfacial area. By this tecnique, the main drawbacks of bilayer configuration; exciton diffusion length and required thickness for light absorption were overcomed [32]. As mentioned before the basic requirement for an efficient solar cell is to collect free charges into anode and cathode and via these interpenetrated networks hole and electron transportation is easier due to suitable channels.

(a) (b)

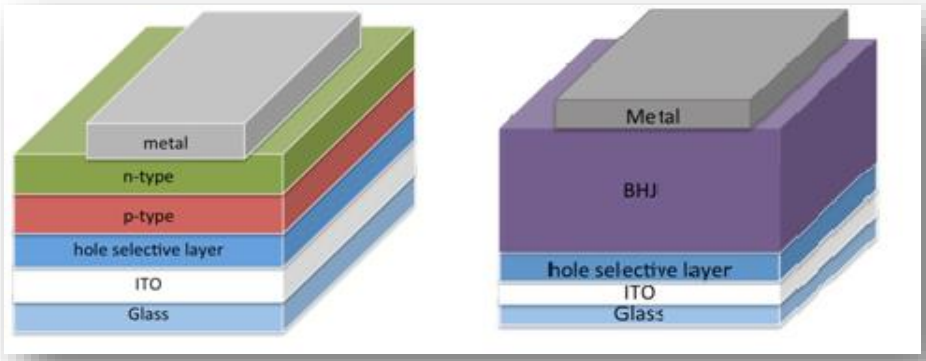

Figure 1. 13. (a) Bilayer device configuration (b) Bulk heterojunction device configuration.

1.6.1.3. Characterization of organic solar cells

For the characterization of constructed solar cells, current vs. voltage curve is drawn both under illumination of AM 1.5 G solar spectrum and dark (Figure 1.14).Open circuit voltage (V_{OC}), short circuit current (J_{SC}) and fill factor (FF) are crucial parameters that affect the power conversion efficiency (PCE) of organic solar cell and the relation can be explained by the equation of PCE.

$$\text{Eq.1.}\eta = \frac{J_{SC} V_{OC}\, FF}{P_{in}}$$

P_{in}: light power incident on the device

V_{OC} : open circuit voltage

J_{SC} : short circuit current

FF: fill factor

$$\text{Eq.2.} \quad FF = \frac{J_{max} V_{max}}{J_{SC} V_{OC}}$$

Open circuit voltage (V_{OC}) can be defined as the maximum voltage obtained from the solar cell when the current is zero and it can be determined as the difference between HOMO level of donor unit and LUMO level of the acceptor unit in the active layer [33].

The band gap of the material and absorption characteristics in the visible region mainlyaffects the *short circuit current (J_{SC})* which can be defined as the current flows when V_{OC}=0 [34].

Fill factor (FF) defined as the ratio of maximum power (P_{max}=J_{max}.V_{max}) to the incident power. FF shows the quality of the photovoltaic devices and affected by resistances (series (Rs) and shunt resistance (Rsh)), carrier recombination and carrier lifetime [35,36].

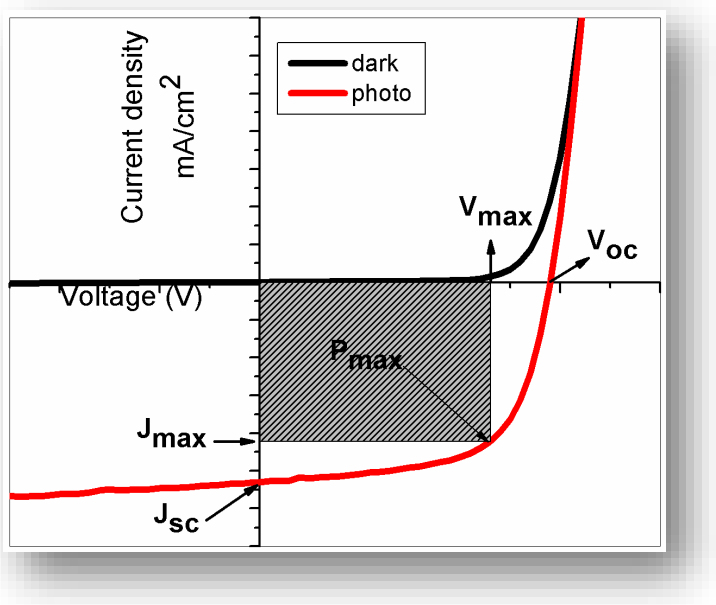

Figure 1. 14. Current-voltage curve under illumination and in dark.

1.6.2. Electrochromic Devices

1.6.2.1. Electrochromism

Electrochromism could be defined as the reversible and visible change in transmittance or reflectance as a result of an applied voltage. During electrochromic studies, color change takes place upon reduction (accept electrons) or oxidation (reject electrons) due to application of an appropriate electrode potential [37].

Electrochromic materials discovered in 1968 and from the first discoverythis phenomenon has been explored by many scientists due to some certain advantages and possible application areas such as: displays, smartwindows, sunglasses and rear-view mirrors. The switching time, optical contrast, coloration efficiency, electrochromic memory and long term stability are some important characteristics of electrochromic materials which affect the application field significantly and will be disscussed in detail.

In this field, basically three classes of electrochromic materials are known namely; metal oxide films (especially tungsten oxide) ,viologens (4,40-bipyridylium salts) and conducting polymers (polypyrrole, polythiophene and polyaniline).The most popular example of metal oxides is the tungsten trioxide (WO_3) system. Nearly cubic structure of tungten oxide satisfy empty spaces inside which provides large number of regions where the dopant ions can be inserted or ejected. While tungsten trioxide has transparent color in the thin film form and at the W_{VI}oxidation state, upon electrochemical reduction $W_V$state appears and the resulting color turns to blue color at that redox state. Coloration mechanism of WO_3 could be explained with the injection and ejection of electrons and metal cations (Li^+, H^+, etc.) .The following equation explains the redox process and corresponding colors for WO_3[38].

$$WO_3 + \quad xM^+ \quad + xe^- \rightarrow \quad M_xWO_3$$

(transparent) (blue)

Viologens are small molecules that are produced by diquaternization of 4,4'-bipyridyl, 1,1'-disubstituted-4,4'-bipyridilium salts and generally known as type II electrochromic materials, Figure 1.15 illustrates the three common redox states of viologen. While the dication form is the most stable state (colorless),reduction of viologen dications yields radical cations which are generally intensely colored with high molar absorption coefficients. In violegen electrochromism, nitrogen substituents significantly affect the color of the resulting radical cation [39].

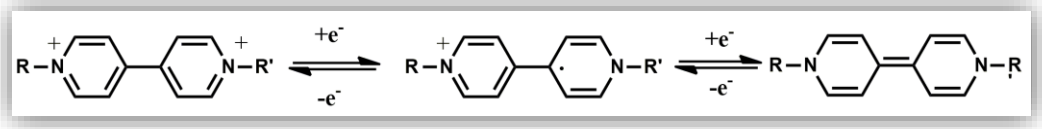

Figure 1. 15. The three common viologen redox states (dication, radical cation, neutral states).

1.6.2.2. Electrochromism in conjugated polymers

Another class of electrochromic materials are conducting polymers which gained significant interest in the field of electrochromism due to some certain advantages, such as, low cost during production and processing, enhanced mechanical properties, high coloration efficiency, fast switching time and fine-tuning of the band gap via the modification of polymer's chemical structure.

Conjugated polymers can undergo redox process (reduction and oxidation) via application of an electrical bias. Figure 1.16shows the changes in chemical structure and bandgap of a conjugated polymer after an oxidation process. Upon stepwise oxidation initiallypolaron (radical cation) will appear with newly generatedmid-gap electronic statessymmetric at the band center. As shown in Figure 1.16 during polaron formation, Ep_1 and Ep_2 which are new lower-energy electronictransitions took place. During this timewhile neutral state absorption is decreasing simultaneously in the visible region, the new absorption bandsare appearing at longer wavelengths. Further oxidation results formation of bioplaron(dication).

During bioplaron formation, the mid-gap electronic states are getting closer in energies and allowed electron transitionoccurs from the HOMO level to the first unpopulated mid-gap state (Ebp) [40].

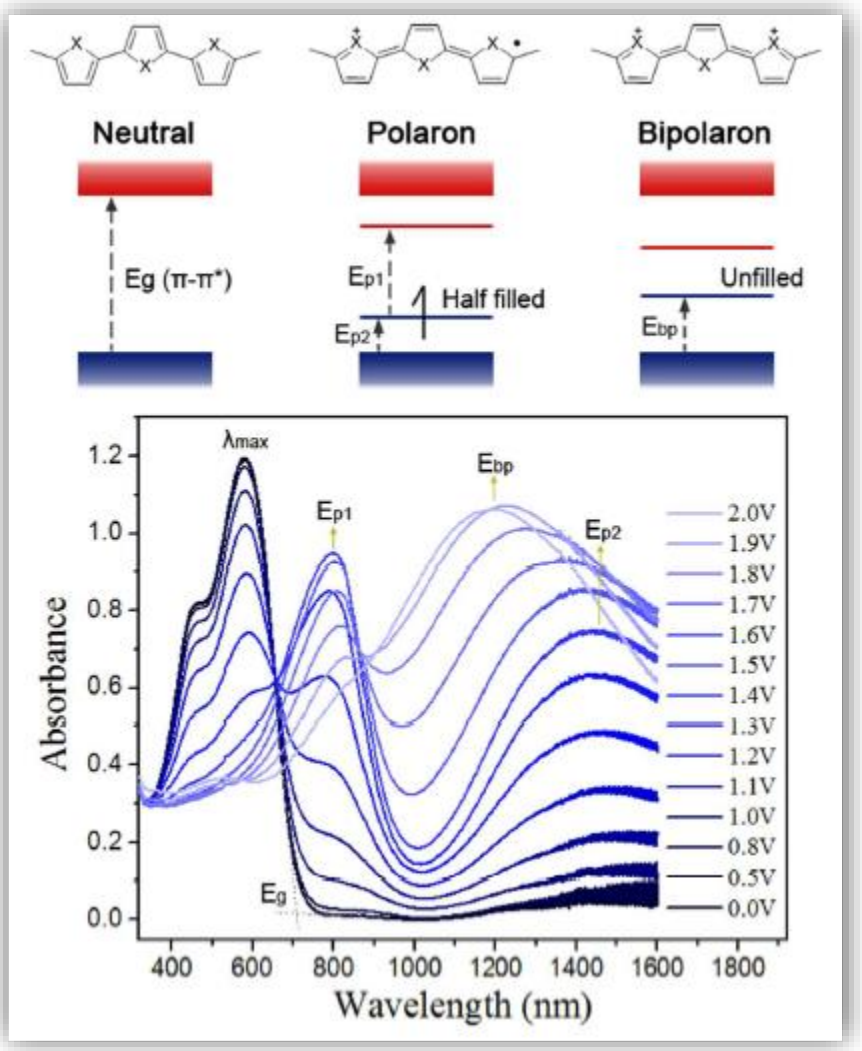

Figure 1. 16. Allowed transitions for neutral, polaron and bipolaron states with illustration of electronic, absorption spectral changes of a conjugated polymer upon oxidation.

While the polymers that have color in their reduced statesare called as cathodically-coloring, polymers that have color in their oxidized states are named as anodically-coloring. Some of electrochromic polymers could reveal two or more different colors (red, green, blue, etc.) and such materials are called as ‘multichromic’.

1.6.2.3. Electrochromic Device Architecture

An electrochromic device (ECD) is a battery in which the electrochromic polymer coated electrodeis separated from a counter electrode which acts as a charge balancing layer by a suitable electrolyte (solid or liquid). Voltage was applied to the constructed device to achive the color changewhich occur by charging and discharging the cell[41]. In literature, there are four different fields within which electrochromic devices were widely explored namely; smart window, variable reflectance mirror, information display and variable emmittance surface. Between them the smart windows have some certain advantages due to vital applications in innovative and energy-efficient architecture (Figure 1.17).

Figure 1. 17. Examples of commercial applications of ECDs a s smart windows[41].

As seen in Figure 1.18, sandwich type device configuration was used to construct the dual type ECDs. As active layer electrochromically complimentary polymers coated onto the transparent ITO coated glass electrodesare used and electrodes are separated via gel electrolyte which contains supporting electrolyte. As commercial application, highly transparent and colored states of resulting devices are very useful in controlling the light intensity in buildings.

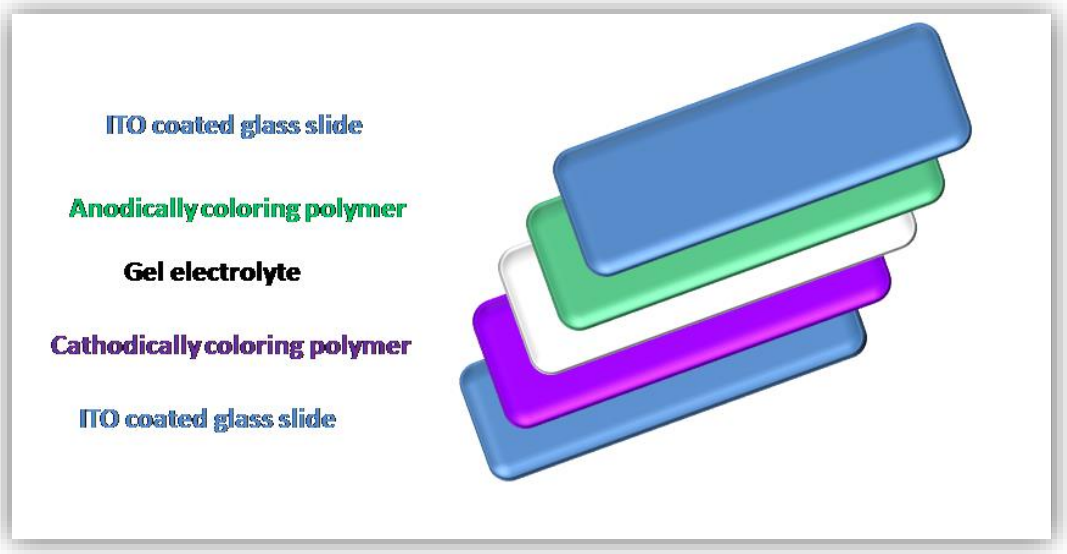

Figure 1. 18. Schematic illustration of dual type sandwich structured electrochromic device configurations.

1.6.2.4. Electrochromic device performance parameters

There are some crucial parameters that significantly determine the performance of electrochromic materials, one or more of the following performance criteria such as; optical contrast, switching time, coloration efficiency, optical memory and lon term stability have to be fulfilled depending on the intended application [40].

Optical contrast: Optical contrast could be defined as the change in percent transmittance($\Delta T\%$) of electrochromic material between its neutral and doped states. Optical contrast also measures the degree of color/transmissivity changes of the material between two extreme states. Generally, the optical contrast is investigated at the maximum wavelengths of the absorptions recorded in spectroelectrochemical studies. For experimental part, the percent transmittance changes were recorded at mentioned wavelengths while the applied potential was swept between two extreme states (neutral and oxidized/reduced).

Switching time: Switch time could be defined as the time required for one full switch between two extreme states whichalso defines how fast materialsswitch between the colored to the bleached state orvice versa. While the former process called as bleaching time, the latter one is named as coloration time. The time required for color change is very important for electrochromic device applications and will significantly affect the performence and applicability of resulting device.

Coloration efficiency: The power consumption of the electrochromic device was usually determined via coloration efficiency. This vital parameter is defined as *the change in optical densityper unit of charge injected/ejected*. Coloration efficiency could be calculated with the equation. The unit for coloration efficiency is cm^2/C.

Eq.3. $$Colorationefficiency, CE = \frac{log\frac{T_{ox}}{T_{red}}}{Q/_A}$$

Tox / Tred: *The percent transmittance changein the oxidized and reduced states.*
Q: *The charge consumed during the process*
A: *The active area of the electrocromic device.*

Open circut memory: The ability of the material to retain its color after the removal of the external bias is measured and reported with the open circut memory. The importance of an optical memory comes from that this parameter determines the approximate capacity of the device to operate without applying continuous potential.

Stability: The long term stability of the electrochromic device shows the ability of the device to maintain itsperformance under repeated operation and doping-dedoping processes. The stability of the electrochromic materials, type of gel electrolyte and the operation potentials of the resulting ECDs significantly affect the stability.

1.7. Building blocks for functional polymers

Band gap is the key parameter to control the physicochemical properties of conjugated polymers. In literature different strategies were used to tune the band gap such as; variation of bond length, increasing planarity of the systems, increasing stability of the polymer by using resonance, interchain effects and donor-acceptor approach. Among all band gap-engineering strategies, donor-acceptor (D-A) approach is the most effective strategy to tune band gap of conjugated polymers. In this approach, different donor and acceptor units are combined in the polymer backbone to tune thephysicochemical properties by controlling the degree of aromaticity, the planarity of polymer chain and the electron density of conjugated polymers[42]. Most widely used donor and acceptor units to tune the band gap and synthesize multifunctional polymers are summarized in Figure 1.19 and Figure 1.20.

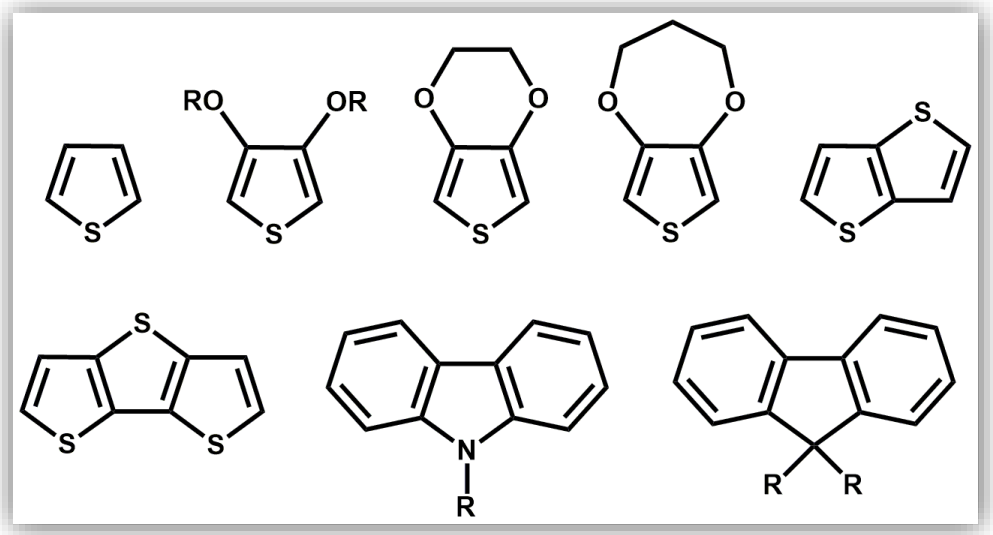

Figure 1. 19. Chemical structures of widely used donor units during the design of conjugated polymers.

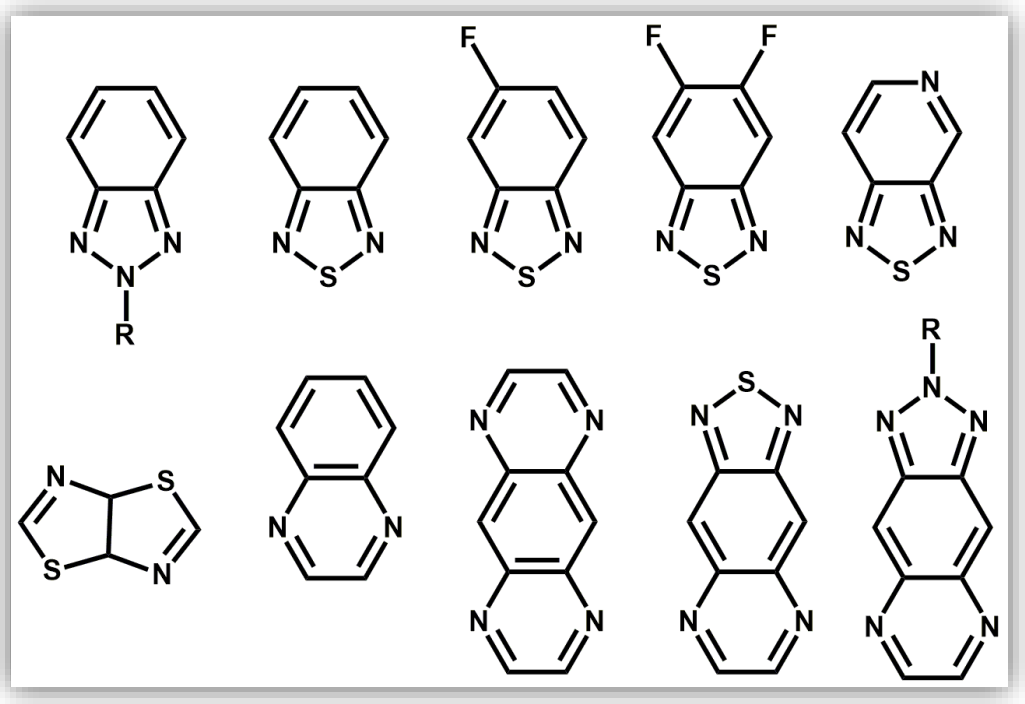

Figure 1. 20. Chemical structures of widely used acceptor units during the design of conjugated polymers.

1.7.1. Triphenylamine (TPA) bearing polymers

TPA exists as a white solid which is almost insoluble in water. Recently, the electron-rich TPA unit has been utilized as an attractive building block due to its high redox activity, fluorescence, ferromagnetism and transportability of positive charges. These desired properties make it good candidate for various applications [43]. In literature, triphenylamine (TPA)-based polymers are well known for their electron-rich groups which are extensively used as hole transport materials and light emitters in the field of optoelectronics such as OLEDs[44].Besides, it has been reported that TPA-containing materials have promising electrochromicfeatures due to its;

- Electron-rich character,
- Highly stable cationic states,

- ❖ Efficient hole-transport ability,
- ❖ Propeller like star-shaped structure

In addition insertion of TPA unit results in amorphous polymers which reveal multichromic behaviorsdue to multiple redox states. TPA based polymersgenerally has large band gaps due to their light yellow or light brown shades intheir neutral states. Finally, generally such polymers are anodically-coloring and they turnintomultiple intense colors upon oxidation, ranging from dark green, blue, purple to black [44].

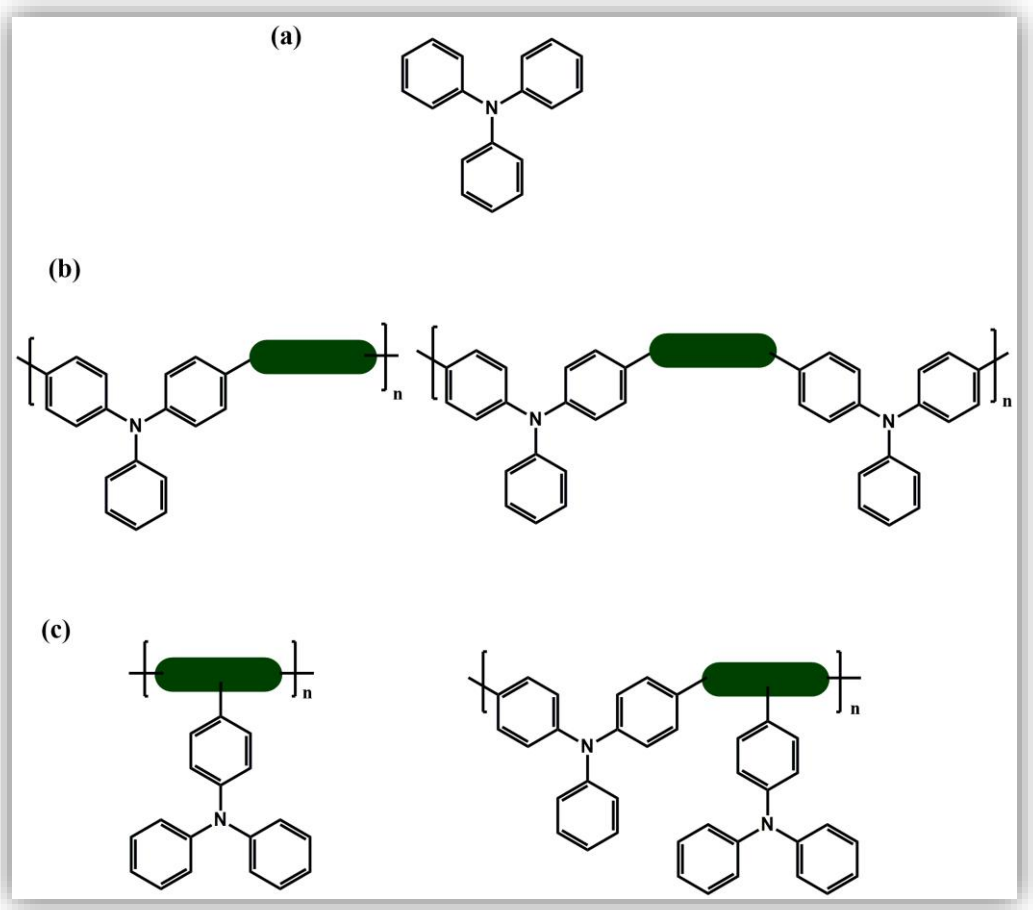

Figure 1. 21. (a) Structure of TPA and (b) possible position of TPA unit in the polymer chain.

As illustrated in the Figure 1.21, TPA may either comprise a repeat unit in a polymer main chain or be attached to the main chain as a side chain. In literature, there are number of examples for TPA bearing polymers. In the following sections some vital examples for TPA functionalized electrochromic polymers (both electrochemically and chemically synthesized) will be summarized.

1.7.1.1. A novel electrochromic polymer containing triphenylamine derivative and pyrrole[45]

In 2011 M. Ouyang et al reported a novel TPA bearing conducting polymer; poly-N1,N4-bis(4-(1H-pyrrol-1-yl)phenyl)-N1,N4-diphenylbenzene-1,4-diamine (PDPTPA). PDPTPA was synthesized electrochemically and resulting polymer film showed sixvarious colors under different neutral and oxidized states. Structure of DPTPA and corresponding colors for electrochemically synthesized polymer is depicted in Figure 1.22.In addtion, authors state that this polymer has high optical contrasts (41% at 852 nm, 52% at 617 nm)and fast switching times (1.3 s at 410 nm, 1.4 s at 852nmand 0.6 s at 617 nm) which are very crucial for electrochromic device applications. As a further characterization, the long-term stability of the prepared polymer film was investigated. Cyclic voltammograms were recorded between 0.0 V and 1.2V for 500 cycles and after experinet only slight shrinkage of redox loop is observed.

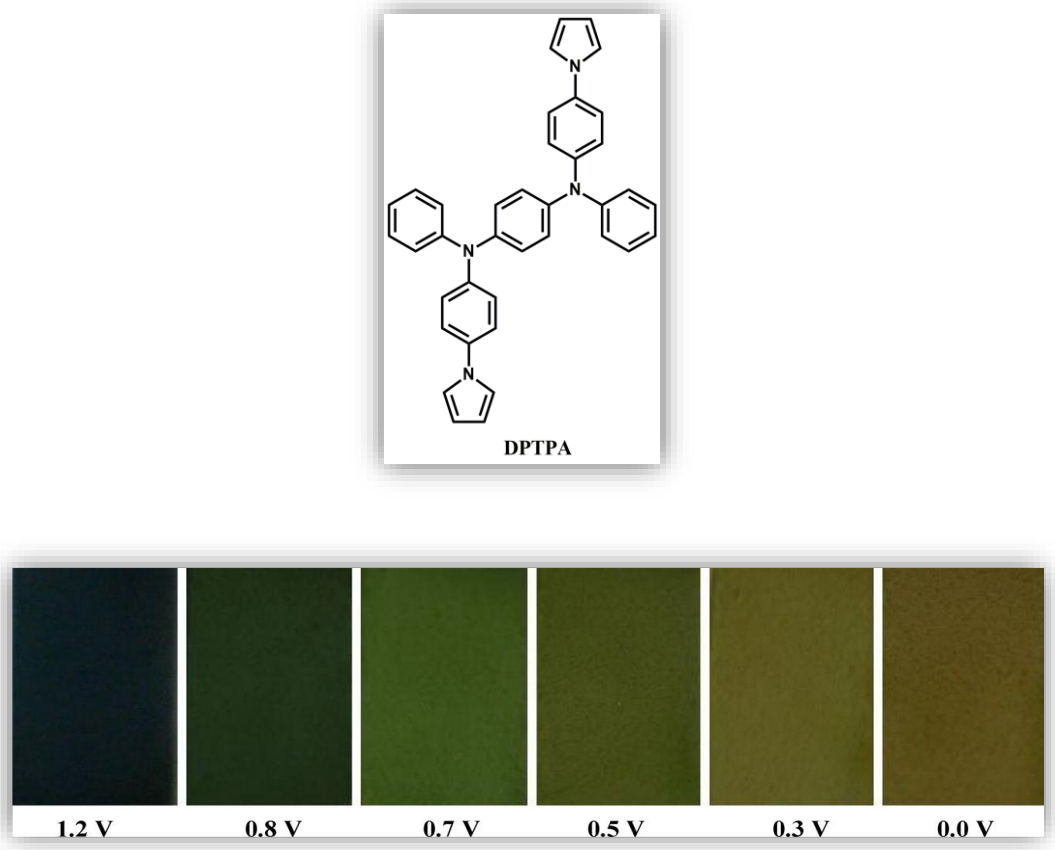

Figure 1. 22. Structure of DPTPA and corresponding colors for electrochemically synthesized polymer [45].

Due to characteristic behavior of TPA, PDPTPA has yellow color in its neutral state and its absorptionis closer to the UV region with 345 nm λ_{max} value. For OPV applications this absorption should be shifted to the NIR region with suitable functional groups for efficient applications.

1.7.1.2. Triphenylamine-based multielectrochromic material and its neutral greenelectrochromic devices [46]

C. Xu et al reported a star-shaped monomer; tris[4-(3,4-ethylenedioxythiophene)phenyl]amine (TEPA). Synthesis, electrochemical polymerization, characterization and ECD applications were reported in 2012.

Resulting polymer (PTEPA) had multielectrochromic behavior and presented six colors from brown to blue in the neutral and different oxidized states. This multicolor property possesses significant potential applications in smart windows or displays and can dedicated to the multiple redox states of TPA unit. Figure 1.23 illustrates the structure and colors of PTEPA.

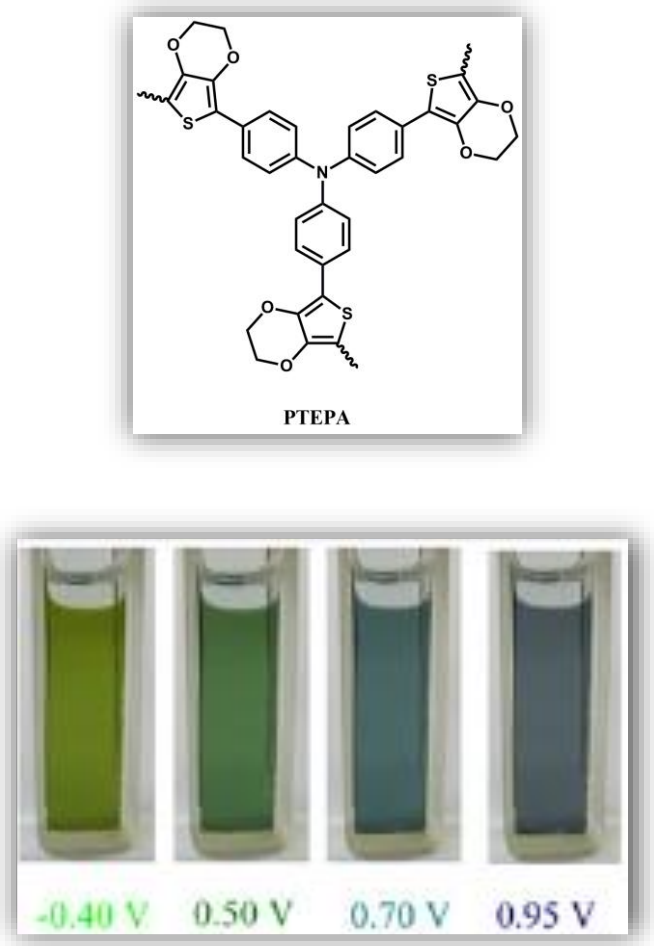

Figure 1. 23. Structure of PTEPA and corresponding colors for electrochemically synthesized polymer [46].

At the neutral state, the polymer film exhibited two absorption peaks at 448 and 686 nm. The absorption band at 448 nm was due to the π-π^* transition and the long wavelength absorption band at 686 nm was probably attributed to the charge transfer

band from TPA to EDOT segment [47]. From kinetic studies, maximum optical contrast and response time of the PTEPA film were reported as 26.84% and 0.94 s at 448 nm, 17.03% and 1.11 s at 686 nm, respectively.

Finally dual type ECD based on PTEPA and PEDOT was also constructed and characterized. Resulting ECD was operated between green and blue colors with 20.46% and 0.44 s at 448 nm, 24.72% and 0.36 s at 628 nm optical contrast and switching times, respectively. In addition, ECD also shows reasonable redox stability after 1000 cycle with unperturbed color change from green to blue.

1.7.1.3. Synthesis and characterization of photoelectronic polymers containing triphenylamine moiety [48]

In this study, Y. Liu et al reported synthesis and characterization of several polymers containing triphenylene moieties in main chain by Knovenagel or Wittig condensations. The polymers were characterized by ^{1}H NMR, UV–vis and CV. Between them structures of benzene, thiophene and furan bearinng derivatives are illustrated in Figure 1.25 and electrochemical and optical properties of corresponding polymers are listed in Table 1.1.

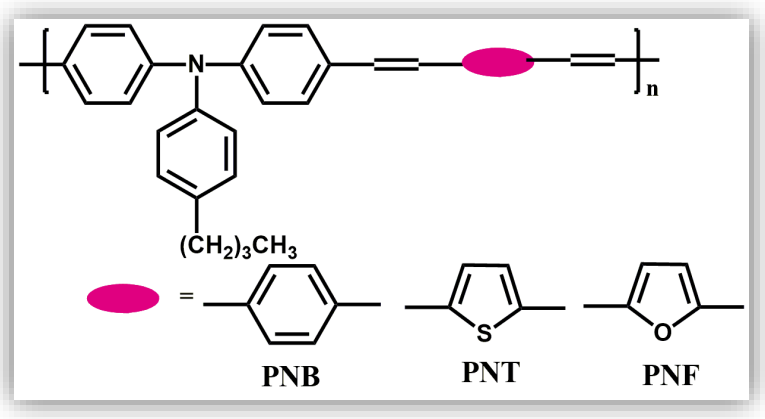

Figure 1. 24. Structures of TPA bearing polymers PNB, PNT and PNF [48].

Table 1. 1. Electrochemical and optical behaviors of PNB, PNT and PNF.

	E_{ox} (V)	E_{red}(V)	HOMO (eV)	LUMO (eV)	λ^{abs}_{max} (nm)	λ^{abs}_{edg} (nm)	E_g (eV)
PNB	1.17	-1.62	-5.91	-3.12	428	478	2.59
PNT	1.30	-1.51/ -2.51	-6.04	-3.23	439/397	520	2.38
PNF	1.24	-1.52/ -2.65	-5.98	-3.22	374	507	2.45

All polymers have a similar CV profile with a reversible oxidation peak and two reduction peaks except that PNB has a single reduction peak. Similar to the other TPA bearing polymers all polymers have neutral state absorptions closer to the UV region. As a results of this absorption range all PNB, PNT and PNF can be called as large band gap polymers. In order to solve these problems TPA unit should be coupled with acceptor units to lower the band gap.

1.7.1.4. Toward the Development of New Textile/Plastic ElectrochromicCells Using Triphenylamine-Based Copolymers [49]

Beaupre´ et al reported the the preparation and characterization of TPA bearing electrochromic polymers. In this study, 4-butyltriphenylamine (BuTPA) unit incorporated on the main chain and all polymers were obtained through the Suzuki-Miyaura cross-coupling reaction between 4-butyl-N,N-bis((4,4,5,5-tetramethyl-1,3,2-dioxaborolan-4- phenyl)aniline) and several aryl dibromide molecules.

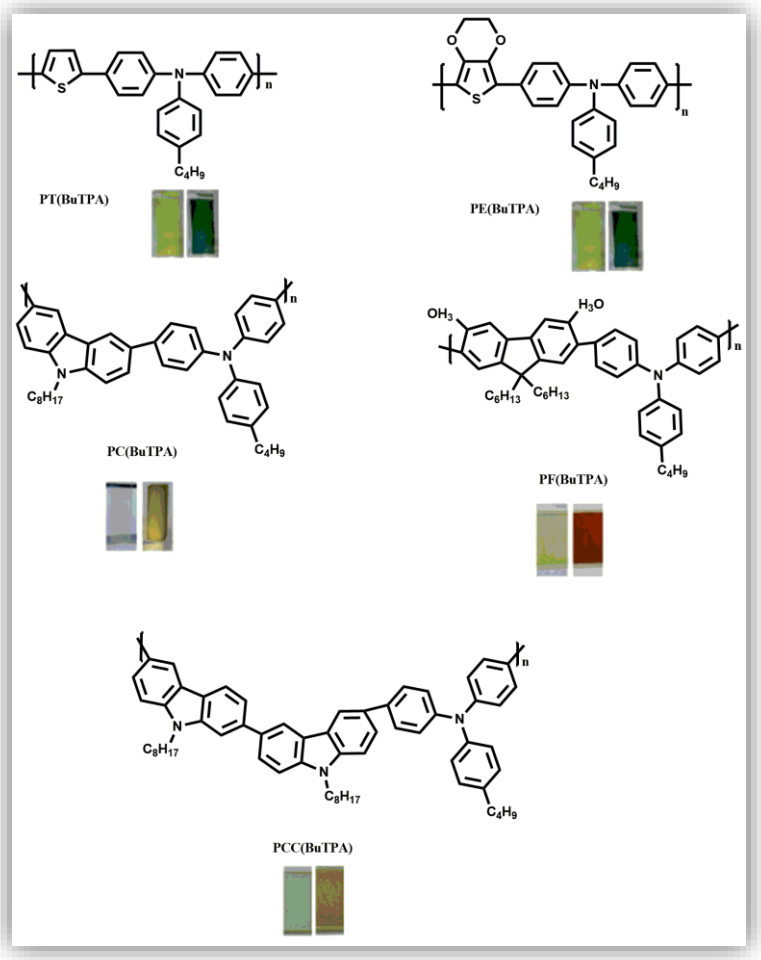

Figure 1. 25. Structures of 4-butyltriphenylamine (BuTPA) bearing polymers and corresponding colors for different states [49].

Resulting five polymers are soluble in common organic solvents, processable, and electrochromic. Interestingly, among them carbazole derivatives PC(BuTPA) and PCC(BuTPA) are colorless in their neutral states and show reversible color transition from colorless to khaki in the oxidized sates. All optical, electrochemical and colorimetric data are summarized in Table 1.2. Similar to the other literature examples, all TPA derivatives have absorption maxima at around 400 nm.

Finally, what important in this study is that Beaupre´ et al reportedflexible hybrid electrochromic cells for the first time. ITO-coated plastic and conductivetextile were

chosen as electrodes and this investigation shows interesting features foradaptive camouflagepolymers.

Table 1. 2. Optical, Electrochemical, and Colorimetric Data of Copolymers.

	E_{ox} (V)	λ^{abs}_{max} (nm)	Color (neutral state)	Color (oxidized state)
PT(BuTPA)	416	1.19	yellow	green
PE(BuTPA)	418	0.95	yellow	green
PC(BuTPA)	344	1.16	colorless	khaki
PCC(BuTPA)	342	1.16	colorless	khaki
PF(BuTPA)	380	1.19	pale green	reddish-brown

1.7.1.5. Electrochemical synthesis and electrochromic properties of new conjugated polycarbazoles from di(carbazol-9-yl)-substituted triphenylamine and N-phenylcarbazole derivatives [50]

Finally in 2015, S.-H. Hsiao, J.-C. Hsueh reported two carbazole end-capped monomers containing triphenylamine or n-phenylcarbazole as an interior core. The electrochemically synthesized polymershas two to three quasi-reversible redox couplesdue to successive oxidation behaviors of the triphenylamine and biscarbazole units. For TPA bearing derivative, spectroelectrochemical studies show that before applying potential, the P(TPA-2Cz) film showed a strongabsorption at 307 nm, and it almost colorless in the visible region. When the applied potential was gradually raised from 0.0 to 0.99 V, semi-oxidized state exhibited dark green color and fully oxidized states showed brown color (Figure 1.26) .

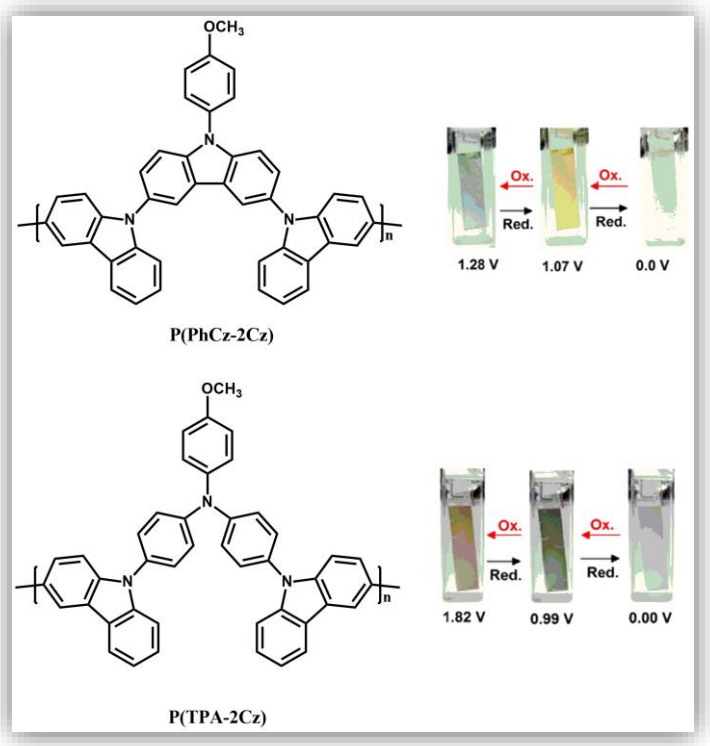

Figure 1. 26. Structures of polymers (P(PhCz-2Cz)) and (P(TPA-2Cz)) and corresponding colors for different states [50].

When P(PhCz-2Cz) polymer film was compared with the TPA bearing derivative, TPA bearing polymer showed better stability and switched more than 50 cycles without much failure incolor contrast. The results are reasonable due to the lower oxidation potential of TPA unit than the N-phenylcarbazole unit and more stable character of TPA radical cations. Kinetic studies illustrate that while P(PhCz-2Cz) has 35 % (1052 nm) and 37 % (741 nm), P(TPA-2Cz) shows 33 % (414 nm) and% 60 (730 nm) optical contrasts.

As a result, due to the high redox stability and good electrochromic performance of the resulting polymer films, these materials are good candidates for electrochromic device applications.

1.7.2. Triazoloquinoxaline bearing polymers

In literature, the very first examples of BTz-containingconjugated polymers were shown by Yamamoto andcoworkers [51,52]. Later on, in 2009, the electrochromic properties ofanother BTz derivative (PTBT) were investigated by our group.This fascinating polymer attracted many researchers and it wasreported as a multipurpose material due to its solubility, processabilityand dual type dopability (both p- and n-dopable) [53].After this discovery, BTz derivatives were in demand due to the achievement of resulting desired properties such as multichromism, transmissive states and photoluminescence, all combined in a single polymer.

In the meantime, quinoxaline based conjugated polymers, which were widely studied in the literature, attracted considerable attention. The lack of available neutral state green coloured polymers with highly transmissive oxidized states was addressed in 2007 by our group. By virtue of synthesizing these EDOT bearing quinoxaline derivatives, the missing element of the RGB (Red, Green, Blue) puzzle was contrived [54,55]. The idea having these two main electron deficient units; benzotriazole and quinoxaline in a single structure leading to the formation of black colored polymers inspired us to synthesize triazoloquinoxaline unit.

The idea is to synthesize a new acceptor unit which contains both benzotriazole and quinoxaline moieties. Owing to the increase in imine bonds (two vs four) with this single structure, the molecule is expected to yield higher electron transporting features [51,52]. For this purpose, the first examples for synthesis and electrochromic characterizations of triazoloquinoxaline bearing donor acceptor type polymers were firstly reported by our group [56]. In earlier reports triazoloquinoxaline unit was generally used for organic solar cell applications [57-61].

1.7.2.1. Triazoloquinoxaline and Fluorene bearing polymers for organic solar cells

J. Hai et al. reported novel donor-acceptor type polymers bearing a new electron-donating unit (thiophenyl-methylene-9H-fluorene) and triazoloquinoxaline unit. This study is the first example for the development and application of thiophenyl-methylene-9H-fluorene for organic solar cells. Resulting poylmer hasa narrow bandgap of 1.92 eV with 0.6 % PCE [57].

Then, Baran et al. reported another fluorene and triazoloquinoxaline based copolymer PTQF. The resulting polymer shows good thermal stability and solubility in common organic solvents and also has low band gap as 1.4 eV. Photovoltaic devices exhibited maximum 1.7% efficiency for 1:2 PTQF:$PC_{61}BM$ blend ratio. Finally, the authors suggested to combine triazoloquinoxaline unit with other donor units such as; dithienosilole, benzodithiophene, or carbazole which may improve the transport and transfer abilities [58].

A narrow-bandgap conjugated polymer (PFDTBTzQ-2OC1) is synthesized by Hai et al. [1,2,3] triazolo[4,5-g]quinoxaline and 9,9-didodecyl-fluorene were chosen as acceptor and donor materials. The resulting polymer PFDTBTzQ-2OC1 has wide absorption range in the visible region ranging from 300–760 nm with a bandgap of 1.63 eV. Bulk heterojunction solar cells fabricated by PFDTBTzQ-2OC1 and [6,6]-$PC_{71}BM$ illustrated a maximum power conversion efficiency of 1.31% [59].

Table 1. 3. Electrochemical and optical results for triazoloquinoxaline based polymers.

	HOMO (eV)	**LUMO (eV)**	**λ_{max}**	**E_g**	**PCE (%)**
PFDTBTzQ	-5.43	-3.51	548	1.92	0.6
PTQF	-5.13	-3.62	790	1.40	1.71
PFDTBTzQ-2OC1	-5.40	-3.77	638	1.63	1.31

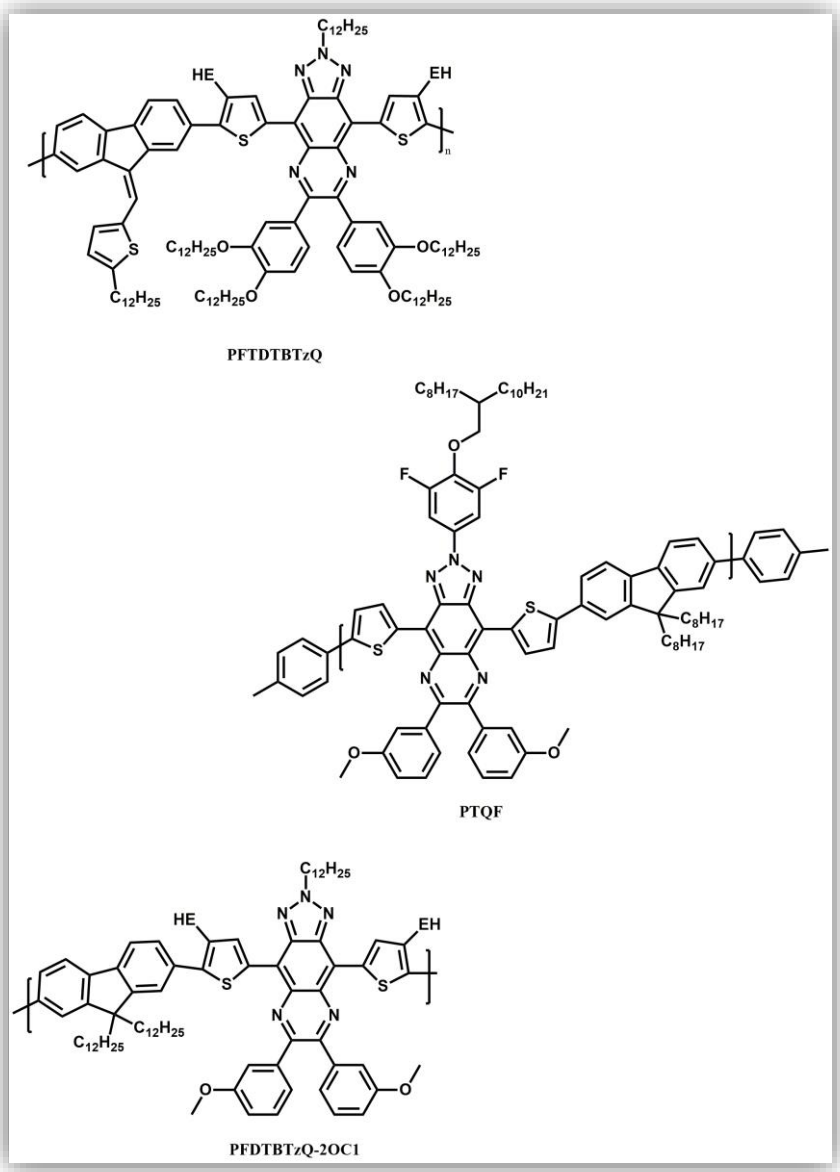

Figure 1. 27. Structures of triazoloquinoxaline and fluorene based polymers [57-59].

1.7.2.2. Design and synthesis of triazoloquinoxaline polymers with alkyl or alkoxyl chains for organic photovoltaics cells [60]

Hai et al. reported four benzodithiophene and triazoloquinoxaline based alternating polymers, PBDTT-BTzQx-EH-C1, PBDT-BTzQx- EH-C1, PBDT-BTzQx-EH-C12 and PBDT-BTzQx-C12 in 2014. They have been investigated the correlation of alkyl side chains with the opto-electronic properties of polymers. Electrochemical and

optical data for resulting polymers are summarized in Table 1. 4. Both organic solar cell and electrochemical studies show that the insertion of alkyl chains onto the thiophene spacer or quinoxaline unit lowers the HOMO level of the polymers, but on the other hand excessive chains prevent the polymer backbone from π-π* stacking which decreases short circuit current and fill factor in a photovoltaic application.

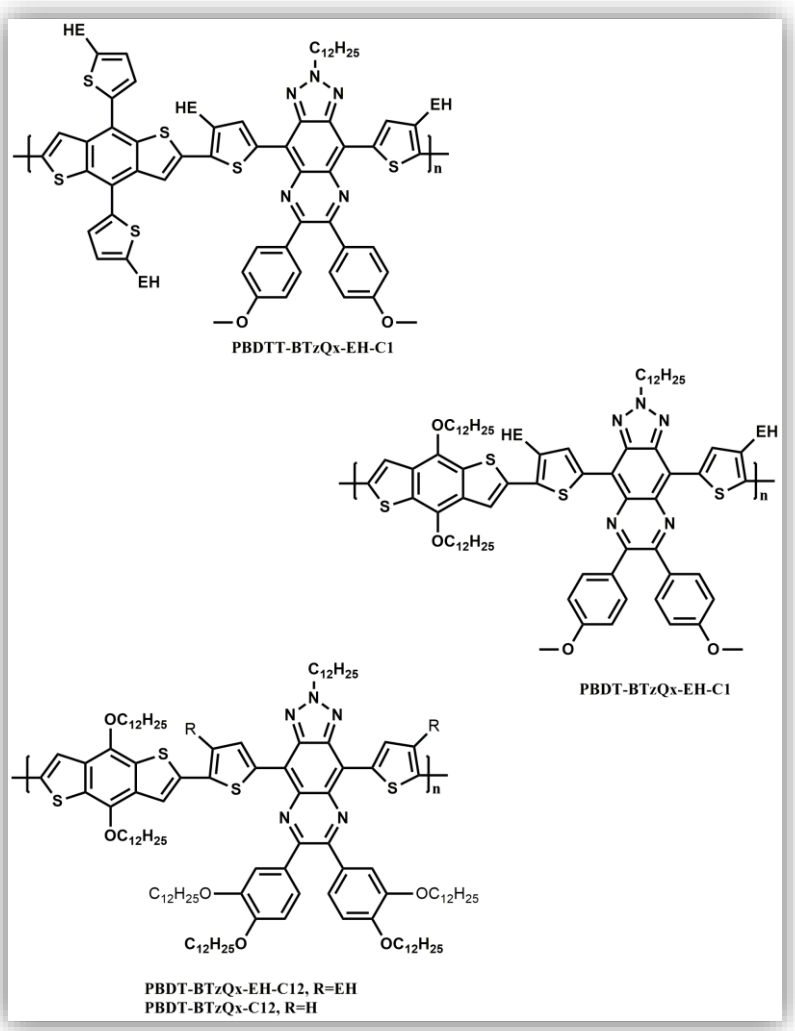

Figure 1. 28. Structures of triazoloquinoxaline and benzodithiophene based polymers [60].

Table 1. 4. Electrochemical and optical results for triazoloquinoxaline based polymers.

	HOMO (eV)	LUMO (eV)	λ_{max}	E_g	PCE (%)
PBDTT-BTzQx-EH-C1	-5.26	-3.78	697	1.48	0.57
PBDT-BTzQx-EH-C1	-5.00	-3.56	704	1.44	1.40
PBDT-BTzQx-EH-C12	-5.30	-3.81	694	1.49	0.28
PBDT-BTzQx-C12	-5.11	-3.73	781	1.38	-

CHAPTER 2

EXPERIMENTAL

2.1. Materials and Methods

All chemicals and reagents were obtained from commercial sources and used without further purification. Tetrahydrofuran (THF) was dried via sodium and benzophenone. Column chromatography was performed for the purification of monomers. TLC was utilized to monitor the reaction. Structures of polymers were determined by NMR. ^{1}H and ^{13}C NMR spectra were recorded on a Bruker Spectrospin Avance DPX-400 Spectrometer with TMS as the internal reference and all shifts were given in ppm. High-resolution mass spectrometer (HRMS) studies were done with a Waters SYNAPT MS system to verify molecular weight of monomers. Molecular weights of the polymers were measured by gel permeation chromatography (GPC) on Polymer Laboratories GPC 220 with polystyrene as the standard and THF as the solvent and molecular weights were reported as g. mol^{-1}. Electrochemical studies were performed in a threeelectrode cell consisting of an indium tin oxide (ITO)-doped glass slide as the working electrode, platinum wire as the counter electrode, and Ag wire as the pseudoreference electrode using a Gamry Reference 600 potentiostat/galvanostat. The reference electrode was subsequently calibrated to Fc/Fc^{+} (0.30 V), and the band energies were calculated relative to the vacuum level taking the value of SHE as 4.75 eV versus vacuum. Cary 5000 UV–vis spectrophotometer was used in order to perform the spectroelectrochemical studies of polymers.

2.1.1. Organic Solar Cell Device Fabrication and Characterization

Performances of PSCs based on PBTP1 and PBTP2 were investigated with the device structure of ITO/PEDOT:PSS/Polymer:$PC_{71}BM$ /LiF/Al. Indium tin oxide (ITO) coated glass substrates were cleaned in ultrasonic bath for 15 min in toluene, detergent, water, and isopropyl alcohol and dried with nitrogen gun. Oxygen plasma cleaning was carried out for 5 min. After that, a thin layer of poly(ethylenedioxythiophene):polystyrenesulfonate (PEDOT:PSS) was spin-coated (40 nm) onto the ITO substrates. Right after baking 135 ^{o}C for 15 min in air, the substrates were transferred to N2filled glovebox. The PBTP1 - $PC_{71}BM$ blends were prepared in chlorobenzene (CB) and the PBTP2 - $PC_{71}BM$ blends were prepared in 1,2-dichlorobenzene (DCB) at several weight ratios. The total concentration of solutions were fixed to 20mg/mL. Blends were filtered through a PTFE filter (0.2 μm). Lithium fluoride (LiF) (0.6 nm) and aluminum (Al) (100 nm) were thermally evaporated on top of the active layer with average deposition rate of 0.08 Å /s and 1 Å/s, respectively. Area of the device was determined as 0.06 cm^2. The current density voltage (J-V) characteristics were measured usingKeithley 2400 source meter under AM 1.5 G illumination. Incident-photon-to-current efficiency (IPCE) of solar cellswas determined using an Oriel Quantum Efficiency MeasurementKit. A calibrated silicon diode was used as the reference.

2.2. Synthetic procedures

2.2.1. Synthesis of 2-dodecylbenzotriazole

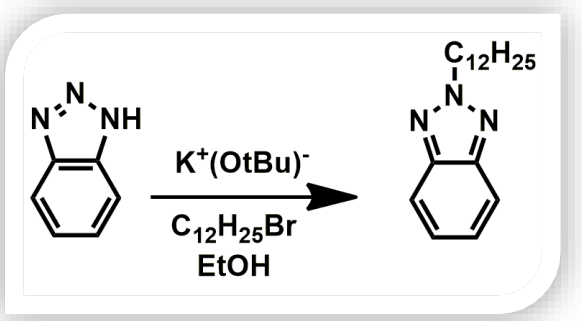

Figure 2. 1. Synthesis of 2-dodecylbenzotriazole

2-Dodecylbenzotriazole was synthesized via modified procedure of a reported procedure [53]. Starting materials 1,2,3-benzotriazole (5.0 g, 42.0 mmol), potassium tert-butoxide (5.0 g, 44 mmol) and bromododecane (12.2 g, 49.0 mmol) were refluxed for 12 hoursin 50 mL ethanol. After alkylation reaction was completed, the mixture wascooled to room temperature and the solvent was evaporated. The remaining residue was dissolved in $CHCl_3$ and the mixture was washed with brine. After drying over $MgSO_4$, the solvent was evaporated under reduced pressure. Finally the compound was purified by columnchromotographywith mixture of hexane/DCM (1:2) as the eluent. The final product was a colorless oil (3.7 g, 31%)
^{1}H NMR (400 MHz, $CDCl_3$, δ): 7.74 (m, 2H), 7.28 (m, 2H), 4.59 (t,J=6.9 Hz 2H), 2.12 (m, 2H), 1.25-1.18 (m, 18H), 0.8 (t, J=6.0 Hz, 3H)^{13}C NMR (100 MHz, $CDCl_3$, δ): 144.2, 126.0, 117.9, 53.5, 31.6, 31.5, 30.0, 29.5, 29.4, 29.3, 29.3, 29.0, 26.5, 22.6, 14.0

2.2.2. Synthesis of 4,7-dibromo-2-dodecylbenzotriazole

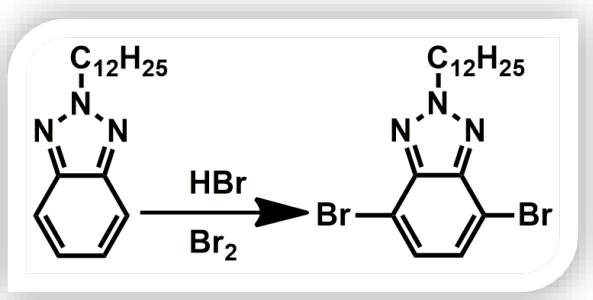

Figure 2. 2. Synthesis of 4,7-dibromo-2-dodecylbenzotriazole

4,7-Dibromo-2-dodecylbenzotriazolewas synthesized via the modified procedure of a reported method [53]. Firstly, 2-dodecylbenzotriazole (3.6 g, 13.0mmol) and an HBr solution (5.8 M, 15 ml) was stirred at 100^{o}C for 1 h. After 1 hour, bromine (5.7 g, 36 mmol) was added to the mixture and stirred for 12 h at 135^{o}C. Then, mixture was cooled to room temperature followed by addition of $CHCl_3$ and $NaHCO_3$. The organic layer was collected, dried (with $MgSO_4$) and the solvent was evaporated. For purification column chromatography was performed with $CHCl_3$: hexane (1:1) as the eluent. The final product was a light yellow solid (4.0 g, 73%).

^{1}H NMR (400MHz, $CDCl_3$, δ): 7.32 (s, 2H), 4.58 (t, J=6.5 Hz, 2H), 2.10 (m, 2H), 1.38-1.12 (m, 18H), 0.85 (t, J=6.7 Hz, 3H). ^{13}C NMR (100 MHz, $CDCl_3$, δ): 142.7, 128.4, 108.9, 56.4, 30.8, 29.1, 28.5, 28.4, 28.3, 27.9, 25.4, 25.3, 21.6, 13.0

2.2.3. Synthesis of 4,7-dibromo-2-dodecyl-5,6-dinitro-2H-benzo[d][1,2,3]triazole (4):

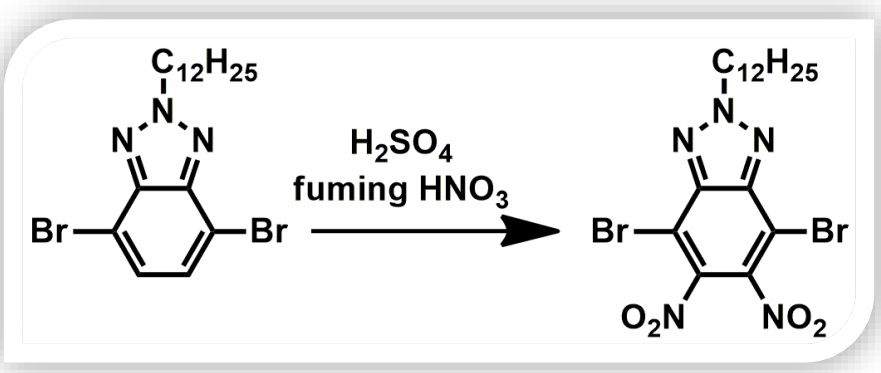

Figure 2. 3. Synthesis of 4,7-dibromo-2-dodecyl-5,6-dinitro-2H-benzo[d][1,2,3]triazole

A mixture of concentrated sulfuric acid (15 ml) and fuming nitric acid (15 ml) was used for the nitration of 4,7-dibromo-2-dodecyl-2H-benzo[d][1,2,3]triazole (3). The acid mixture was cooled to 0 ^{o}C and compound **3** (1.50 g, 3.37 mmol) was added to the mixture in small portions to keep the temperature below 5 ^{o}C. After addition completed, reaction mixture was stirred at room temperature for 3 hours and then the mixture was poured into ice-bath. The precipitate was collected by filtration and recyrstallized with acetone-water mixture yield 1.0 g4,7-dibromo-2-dodecyl-5,6-dinitro-2H-benzo[d][1,2,3]triazole as a yellow solid (56 % yield).

^{1}H NMR (400 MHz, $CDCl_3$) δ 4.93 (m, 2H), 2.31 (m, 2H), 1.55 – 1.02 (m, 18H), 0.88 (t, *J* = 6.8 Hz, 3H).^{13}C NMR (101 MHz, $CDCl_3$) d 141.7, 140.5, 105.7, 33.2, 30.4, 28.5, 28.2, 28.1, 27.9, 27.8, 27.7, 27.3, 24.9, 21.2, 12.6.

2.2.4. Synthesis of 2-dodecyl-5,6-dinitro-4,7-di(thiophen-2-yl)-2H-benzo[d][1,2,3]triazole(5):

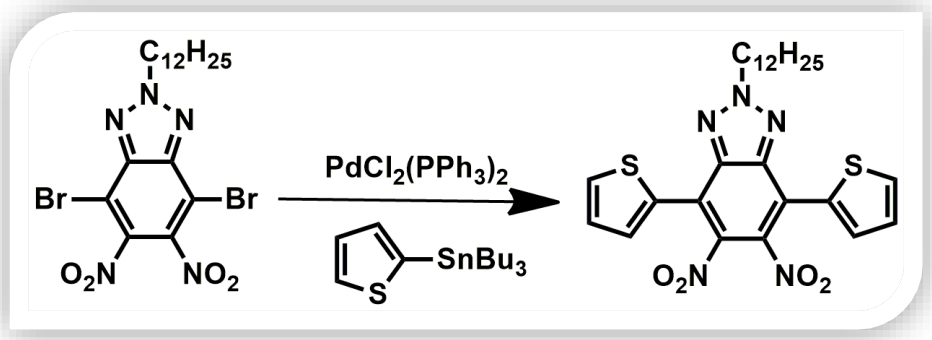

Figure 2. 4. Synthesis of 2-dodecyl-5,6-dinitro-4,7-di(thiophen-2-yl)-2H-benzo[d][1,2,3]triazole

4,7-Dibromo-2-dodecyl-5,6-dinitro-2H-benzo[d][1,2,3]triazole (4) (1.5 g, 2.80 mmol) and tributyl(thiophen-2-yl)stannane (5.22 g, 14.0 mmol) were dissolved in dry THF (60 mL). $PdCl_2(PPh_3)_2$ was added after 1 hour reflux and the mixture was stirred at 100 ^oC under argon atmosphere for 18 h. After stirring overnight the residue was subjected to column chromatography (silica gel, $CHCl_3$: hexane, 1:2) to afford compound **5**(660 mg, 1.22 mmol, 45 %).Then, 2-dodecyl-5,6-dinitro-4,7-di(thiophen-2-yl)-2H-benzo[d][1,2,3]triazole (217 mg, 0.406 mmol), iron dust (272 mg) and acetic acid (18 mL) were refluxed under ambient conditions for 4 hours to synthesize 2-dodecyl-4,7-di(thiophen-2-yl)-2H-benzo[d][1,2,3]triazole-5,6-diamine. After reaction was completed the crude product was achieved via extraction of NaOH solution and ether. Due to instability of the diamine unit the product could not be characterized with NMR technique and 2-dodecyl-4,7-di(thiophen-2-yl)-2H-benzo[d][1,2,3]triazole-5,6-diamine was used for condensation reactions as soon as possible.

^{1}H NMR (400 MHz, $CDCl_3$) δ 7.67 (dd, *J* = 5.1, 1.1 Hz, 2H), 7.54 (dd, *J* = 3.7 Hz, 2H), 7.21 (dd, *J* = 5.0 Hz, 2H), 4.81 (m, 2H), 1.62 (m, 2H), 1.38 – 1.29 (m, 18H), 0.94 (t, 3H).^{13}C NMR (101 MHz, $CDCl_3$) δ 141.9 , 140.1, 130.4 , 130.4 , 130.1 , 127.9 , 119.8, 32.1, 30.0, 29.6, 29.4, 29.3, 29.0, 28.3, 26.7, 26.5, 22.7 , 17.3 , 13.5.

2.2.5. Synthesis of 2-dodecyl-6,7-diphenyl-4,9-di(thiophen-2-yl)-2H-[1,2,3]triazolo[4,5-g]quinoxaline (M1):

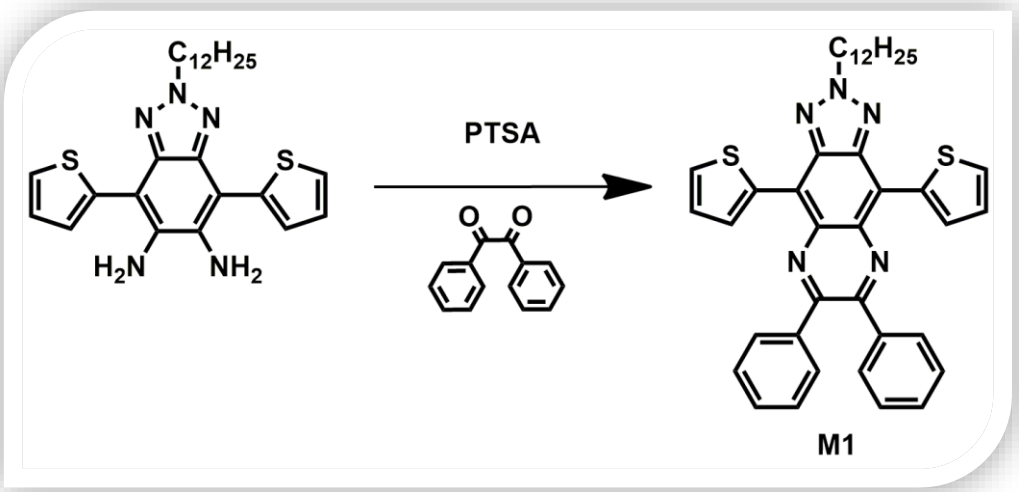

Figure 2. 5. Synthesis of 2-dodecyl-6,7-diphenyl-4,9-di(thiophen-2-yl)-2H-[1,2,3]triazolo[4,5-g]quinoxaline

Iron dust (350 mg) in acetic acid (25 ml) was used for the reduction of 2-dodecyl-5,6-dinitro-4,7-di(thiophen-2-yl)-2H-benzo[d][1,2,3]triazole (240 mg, 0.44 mmol) at 50˚C for 4 hours. At the end of the reaction, the mixture were poured into cold NaOH solution and then extracted with ether. 2-Dodecyl-4,7-di(thiophen-2-yl)-2H-benzo[d][1,2,3]triazole-5,6-diamine (6) was used without any purification. Then condensation reaction was performed to get the desired monomer. A solution of compound 6 (200 mg,0.420 mmol) and benzil (230 mg, 1.09 mmol) in EtOH (40 ml)

was refluxed overnight with a catalytic amount of p-toluene sulfonic acid (PTSA). The residue was subjected to column chromatography (silica gel, $CHCl_3$: hexane, 1:1) to purify a purple oily product (110 mg, 0.170 mmol, 40 %).

^{1}H NMR (400 MHz, $CDCl_3$) δ 8.92 (dd, *J* = 3.9 Hz, 2H), 7.76 – 7.70 (m, 4H), 7.56 (dd, *J* = 5.2, 1.0 Hz, 2H), 7.37 – 7.32 (m, 6H), 7.23 (dd, *J* = 5.1 Hz, 2H), 4.91 (m, *J* = 7.3 Hz, 2H), 1.48 – 1.45 (m, 2H), 1.21 – 1.16 (m, *J* = 2.9 Hz, 18H), 0.80 – 0.78 (m, *J* = 6.9 Hz, 3H).^{13}C NMR (101 MHz, $CDCl_3$) d 151.7, 142.9, 138.8, 136.2, 134.8, 133.0, 131.7, 130.7, 129.9, 129.0, 128.1, 126.5, 57.9, 47.1, 32.0, 30.1, 30.0, 29.6, 29.5, 29.4, 29.4, 29.1, 26.7, 22.8. HRMS (EI) for $C_{40}H_{41}N_5S_2$ calculated656.2882, found 656.2880.

2.2.6. Synthesis of 2-dodecyl-4,6,7,9-tetra(thiophen-2-yl)-2H-[1,2,3]triazolo[4,5-g]quinoxaline (M2):

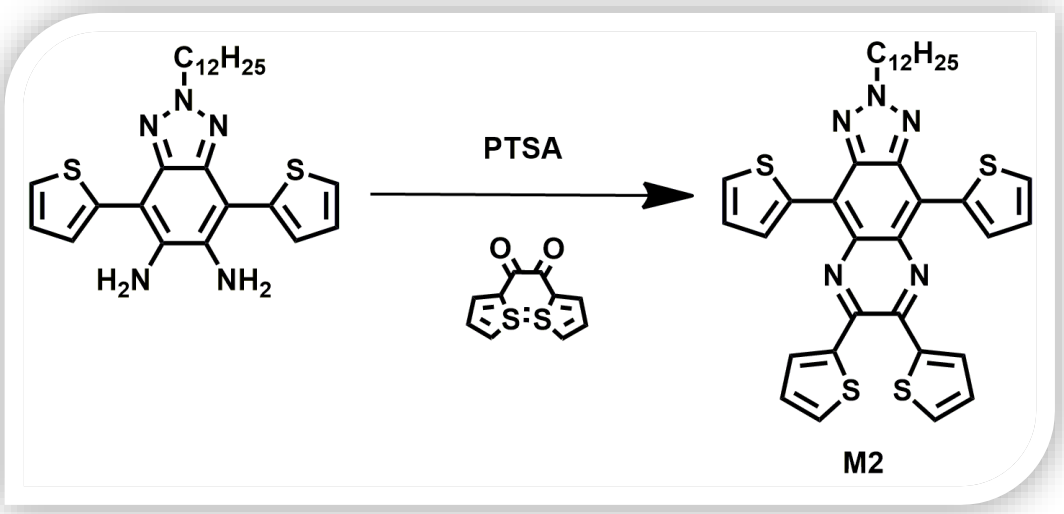

Figure 2. 6. Synthesis of 2-dodecyl-4,6,7,9-tetra(thiophen-2-yl)-2H-[1,2,3]triazolo[4,5-g]quinoxaline

2-Dodecyl-4,7-di(thiophen-2-yl)-2H-benzo[d][1,2,3]triazole-5,6-diamine was synthesized according to previously described procedure. A solution of compound

6(250 mg, 0.520 mmol) and 1,2-di(thiophen-2-yl)ethane-1,2-dione (115 mg, 0.52 mmol) in EtOH (40 ml) was refluxed overnight with a catalytic amount of p-toluene sulfonic acid (PTSA). The residue was subjected to column chromatography (silica gel, $CHCl_3$: hexane, 1:1) to purify a bluish purple solid in 26 % yield (90 mg, 0.13 mmol).

^{1}H NMR (400 MHz, $CDCl_3$) δ 8.81 (dd, *J* = 3.8 Hz, 2H), 7.56 (dt, *J* = 9.6 Hz, 2H), 7.50 (dd, *J* = 5.0 Hz, 2H), 7.41 (dd, *J* = 3.7 Hz, 2H), 7.19 (dt, *J* = 7.1 Hz, 2H), 6.98 (dd, *J* = 5.0 Hz, 2H), 4.83 (t, *J* = 7.3 Hz, 2H), 2.24 – 2.16 (m, 2H), 1.23 – 1.07 (m, 18H), 0.80 (t, *J* = 4.7 Hz, 3H). ^{13}C NMR (101 MHz, $CDCl_3$) δ 144.1, 141.7, 140.7, 134.7, 131.9, 130.7, 129.7, 129.5, 128.8, 126.3, 125.6, 118.3, 30.9, 29.0, 28.9, 28.6, 28.5, 28.4, 28.3, 28.0, 26.0, 24.3, 21.9, 13.5.

.

HRMS (EI) for $C_{36}H_{37}N_5S_4$ calculated 668.2010, found 668.1979.

2.2.7. Synthesis of 6,7-bis(4-tert-butylphenyl)-2-dodecyl-4,9-di(thiophen-2-yl)-2H-[1,2,3]triazolo[4,5-g]quinoxaline (M3):

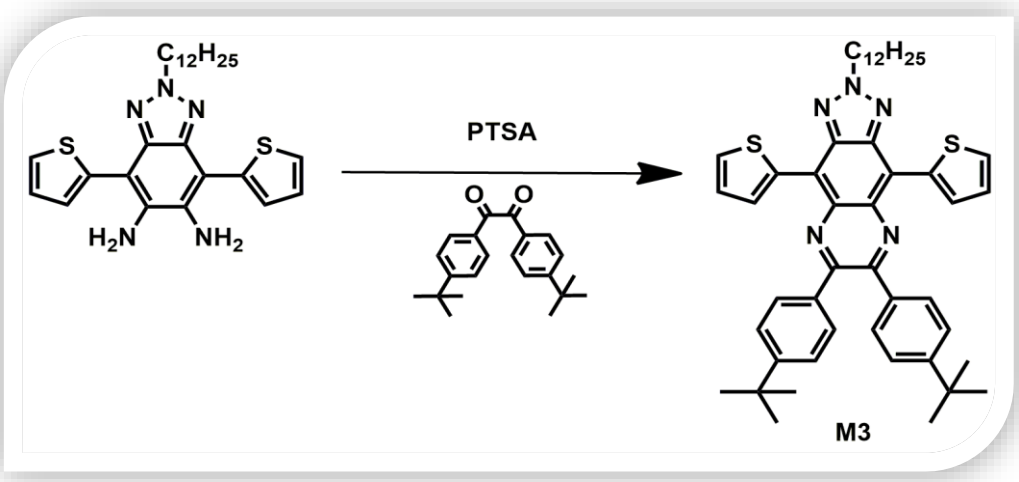

Figure 2. 7. Synthesis of 6,7-bis(4-tert-butylphenyl)-2-dodecyl-4,9-di(thiophen-2-yl)-2H-[1,2,3]triazolo[4,5-g]quinoxaline

2-Dodecyl-4,7-di(thiophen-2-yl)-2H-benzo[d][1,2,3]triazole-5,6-diamine was synthesized according to previously described procedure. A solution of compound 6 (250 mg,0.52 mmol) and 1,2-bis(4-tert-butylphenyl)ethane-1,2-dione (170 mg, 0.520 mmol) in EtOH (40 ml) was refluxed overnight with a catalytic amount of p-toluene sulfonic acid (PTSA). The residue was subjected to column chromatography (silica gel, $CHCl_3$: hexane, 1:2) to purify a puple oily product in 20 % yield (80 mg, 0.10 mmol).

^{1}H NMR (400 MHz, $CDCl_3$) δ 8.90 (dd, *J* = 3.9 Hz, 2H), 7.71 (d, *J* = 8.4 Hz, 4H), 7.57 (dd, *J* = 5.1 Hz, 2H), 7.35 (d, *J* = 8.5 Hz, 4H), 7.23 (dd, *J* = 5.1 Hz, 2H), 4.90 (t, *J* = 7.3 Hz, 2H), 2.25 – 2.19 (m, 2H), 1.36 – 1.24 (m, 36H), 0.78 (t, 3H).

^{13}CNMR (101 MHz, $CDCl_3$) d 152.3, 151.8, 142.3, 135.9, 135.7, 131.5, 130.5, 130.4, 126.5, 125.0, 124.0, 122.6, 34.8, 33.7, 33.5, 33.4, 31.9, 31.3, 30.1, 29.6, 29.5, 29.4, 29.3, 29.0, 27.0, 26.7, 26.6, 26.5.HRMS (EI) for $C_{48}H_{57}N_5S_2$ calculated 768.4134, found 768.4134.

2.2.9. Synthesis of 2-dodecyl-4,7-di(thiophen-2-yl)-2H-benzo[d][1,2,3]triazole

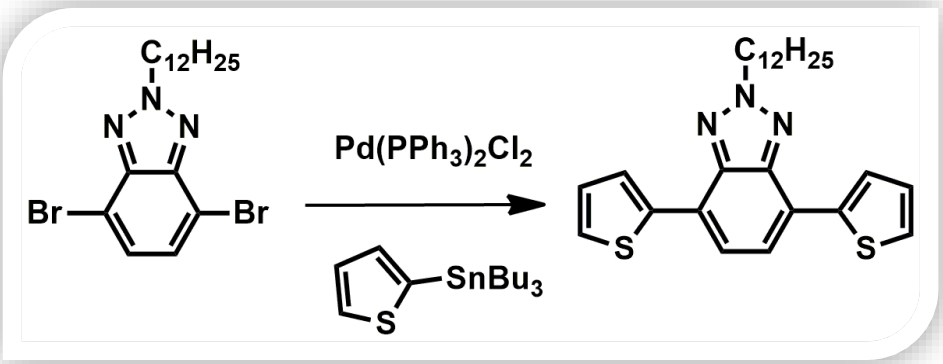

Figure 2. 8. Synthesis of 2-dodecyl-4,7-di(thiophen-2-yl)-2H-benzo[d][1,2,3]triazole

Stille coupling reaction was used for the synthesis of 2-dodecyl-4,7-di(thiophen-2-yl)-2H-benzo[d][1,2,3]triazole. Initially statrting materials 4,7-Dibromo-2-dodecylbenzotriazole (100 mg, 0.22 mmol), and tributyl(thiophen-2-yl) stannane

were dissolved in anhydrous THF (80 ml) and the mixture was refluxed for 1 hour. Then, dichlorobis (triphenylphosphine)-palladium(II) (50 mg, 0.045 mmol)was added to the reaction medium. The resulting mixture was refluxed for 12 hours under argon atmosphere. After coupling reaction was completed, solvent was evaporated under vacuum and the product was purified by column chromatography(silica gel, $CHCl_3$: hexane, 1:1). Final product was obtained as a yellow solid (70 mg,71%)
^{1}H NMR (400MHz, $CDCl_3$, δ): 8.1 (dd, *J*=1.1, 4.7 Hz, 2H), 7.63 (s, 2H), 7.38 (dd, *J*=1.0, 6.2 Hz, 2H), 7.19 (dd, *JA*=8.7 Hz, *JB* = 3.8, 2H), 4.80 (t, *J*=7.2 Hz, 2H), 2.20 (m, 2H), 1.38-1.2 (m, 18H), 0.87 (t, *J*=6.9 Hz, 3H); ^{13}C NMR (100 MHz, $CDCl_3$, δ): 142.1, 140.0, 128.1, 127.0, 125.5, 123.6, 122.7, 56.8, 32.2, 30.3, 29.9, 29.8, 29.7, 29.6, 29.5, 29.3, 26.9, 22.9, 14.4.

2.2.10. Synthesis of 4,7-bis(5-bromothiophen-2-yl)-2-dodecyl-2Hbenzo[d][1,2,3]triazole

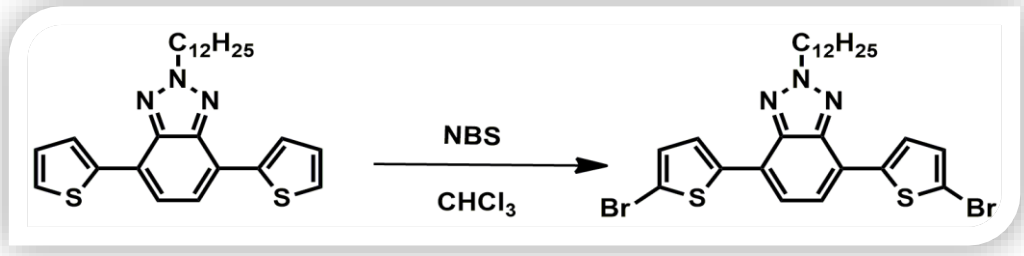

Figure 2. 9. Synthesis of 4,7-bis(5-bromothiophen-2-yl)-2-dodecyl-2Hbenzo[d][1,2,3]triazole

For the bromination of TBT mild bromination conditions were applied. Firstly, TBT (200 mg,0.45 mmol) was dissolved in 100 mL of $CHCl_3$ at room temperature and then N-bromosuccinimide (190 mg,1.06 mmol) were added slowly to the mixture in inthe dark. The reaction was stirred at room temprature for 12 h and the solvent was removed under reducedpressure. After filtration over silica (eluent:$CHCl_3$) brominated product was obtained as a white solid (92 %)

^{1}H NMR (400 MHz, $CDCl_3$, d): 7.72 (d, J = 4.0 Hz, 2H), 7.43 (s, 2H), 7.05 (d, J = 4.0 Hz, 2H), 4.72 (t, J = 7.0 Hz, 2H), 2.10 (m, 2H), 1.3–1.15 (m, 18H), 0.80 (t, J = 6.6 Hz, 3H)^{13}C NMR (100 MHz, DMSO-d6, d): 144.2, 139.8, 126.9, 122.2, 118.1, 115.2, 113.2, 56.1, 43.0, 30.0, 29.9, 29.8, 29.7, 29.6, 29.5, 29.3, 26.9, 22.6,13.1.

2.2.11. Synthesis of Poly4-(5-(2-dodecyl-7-methyl-2H-benzo[d][1,2,3]triazol-4-yl)thiophen-2-yl)-N-(4-(5-methylthiophen-2-yl)phenyl)-N-phenylaniline (PTPB1):

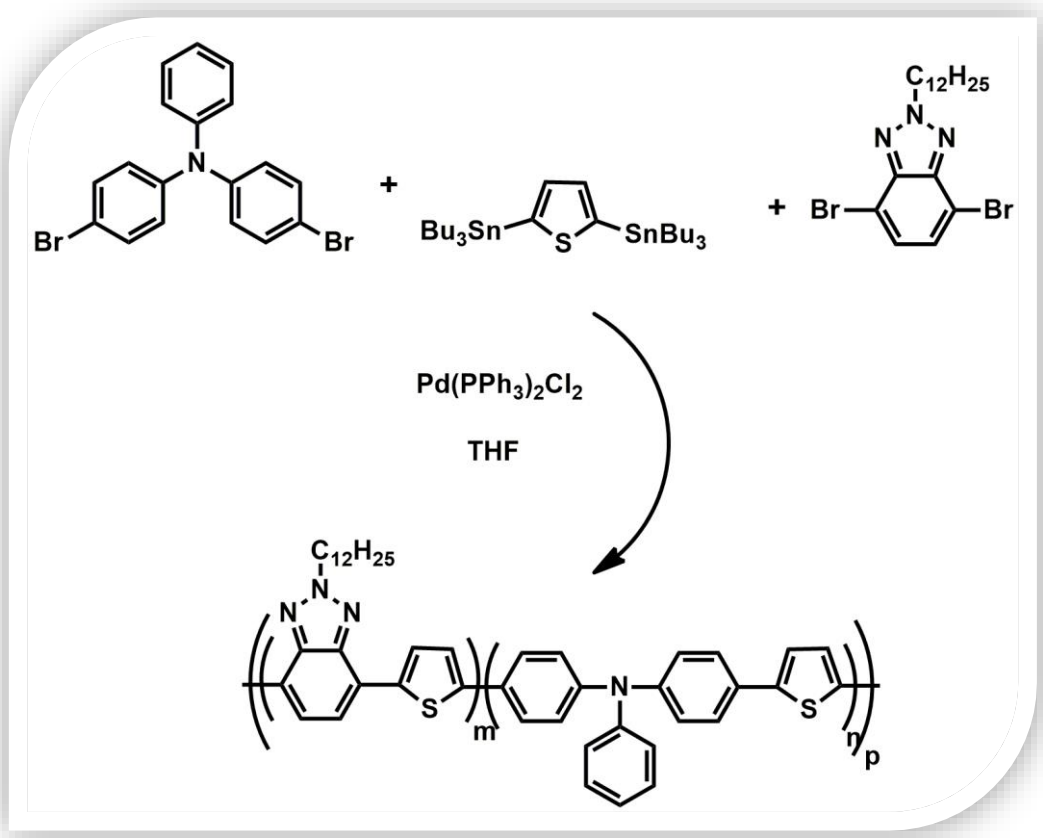

Figure 2. 10. Synthesis of poly4-(5-(2-dodecyl-7-methyl-2H-benzo[d][1,2,3]triazol-4-yl)thiophen-2-yl)-N-(4-(5-methylthiophen-2-yl)phenyl)-N-phenylaniline (PTPB1)

4,7-Dibromo-2-dodecyl-2H-benzo[d][1,2,3]triazole (150 mg, 0.34 mmol), 4-bromo-N-(4-bromophenyl)-N-phenylaniline (135 mg, 0.34 mmol) and 2,5-bis(tributylstannyl)thiophene (448 mg, 0.68 mmol)were dissolved in anhydrous THF. The mixture was heated under reflux and purged with nitrogen for 60 min. Then dichlorobis(triphenylphosphine)-palladium(II) (10% by mol) was added to the reaction mixture. Bromobenzene and after eight hours tributyl(thiophen-2-yl)

stannane were added to the reaction mixture as the end capper after the mixture was heated for 3 days. Then the mixture was poured into 200 mL cold methanol. Collected precipitates were washed with methanol, acetone and hexane via soxhlet extraction several times. FinallyPTPB1was collected as a red solid with 28% yield.
GPC: Number-average molecular weight (M_n) =14600,weight-average molecularweight (M_w) =24400, polydispersity index (PDI) = 1.7

^{1}H NMR (400 MHz, $CDCl_3$), δ (ppm):8.2 (benzotriazole), 7.7 (triphenylamine), 7.2 (thiophene) 7.1 (thiophene), 4.8 (N-CH_2), 2.1 (CH_2), 1.6–0.8 (pendant alkyl chain).

2.2.12. Synthesis of Poly4'-(2-dodecyl-7-methyl-2H-benzo[d][1,2,3]triazol-4-yl)-N-(4'-methyl-[1,1'-biphenyl]-4-yl)-N-phenyl-[1,1'-biphenyl]-4-amine (PTPB2):

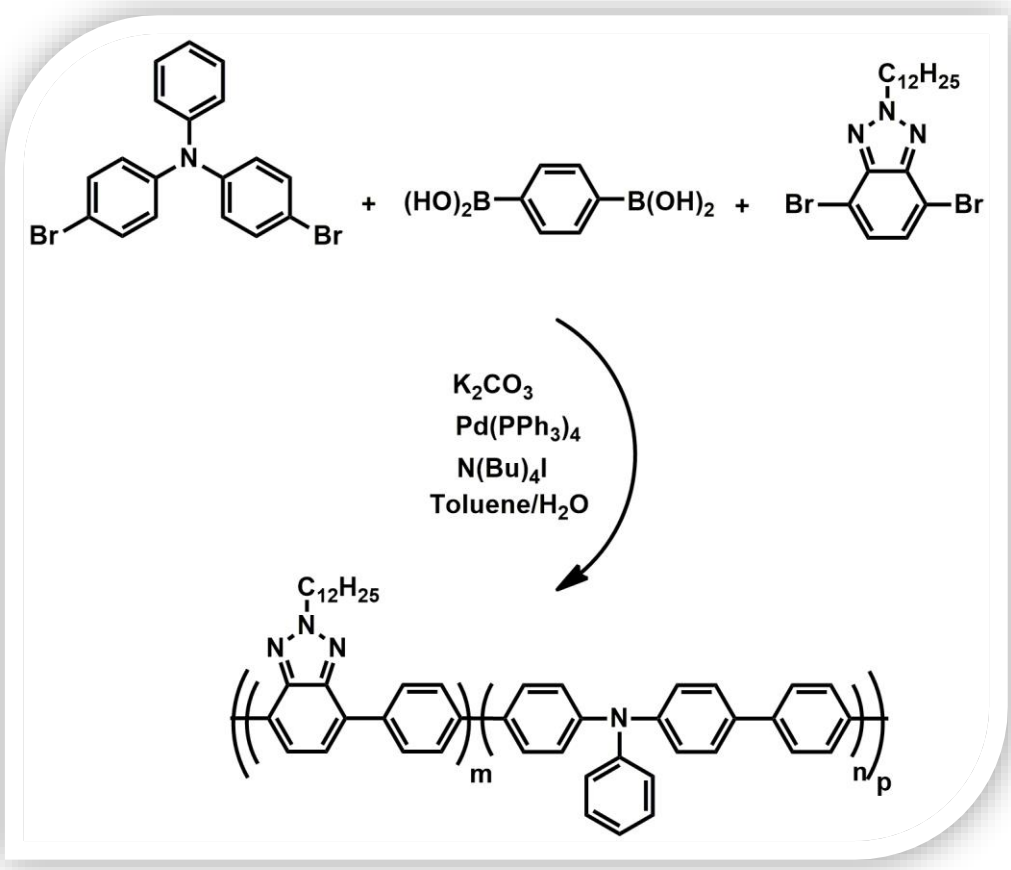

Figure 2. 11. Synthesis of poly4'-(2-dodecyl-7-methyl-2H-benzo[d][1,2,3]triazol-4-yl)-N-(4'-methyl-[1,1'-biphenyl]-4-yl)-N-phenyl-[1,1'-biphenyl]-4-amine

4,7-Dibromo-2-dodecyl-2H-benzo[d][1,2,3]triazole (200 mg, 0.45 mmol), 4-bromo-N-(4-bromophenyl)-N-phenylaniline (180 mg, 0.45 mmol) and 1,4-phenylenediboronic acid (150 mg, 0.90 mmol), were refluxed under an argon atmosphere for 60 min in the presence of potassium carbonate (K_2CO_3, 2 M in H_2O) and toluene (3: 2toluene: water). Then $Pd(PPh_3)_4$ (5 mol%), and tetrabutylammonium iodide ($N(Bu)_4I$, 1 mol%) were added to the mixture and refluxed for 3 days. After the solvent was removed and extracted with $CHCl_3$, the mixture was poured into 200

mL cold methanol. Precipitate was washed with methanol, acetone and hexane several times. Finally PTPB2 was obtained as a yellow solidwith 15% yield.

GPC: Number-average molecular weight (M_n) = 3400, weight-average molecular weight (M_w) = 8200, polydispersity index (PDI) = 2.4

^{1}H NMR (400 MHz, $CDCl_3$), δ (ppm):7.5 (benzotriazole), 7.3 (triphenylamine), 7.2 (benzene) 7.1 (thiophene), 4.3 (N-CH_2), 2.2 (CH_2), 1.6–0.8 (pendant alkyl chain).

2.2.13. Synthesis of Poly4-(5'-(2-dodecyl-7-(5-methylthiophen-2-yl)-2H-benzo[d][1,2,3]triazol-4-yl)-[2,2'-bithiophen]-5-yl)-N-(4-(5-methylthiophen-2-yl)phenyl)-N-phenylaniline (PTPB3):

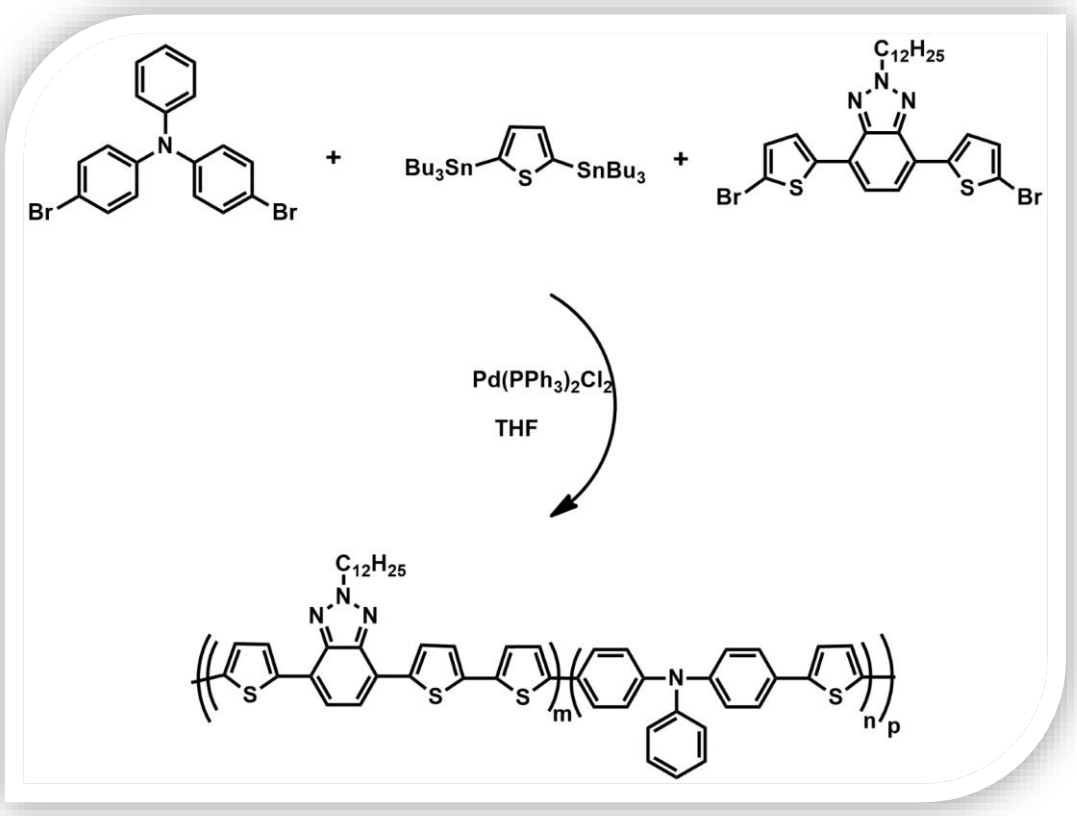

Figure 2. 12. Synthesis of poly4-(5'-(2-dodecyl-7-(5-methylthiophen-2-yl)-2H-benzo[d][1,2,3]triazol-4-yl)-[2,2'-bithiophen]-5-yl)-N-(4-(5-methylthiophen-2-yl)phenyl)-N-phenylaniline (PTPB3)

The same procedure for PTPB1 was applied for the synthesis of PTPB3, using 4-bromo-N-(4-bromophenyl)-N-phenylaniline (118 mg, 0.297 mmol), 4,7-bis(5-bromothiophen-2-yl)-2-dodecyl-2H-benzo[d][1,2,3]triazole (180 mg, 0.297 mmol) and 2,5-bis(tributylstannyl)thiophene (395 mg, 0.59 mmol). After similar purification, desired polymer PTPB3 was obtained as an orange solid with 24% yield.

GPC: Number-average molecular weight (M_n) = 12000, weight-average molecular weight (M_w) = 16500, polydispersity index (PDI) = 1.4,

^{1}H NMR (400 MHz, $CDCl_3$), δ (ppm):8.1 (benzotriazole), 7.6 (triphenylamine), 7.4 (thiophene) 7.1 (thiophene), 4.2 (N-CH_2), 2.1 (CH_2), 1.5–0.8 (pendant alkyl chain).

2.2.14. Synthesis of Poly4-(5-(2-dodecyl-7-methyl-2H-benzo[d][1,2,3]triazol-4-yl)thiophen-2-yl)-N-(4-(5-methylthiophen-2-yl)phenyl)-N-phenylaniline (PBTP1):

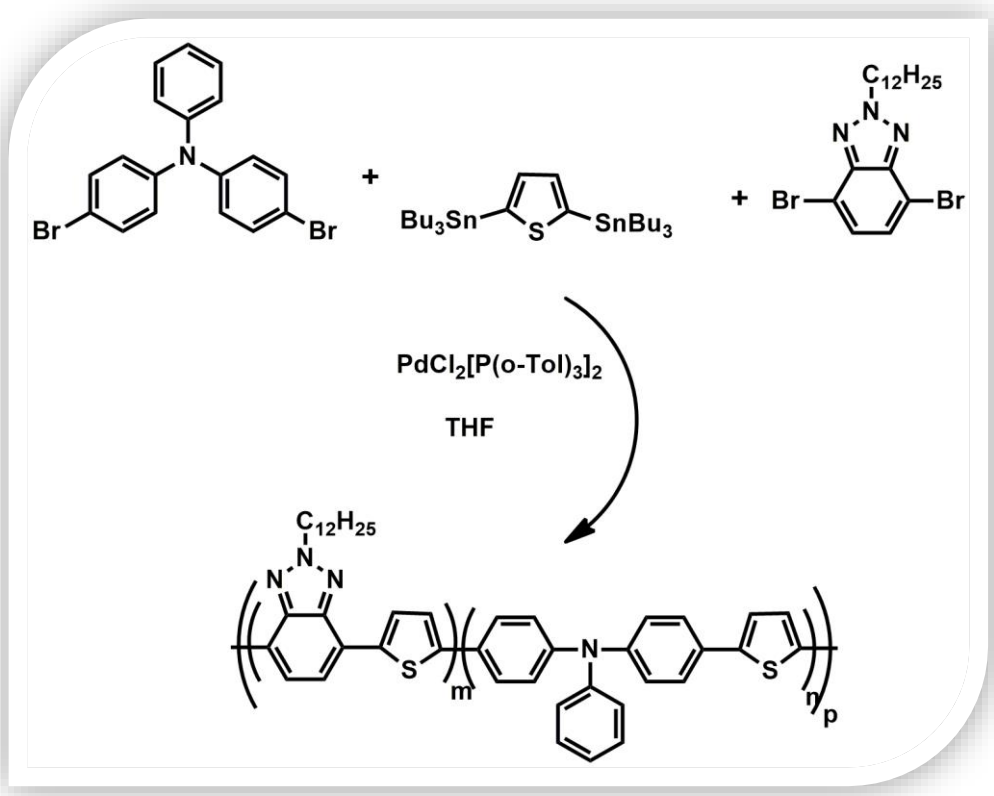

Figure 2. 13. Synthesis of poly4-(5-(2-dodecyl-7-methyl-2H-benzo[d][1,2,3]triazol-4-yl)thiophen-2-yl)-N-(4-(5-methylthiophen-2-yl)phenyl)-N-phenylaniline (PBTP1)

4,7-Dibromo-2-dodecyl-2H-benzo[d][1,2,3]triazole (198 mg, 0.445 mmol), 2,5-bis(tributylstannyl)thiophene (590 mg, 0.890 mmol) and 4,4′-dibromotriphenylamine (180 mg, 0.445 mmol) were added in a 50 mL three-neckflask and purged with argon for 2 h. After addition of THF (30 mL) and dichlorobis(tri-o-tolylphosphine)palladium(II) (5 mol %) to the solution, the mixture was heated at 90 °C for 48 h under inert atmosphere. Phenyl end-groups were used to end-capped the polymerization to remove reactive trimethyltin or bromide groups. After evaporation of solvent under reduced pressure, methanol was added to the crude product. Then, sodiumdiethyldithiocarbamate (15 mg) was added as a palladium scavanger and the solution was stirred for1.5 hours. After filtration, the crude product was washed with methanol, acetone, and hexane using Soxhlet extract to remove oligomers. The polymer was extracted with chloroform. The product was concentrated on rotary evaporator and the crude product was obtained as dark red solid. Yield: 81 %

^{1}H NMR (400MHz, $CDCl_3$): δ (ppm) 8.22, 8.09, 7.25, 4.80, 3.73, 2.17, 1.55, 1.23, 0.85

Mw: 11500, Mn: 8400, PDI: 1.37

2.2.15. Synthesis of Poly4-(5'-(2-dodecyl-7-(5-methylthiophen-2-yl)-2H-benzo[d][1,2,3]triazol-4-yl)-[2,2'-bithiophen]-5-yl)-N-(4-(5-methylthiophen-2-yl)phenyl)-N-phenylaniline (PBTP2):

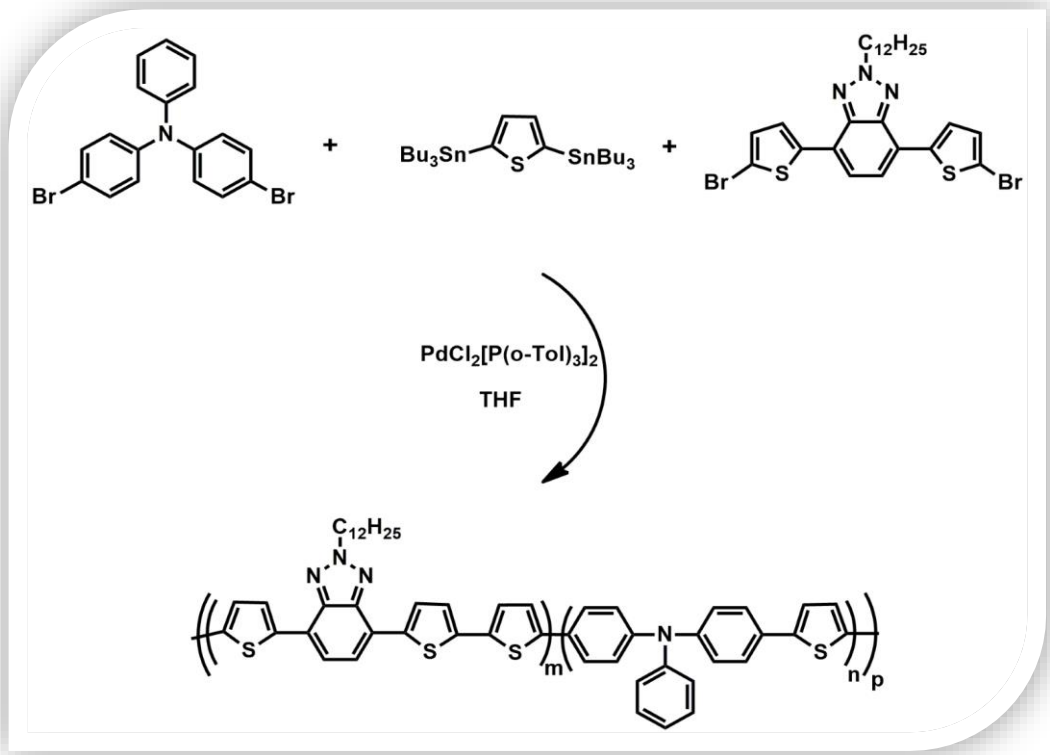

Figure 2. 14. Synthesis of poly4-(5'-(2-dodecyl-7-(5-methylthiophen-2-yl)-2H-benzo[d][1,2,3]triazol-4-yl)-[2,2'-bithiophen]-5-yl)-N-(4-(5-methylthiophen-2-yl)phenyl)-N-phenylaniline (PBTP2)

Similarly, a mixture of 4,7-bis(5-bromothiophen-2-yl)-2-dodecyl-2H-benzo[d][1,2,3]triazole (150 mg, 0.246 mmol), 2,5-bis(tributylstannyl)thiophene (326 mg, 0.492 mmol), 4,4′-dibromotriphenylamine (99.2 mg, 0.246 mmol) and dichlorobis(tri-o-tolylphosphine)palladium(II) (5 mol %) were dissolved in anhydrous THF (25 mL) and polymerized to give P2. Yield: 30 %

^{1}H NMR (400MHz, CDCl3): δ (ppm) 8.05, 7.52, 4.85, 1.55, 1.24, 0.85

Mw: 48400 , Mn: 47300 , PDI: 1.03

CHAPTER 3

RESULTS AND DISCUSSION

3.1. A promising combination of benzotriazole and quinoxaline units: A new acceptor moiety toward synthesis of multipurpose donor–acceptor type polymers

The idea having two important electron deficient units; benzotriazoleand quinoxaline in a single structure leading to theformation of black coloured polymers inspired us to conduct thisstudy. Here, we basically aim to synthesize a new acceptor unitwhich contains both benzotriazole and quinoxaline moieties. Owing to the increase in imine bonds (two vs. four) with thissingle structure, the novel molecule is expected to yield higher electrontransporting features.

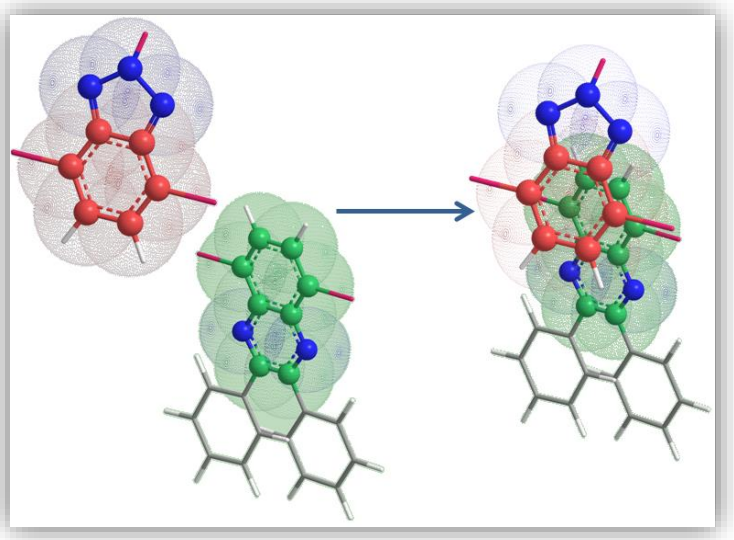

Scheme 3. 1. Schematic illustration for the combination of benzotriazole and quinoxaline units to get new and stronger acceptor unit[56].

3.1.1. Synthesis

The synthetic route to the monomers was outlined in Scheme 3.2. 4,7-Dibromo-2-dodecyl-2H-benzo[d][1,2,3]triazole (3) was synthesized firstly by alkylation of 1H-benzo[d][1,2,3]triazole and then by bromination with HBr and bromine. Nitration of the resulting brominated product gave 4,7-dibromo-2-dodecyl-5,6- dinitro-2H-benzo[d][1,2,3]triazole (4). Compound 5 was obtained by the Stille coupling reaction of compound 4 and tributyl(thiophen-2-yl) stannane. The reduction of 5 with iron dust in acetic acid yielded 2-dodecyl-4,7-di(thiophen-2-yl)-2H-benzo[d][1,2,3]triazole-5,6- diamine (6). Finally, a condensation reaction of compound 6 with three different diketones, (benzyl 7, 1,2-di(thiophen-2-yl)ethane-1,2- dione 8 and 1,2-bis(4-tert-butylphenyl)ethane-1,2-dione 9), in the presence of PTSA and ethanol gave the desired monomers (M1, M2, M3)

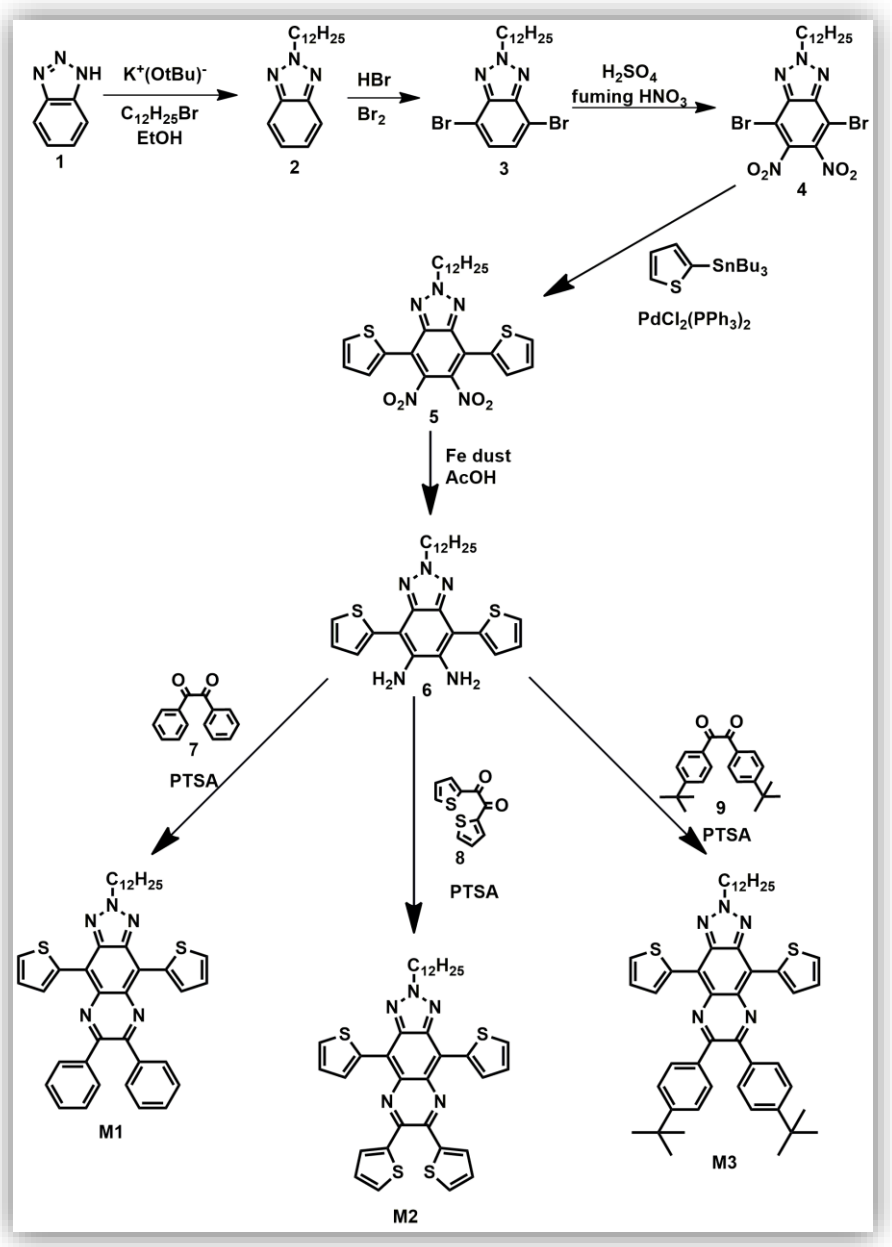

Scheme 3. 2. Synthetic route for the monomers.

3.1.2. Electrochemistry

Electrochemical polymerization of the monomers on ITO electrodeswas performed in 0.1 M $TBAPF_6$ and 0.01 M correspondingmonomer solutions in acetonitrile (ACN)–CH_2Cl_2(95 : 5, v/v) by applying potentials between 0 V and +1.0 V forM1 and M3, and 0 V and +1.2 V for M2 at a scan rate of 100 mV/s (Fig. 3.1). The

monomer oxidation potentials were around 1.0V due to the same electron rich unit, thiophene in their structures. On the other hand, the polymer oxidation potentials weredistinct from each other due to the different electron densities ofthe electrochemically synthesized polymer chains. In all electrochemicalpolymerizations, reversible redox peaks with increasingcurrent density by repeated cycling were observed.

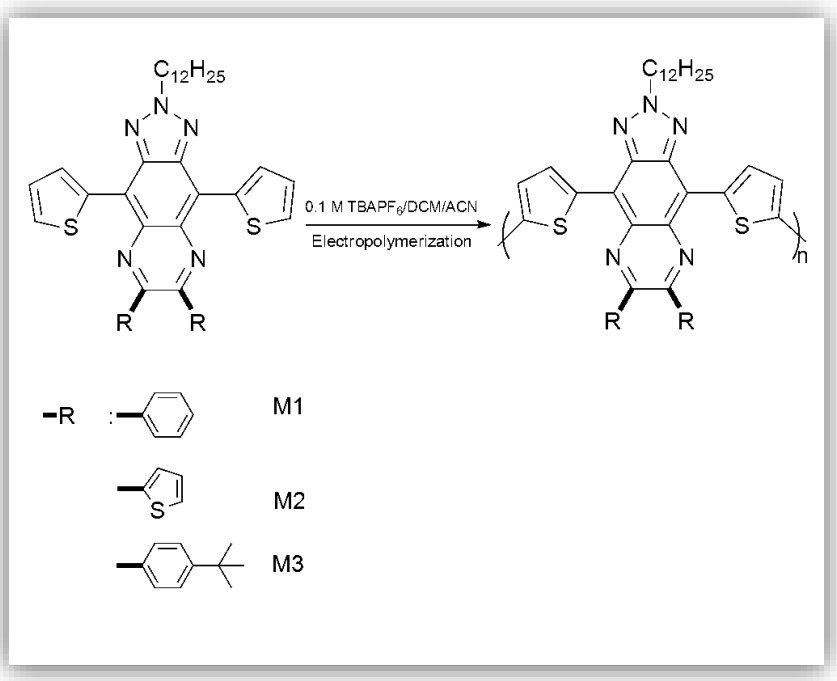

Scheme 3. 3. Electrochemical polymerization of the monomers.

Both benzotriazole and quinoxaline derivatives have strong electron accepting abilities. Hence, the combination of thesetwo strong acceptor derivatives resulted in stronger acceptorability than either benzotriazole or quinoxaline alone. In otherwords, increasing the number of imine bonds in a structure yieldsa stronger electron acceptor moiety. As a result, all polymersrevealed two reversible peaks as regards to n-doping at ambientconditions. The HOMO–LUMO energy levels of the

polymerswere estimated using the onset of the corresponding oxidationby calibrating the reference electrode against Fc/Fc^{+} andcalculating the energy levels relative to the vacuum level.

The LUMO levels differ from each other as regards to theelectron density on the quinoxaline units which leads toa decrease in the strength of the acceptor ability with increasingelectron density. Although such an assumption is valid forLUMO levels of the polymers, experimentally calculated HOMO levels from their single scan cyclic voltammograms did not revealplausible results. This may result from the unequal dopingfeatures of the polymers, especially for P3. When the chargeinjection/ejection is compared, P3 revealed the lowest charge, asseen in Fig. 3.1 This is most probably due to the presence of thetertiary butyl group on the phenyl units which obstructs theejection/injection of the dopant ions. Since all the polymers wereboth n- and p-type dopable, the electrochemical band gap Eg^{ec} andHOMO/LUMO values were calculated experimentally and allthe related electrochemistry data were summarized in Table 3.1.

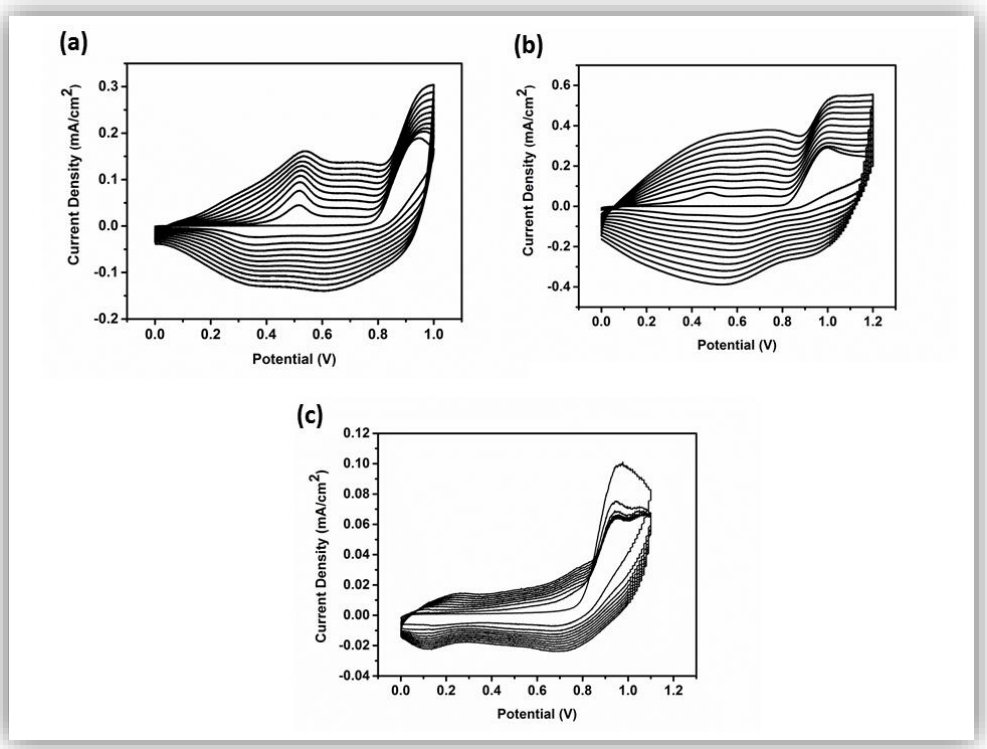

Figure 3. 1. Electrochemical polymerizations of (a) M1 (b) M2 (c) M3 at 100mVs^{1-} in 0.1M $TBAPF_6/CH_2Cl_2$/ACN on ITO electrodes.

Table 3. 1. Summary of electrochemical and spectroelectrochemical properties of P1, P2 and P3.

	E_{mon}^{ox}(V)	$E_{p\text{-}doping}$ (V)	$E_{p\text{-}dedoping}$ (V)	$E_{n\text{-}doping}$ (V)	$E_{n\text{-}dedoping}$ (V)	HOMO (eV)	LUMO (eV)	λ_{max} (nm)	E_g^{op} (eV)	E_g^{ec} (eV)
P_1	0.95	0.54	0.36	-1.38/-1.75	-0.88/-1.46	-5.00	-3.77	450/950	1.02	1.23
P_2	1.00	0.70	0.52	-1.13/-1.60	-0.60/-1.11	-5.07	-3.89	432/1020	0.98	1.18
P_3	0.94	0.78	0.70	-1.38/-1.91	-1.04/-1.54	-5.37	-3.88	400/886	0.92	1.49

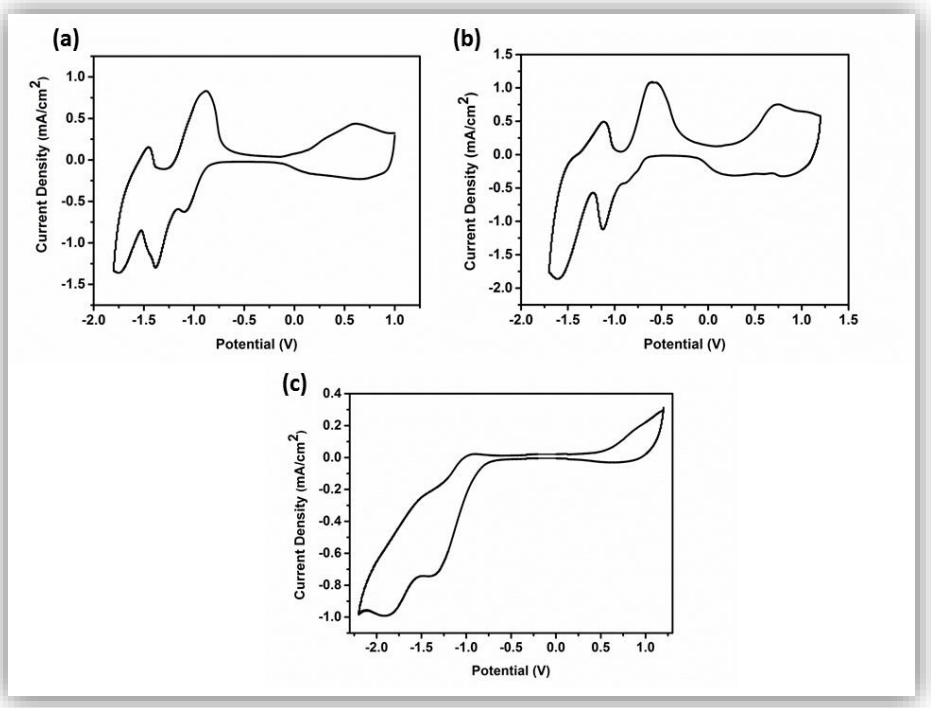

Figure 3. 2. Single scan cyclic voltammograms of P1, P2 and P3 films using ACN as the solvent and 0.1 M $TBAPF_6$ as the supporting electrolyte at a scan rate of 100 mV s^{-1} and reduction peaks.

3.1.3.Electronic and optical studies

To probe the spectral response of the polymers to the dopingprocesses, in situ UV-Vis-NIR spectra were monitored ina monomer free, 0.1 M $TBAPF_6$–ACN solution. All threepolymers revealed two absorption maxima, the first one in theshort wavelength region ranging from 300 to 450 nm is due to theπ-π* transition, whereas the second at the long wavelengthregion covering 700–1000 nm which refers to intramolecular chargetransfer transitions between the donor and the acceptor moieties(Fig.3.3). The absorption of the polymers covered both red andblue color regions of the visible spectrum, hence reflecting theevolution of the green color in their neutral state (Fig.3.3). As thepotential was increased, the short and long wavelength absorptionbands were depleted and new transitions in the NIR regionwere evolved, indicating the formation of charge carriers. Atfurther doping

stages, the formation of polarons was followed by the introduction of bipolarons with increasing external potential.

Since polaron and bipolaron formations were in the NIR region, all polymers were transparent in their oxidized states. As calculated from the onset of their lowest π-π* transitions, P1 and P2 exhibited optical band gaps of 1.02 eV and 0.95 eV, respectively. P3 revealed the lowest optical band gap of 0.92 eV due towiderπ-π* transitions at around 882 nm. Electronic band gaps can be higher than the optical ones since electronic band gaps are calculated using CV data where the polymers contain charged species like polarons. Although all monomers and polymers contain bulky groups attached to quinoxaline units, P3 has an additional tertbutyl bulky group on the quinoxaline unit. As a result it may affect thedegree of polymerization and arrangement of repeating units in the polymer chains. This may be the reason why the spectral behaviours of P1 and P2 are different from that of P3.

Recently both p- and n-dopable polymers made several application areas feasible under atmospheric conditions such as light emitting diodesand organic solar cells. Although P1, P2 and P3 revealed reversible n-type redox couples, there should be additional evidence such as considerable structuraland especially optical differences after the introduction ofcharge carries to the conjugated system. Accretion of bands inthe NIR absorption region upon n-type doping of P1, P2 and P3 isclear evidence for the formation of negative charge carriers(Fig.3.4).

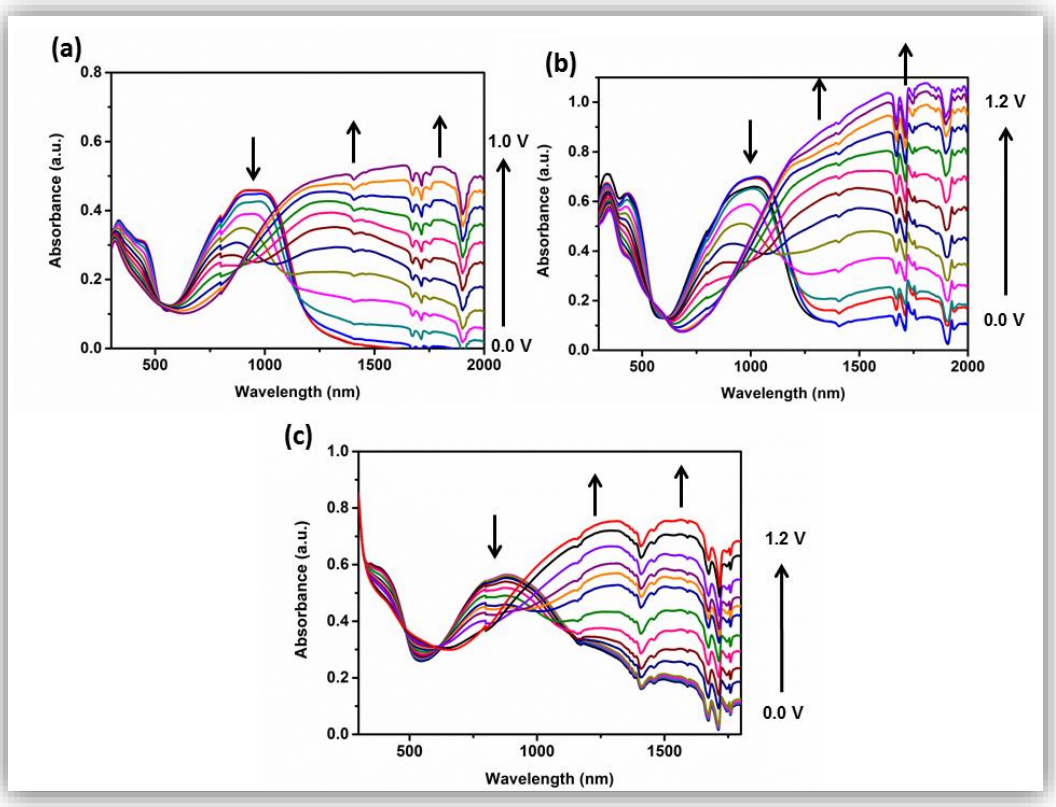

Figure 3. 3. p-type doping spectra for P1 (a), P2 (b) and P3 (c) in 0.1 M 0.1 M $TBAPF_6$ /ACN supporting electrolyte/ solvent system .

The normalized absorbance spectra of monomers in bothCH_2Cl_2 and thin film form are shown in Fig. 3.5 In the solution, monomers revealed absorption in visible region centered at 550nm, 567 nm and 548 nm for M1, M2 and M3, respectively. Asregards the ones in thin film form, reduction in conformationalfreedom diminishing of solvent–monomer interactions and a tendency toaggregate in thin film form mostly causes a red shift absorptioncompared to the ones taken in solutions. In addition to red shift absorption, broadening of absorptions covering between 550 nm and 650 nm were observed.

During the n-doping process, all polymers showed multichromic behavior which is rarely seen in donor–acceptor type polymers (Fig. 3.6). This multichromic behavior of the polymers during the n-doping process may arise from two features: firstly, the

presence of two reversible redox couples as given in Fig. 3.2 and secondly the presence of alkyl chains bonded to triazole units which affects the doping rate.

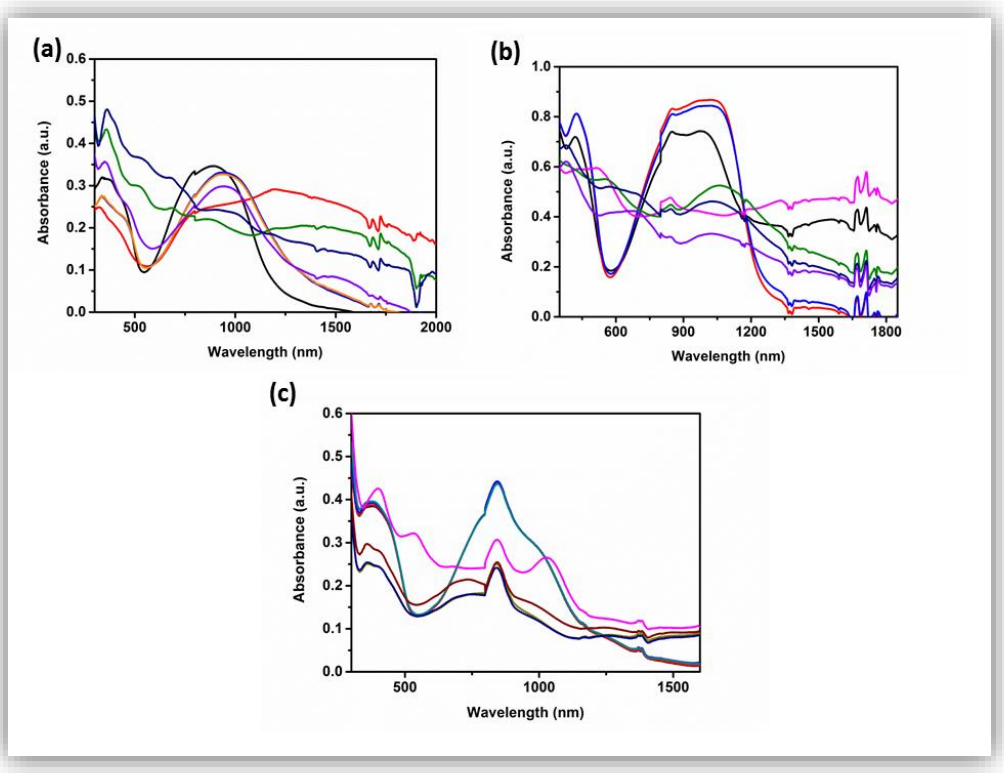

Figure 3. 4. n-type doping spectra for P1 (a), P2 (b) and P3 (c).

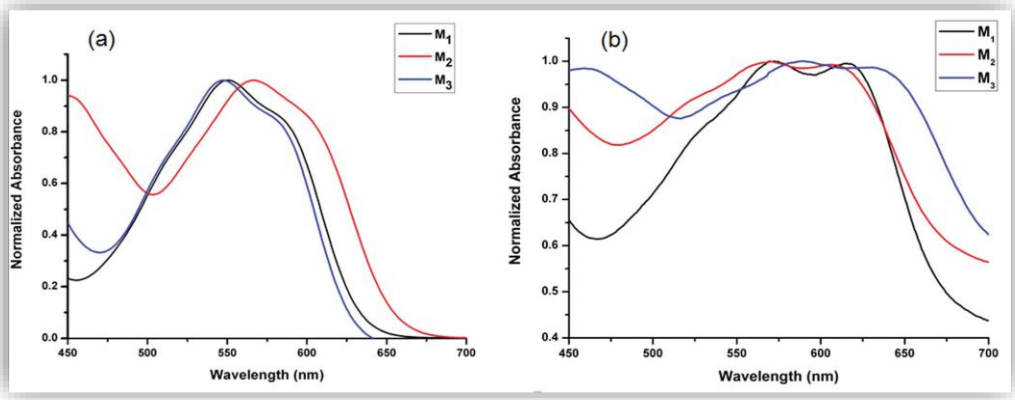

Figure 3. 5. Absorption spectra of monomers in solution (a) and thin film form (b).

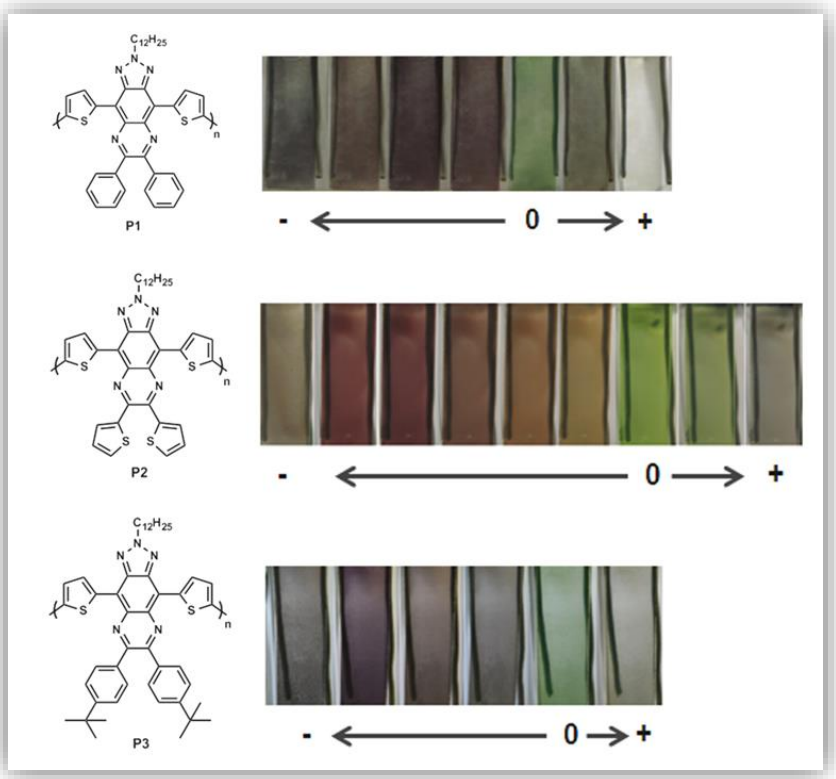

Figure 3. 6. Structures of the polymers and their colors under different applied potentials.

3.1.4. Electrochromic switching studies

To investigate switching studies, the polymer films on ITO surfaces were studied via switching the potentials corresponding to their doped and dedoped states. During the switching, the absorbance at the specific wavelengths determined from the spectra of polymers, were monitored as a function of time with a UV-Vis-NIR spectrophotometer. Due to their strong absorption in the NIR region, all polymers showed a high optical contrast inNIR region; P1 showed 93% contrast at 2000 nm with 2 s of switching time, P2 revealed 71% with 1.7 s at the same wavelength and P3 presented 69% with 1.6 s at 1800 nm (Fig. 3.7). In thestudies as the wavelength in concern decreased, the optical contrasts revealed by the polymers increased; on the other hand, switching times decreased. Optical contrasts, switching times and percent loss in optical contrasts were summarized in Table 3.2.

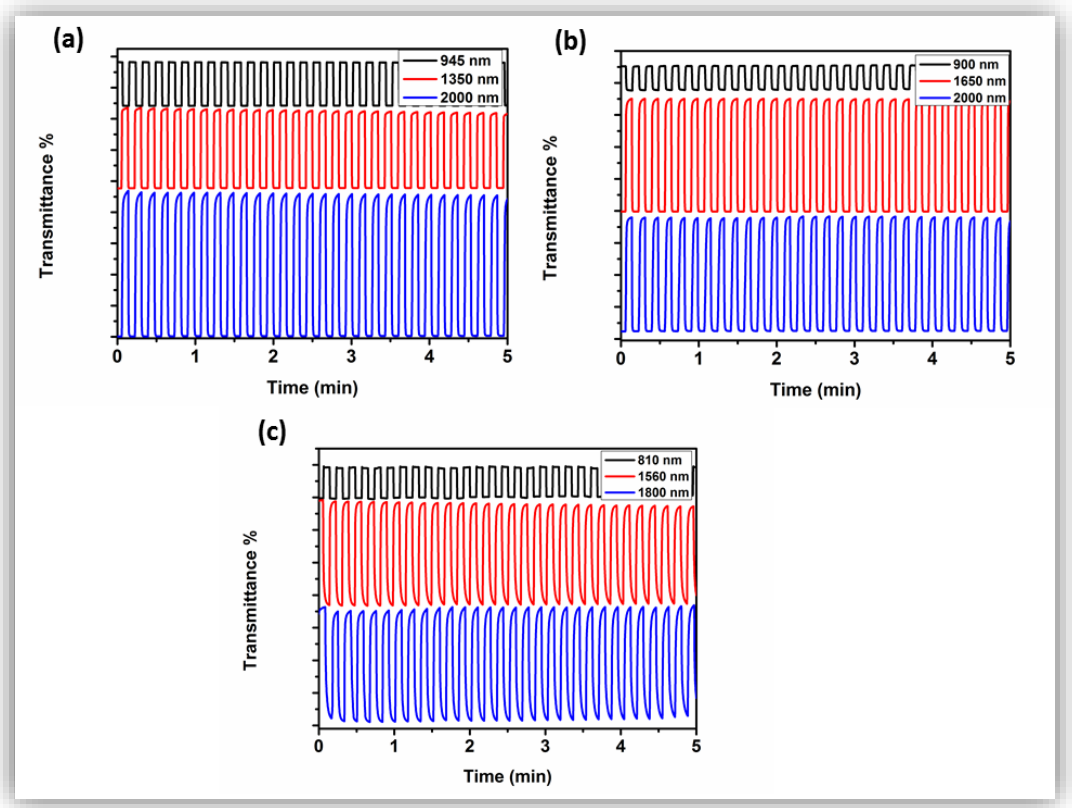

Figure 3. 7. Optical contrasts and switching times of (a) P1, (b) P2 and (c) P3 at different wavelengths.

Table 3. 2. Summary of kinetic and optic studies of P1, P2 and P3.

	P_1			**P_2**			**P_3**		
	945 nm	**1350 nm**	**2000 nm**	**900 nm**	**1650 nm**	**2000 nm**	**810 nm**	**1560 nm**	**1800 nm**
T %	29	52	93	18	70	71	20	62	69
t (s)	0.1	0.5	2	0.8	1.2	1.7	0.3	1.4	1.6
T % lost	1.7	4.9	2.8	3.1	0.8	1.5	3.7	7.2	1.9

3.2.Synthesis and electrochromic properties of triphenylamine containing copolymers: Effect of π-bridge on electrochemical properties

3.2.1 Synthesis

Synthetic pathway for polymers; PTPB1, PTPB2 and PTPB3 is outlined in Scheme 3.4. The synthesis of4,7- bis(thien-2-yl) 2-dodecyl-benzo[1,2,3]triazole (TBT) [53] was reported previously by our group. After succesive synthesis TBT was brominated by N-bromosuccinimide (NBS) in chloroform ($CHCl_3$).PTPB1 was synthesized via a Stille coupling reaction between 4-bromo-N-(4-bromophenyl)-N-phenylaniline **(12)** ,4,7-dibromo-2-dodecyl-2H-benzo[d][1,2,3]triazole**(3)**and 2,5-bis(tributylstannyl)thiophene, PTPB2 was synthesized via Suzuki coupling reaction between 4-bromo-N-(4-bromophenyl)-N-phenylaniline **(12)** , 4,7-dibromo-2-dodecyl-2H-benzo[d][1,2,3]triazole **(3)**and 1,4-phenylene diboronic acid and finally PTPB3 was synthesized via Stille coupling reaction between 4-bromo-N-(4-bromophenyl)-N-phenylaniline **(12)**, 4,7-bis(5-bromothiophen-2-yl)-2-dodecyl-2H-benzo[d][1,2,3]triazole **(11)** and 2,5-bis(tributylstannyl)thiophene(Scheme 3.4).As summerized in the experimental part, the average molecular weights (Mn) of polymers as determined by gel permeation chromatography (GPC) are 14600, 3400 and 12000, respectively, with relatively low polydispersity indexes.(1.7, 2.4, 1.4). When GPC results were compared, the lower Mn value of PTPB2 may be attribured to the difference of synthetic pathways. While PTPB1and PTPB3 were sythesized by using Stille coupling, Suzuki coupling which is more sensitive compared to Stille coupling was used for PTPB2.

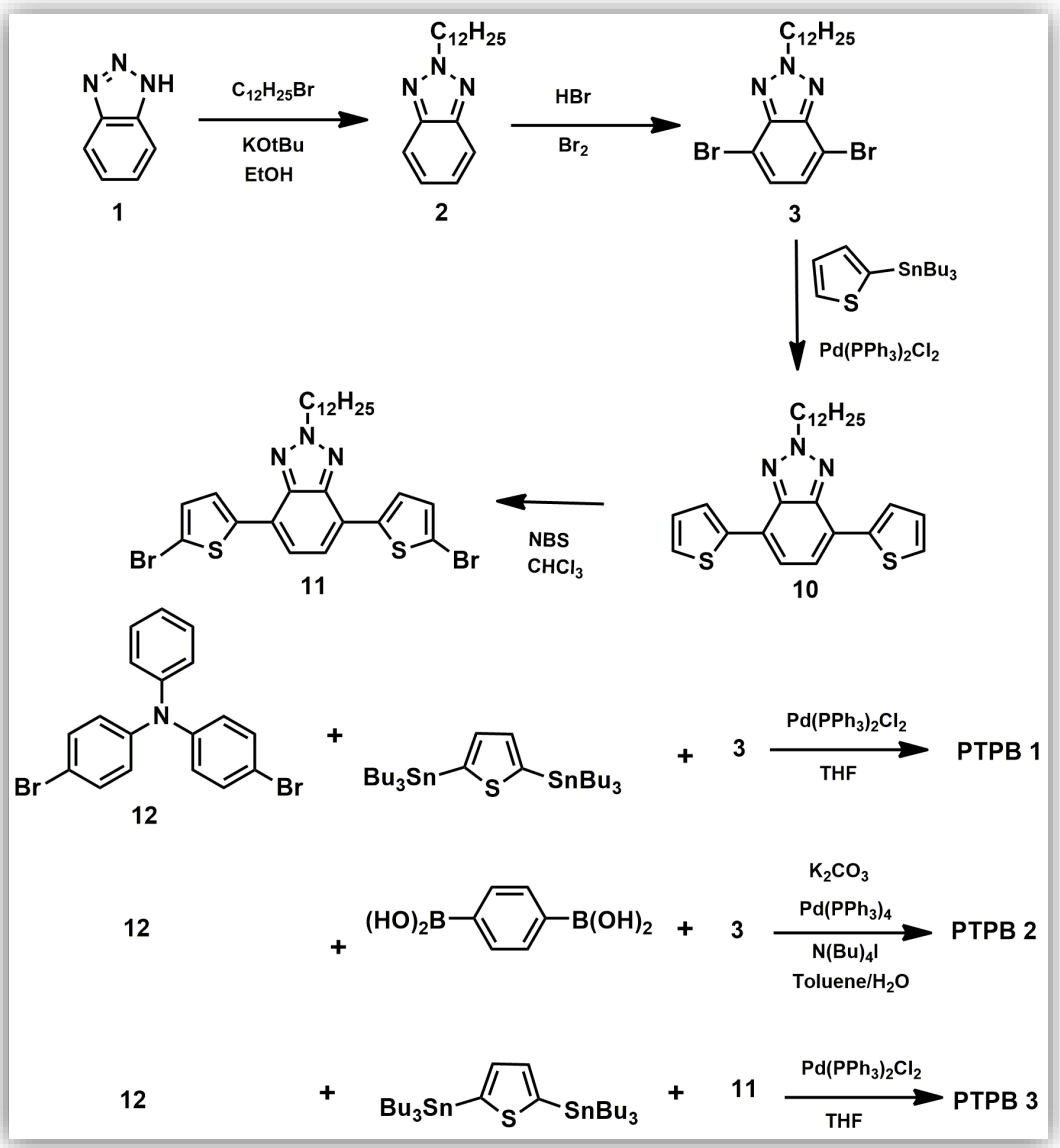

Scheme 3. 4. Synthetic route for the polymers.

3.2.2. Electrochemical Properties

The redox properties of PTPB1, PTPB2 and PTPB3 were investigated via cyclic voltammetry (CV) in order to explore the HOMO and LUMO energy levels and the redox potentials of corresponding random copolymers. All polymers were dissolved in chloroform (5 mg/mL) and spray coated on indium tin oxide (ITO) coated glass slides for electrochemical and optical studies. The cyclic voltammograms of films

were recorded in 0.1 M tetrabutylammonium hexafluorophosphate ($TBAPF_6$)/acetonitrile (ACN) solutions vs. Ag wire pseudo reference electrode (0.3 V vs. Fc/Fc^+) at a scan rate of 100 mV/s.

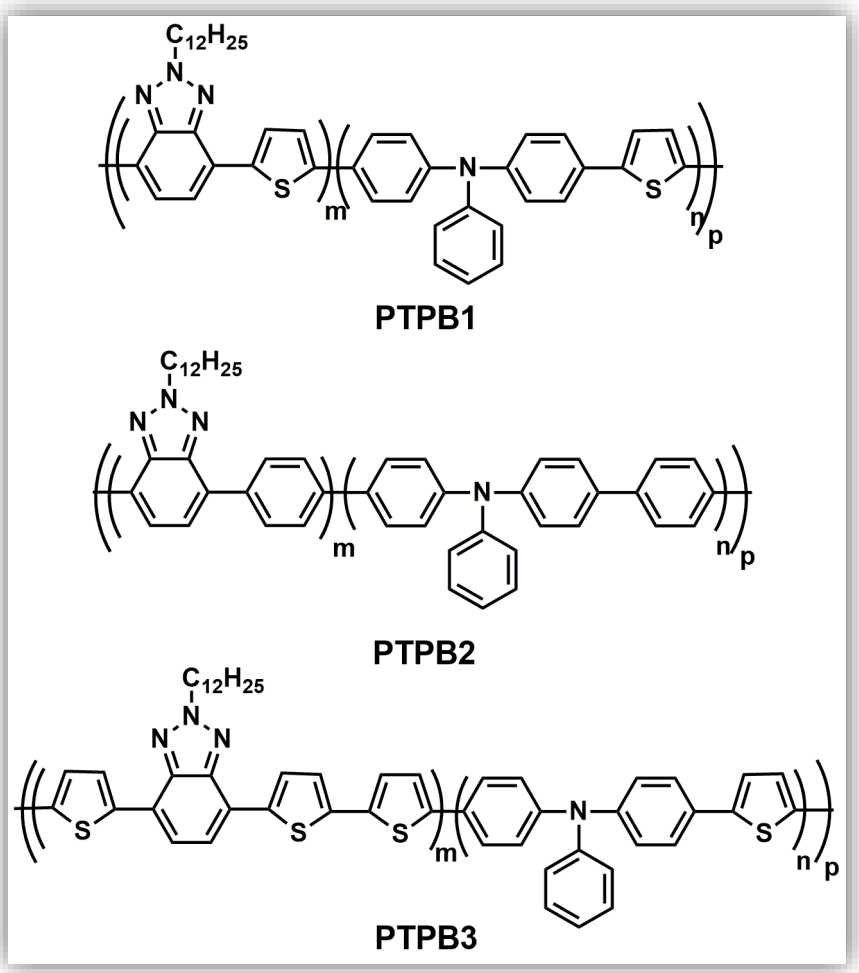

Figure 3. 8. Structures of PTPB1, PTPB2 and PTPB3.

P-type and n-type doping properties of the polymers were also investigated using the same solvent- supporting electrolyte couple via CV. While PTPB1has an ambipolar character, PTPB2 andPTPB3 have only p-doping property as illustrated in Fig.3.9. It is worth considering thata material exhibiting anambipolar character is a good candidate for different applications in batteries, supercapacitors and light-emitting diodes.

Differences in oxidation potentials can be attributed to the different electron densities on polymer chains. As explained before, two different π-bridges (thiophene, benzene) were inserted into the polymer backbone which strongly affect the electronic nature of resulting polymers. As summarized in Table 3.3, PTPB1 film revealed lower redox potentials at 1.38 V / 1.51 V compared to those of PTPB2 at 1.45 V due to the electron-rich thiophene units inPTPB1. Also same trend can be observed when oxidation potentials of PTPB1 and PTPB3 are compared. In this case, for PTPB3 spacer is two thiophene units in the polymer backbone which is more electron rich compared to pristine thiophene hence, the lowest E_{ox} at 0.86 V /1.16 V was observed for PTPB3**.**

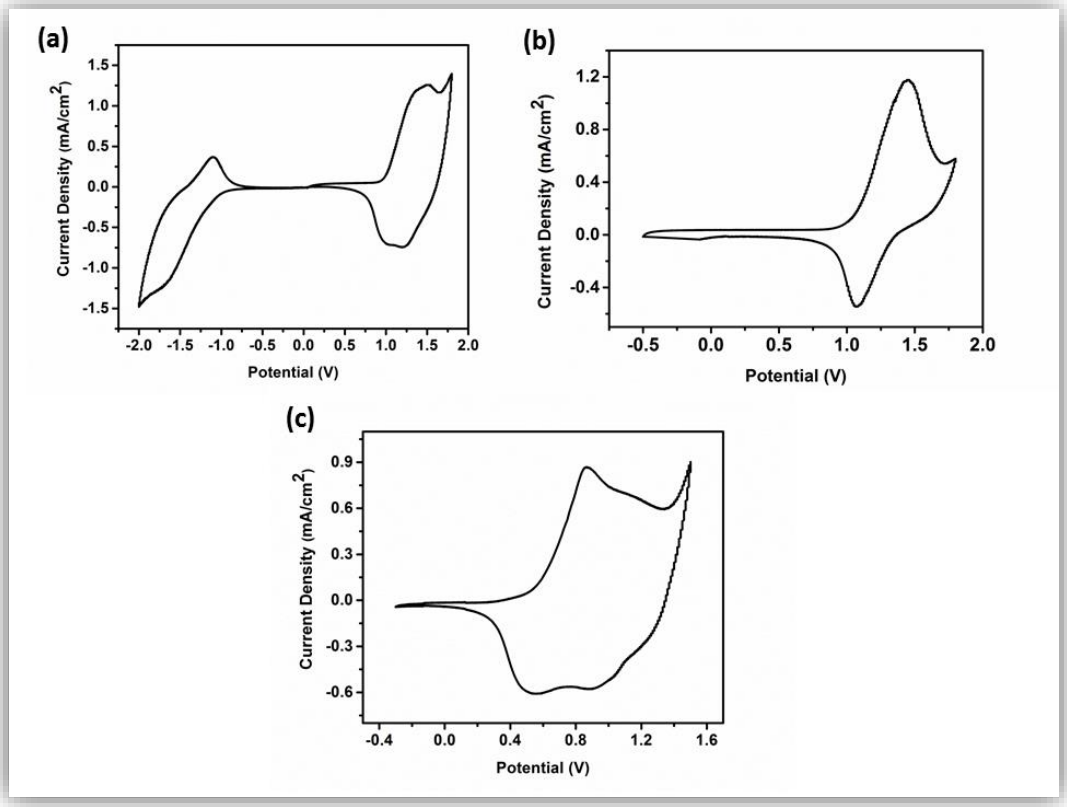

Figure 3. 9. Single scan cyclic voltammograms of a) PTPB1, b) PTPB2 and c) PTPB3 films using ACN as the solventand 0.1 M $TBAPF_6$ as the supporting electrolyte at a scan rate of 100 mV s^{-1}.

The HOMO energy levels of the polymers were estimated using the onset of the corresponding oxidation (Fig. 3.9) by calculating the energy levels relative to the

vacuum level and calibrating the reference electrode against Fc/Fc^{+}. HOMO levels were calculated as -6.04 eV, -6.11 eV and-5.63 eV respectively (Table 3.3). While LUMO energy level of PTPB1 was found from the reduction onset as -3.98 eV, those for PTPB2 andPTPB3 were calculated using optical band gap values. The estimated HOMO energy levels also support the previous argument referring to theelectron densities of the two bridges; thiophene and benzene. All related electrochemistry data were summarized in Table 3.3.

Table 3. 3. Summary of electrochemical and spectroelectrochemical properties of PTPB1, PTPB2 and PTPB3.

	$E_{p\text{-doping}}$ (V)	$E_{p\text{-dedoping}}$ (V)	$E_{n\text{-doping}}$ (V)	$E_{n\text{-dedoping}}$ (V)	HOMO (eV)	LUMO (ev)	E_g^{ec} (eV)	λmax (nm)	E_g^{op} (eV)
PTPB1	1.38 /1.51	1.02/1.2	-1.7	-1.1	-6.04	-3.98	2.06	497	1.86
PTPB2	1.45	1.07	-	-	-6.11	-2.97	-	328	3.12
PTPB3	0.86/1.16	0.53/0.9	-	-	-5.63	-3.76	-	472	1.89

As mentioned before, while all polymers have p-type doping property, only PTPB1 has a reversible redox couple in the n-doped state. Because PTPB2 and PTPB3have an irreversible reduction, they do not any n-type doping property. As a result, it can be state that only PTPB1 has an ambipolar character.

3.2.3. Spectroelectrochemical Properties

Spectroelectrochemical properties of the polymers wereinvestigated by monitoring the changes in the electronic absorption spectra under different applied

potentials.PTPB1, PTPB2 and PTPB3 were dissolved in chloroform to obtain 5 mg/mL polymer solution and spray coated onto ITO substrate until acquiring homogeneous films. Then, spectroelectrochemistry analyses were performed using 0.1 M $TBAPF_6$/ACN solutions via incrementally increasing applied potential between 0.0 V and 1.8 V for PTPB1, 0.0 V and 1.7 V for PTPB2 and 0.0 V and 1.5 V for PTPB3.

Polymer films on ITO were reduced to their neutral states in order to remove any trapped charge and dopant ion. Following the neutral film absorptions, changes in the absorption spectra under a variety of applied potentials were recorded.(Fig.3.10)

During stepwise oxidation, the neutral state absorptions at around 300 nm for PTPB2 and 500 nm for PTPB1 and PTPB3 depleted while new absorptions arouse owing to formation of free charge carriers (polarons and bipolarons). The optical band gaps (E_g^{op}) of all polymers were calculated from the onsets of lowest energy π–π* transitionsas 1.86 eV, 3.12 eV, and 1.89 eV respectively (Table 3.3). As mentioned before onlyPTPB1 has an ambipolar character hence, the LUMO levels of other polymers were calculated using the optical band gaps and previously calculated HOMO levels. All data are summarized in Table 3.3.

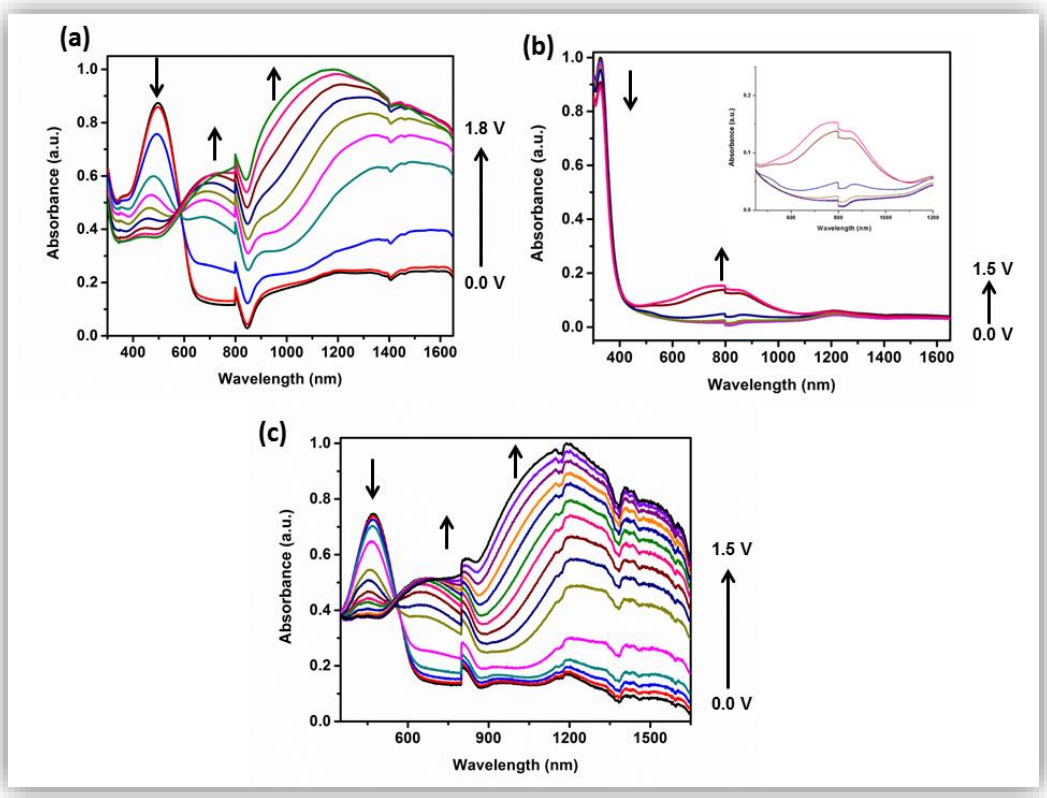

Figure 3. 10. Electronic absorption spectra of a) PTPB1 switching between 0.9 V and 1.8 V, b) PTPB2 between 0.5 V and 1.5 V, c) PTPB3 between 0.4 V and 1.5 V in 0.1 M $TBAPF_6$/ACN solution.

As summarized in Table 3.4, PTPB1 revealed a maximum (λ_{max}) at 497 nm corresponding to the π–π* transition of the polymer. The polymer was red in its neutral state and during stepwise oxidation different intermediate (green) and oxidized (blue)colors were observed for PTPB1 as a result of the polaron and bipolaron bands centered at different wavelengths. Only PTPB1 has a multichromic character among these derivatives.

When PTPB1 and PTPB2 were compared in terms of their electron densities on the polymer chain and optical absorptions, thiophene unit displays a more electron rich character, thus$\lambda_{max}$for the neutral film of PTPB1 was red shifted by 169 nm. As a result, while red color observed for PTPB1, PTPB2 was yellow with a λ_{max} centered

at 328 nm. Although the similar trend was expected when spacer was changed from thiophene to two thiophene units, different molecular weights and conjugation length affectedthe results significantly. Orange color was observed for PTPB3 with λ_{max} centered at 472 nm. This unexpected blue shift can be attributed to the higher M_n value of PTPB1. Higher molecular weight will probably result in longer conjugation and higher λ_{max} value. As illustrated in Figure 3.11,in their oxidized states both PTPB2 and PTPB3 revealed blue color similar to PTPB1 .

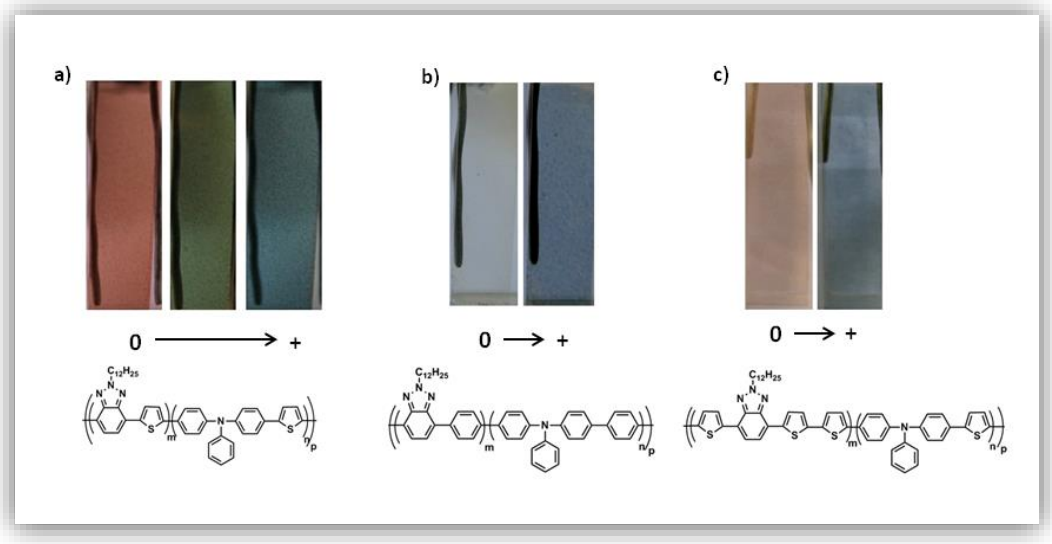

Figure 3. 11. Structures of the polymers and their colors at their neutral and oxidized states.

Neutral absorptions for all polymers could be seen in Fig 3.10. When the colors (Fig. 3.11) are compared with those of neutral state absorptions, the obvious blue shift for PTPB2 could be seen which can be dedicated to the benzene unit inserted into the polymer backbone. In addition, benzene bearing derivative PTPB2 has yellow color which is responsible for the differences in the spectroelectrochemical studies. Higher optical band gap of corresponding derivative can be explained by blue shift.

3.2.4.Electrochromic contrast and switching studies

The capacity of a material rapidly changing its color betweenneutral and oxidized statesand illustrating asignificant change which are importantand desired properties for the electrochromicpolymers to widen their application area.

To investigate the mentioned properties, electrochromic contrast and switching studies were performed on ITO coated glass slides where the polymers were subjected to potential switches between their neutral and oxidized states using a UV–vis–NIR spectrophotometer at their local maximum absorption wavelengths. Polymer films were prepared by spray coating as described before andstudies were monitoredin 0.1 M $TBAPF_6$/ACN solvent/electrolyte couple. As a result, percent transmittance and switching times were recorded as illustrated in Fig 3.12. Switching time is defined as the time required for the color change of a material between its neutral and oxidized states.

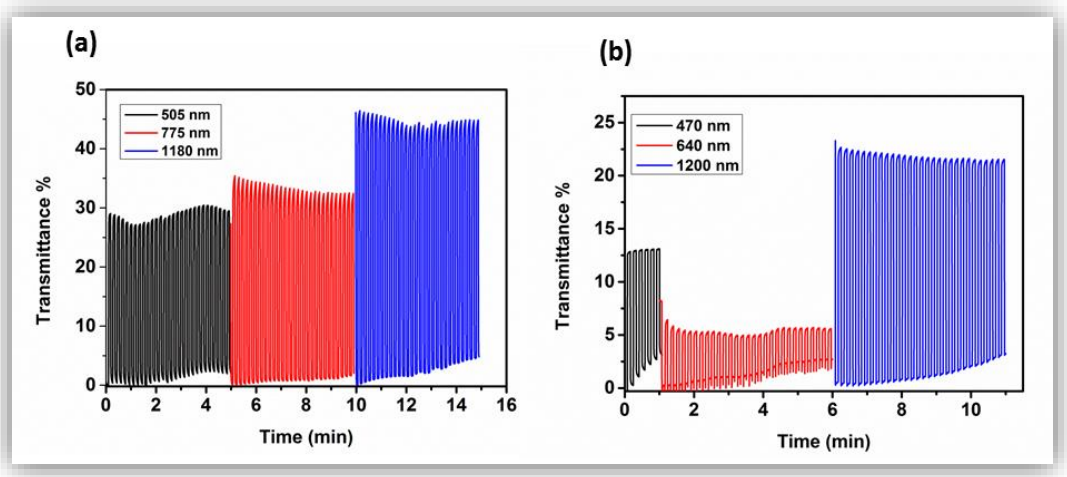

Figure 3. 12. Optical contrasts and switching times monitored at different wavelengths for (a) PTPB1 and (b) PTPB3 in 0.1 M $TBAPF_6$/ACN solution.

Kinetic studies were carried out for PTPB1 and PTPB3 at all absorption regions. Due to the small changes in the π-π* and bipolaron absorption intensities, PTPB2 was not subjected to such a study. As illustrated in Table 3.4, PTPB1 showed 47% transmittancechange upon doping/dedoping processes at 1180 nm, 36 % at 775 nm and 29 % at 505 nm. Percent transmittance results for PTPB3 are 23 % at 1200 nm, 6 % at 640 nm and 13 % at 470 nm. Switching times were reportedas 0.9 s, 1.9 s, 1.4 s for PTPB1and 0.4 s, 2.0 s, 0.4 s for PTPB3 at corresponding wavelengths(Table 3.4).

Table 3. 4. Summary of kinetic studies of polymers.

	Optical contrast (ΔT %)		**Switching times (s)**
PTPB1	29 %	505 nm	1.4 s
	36 %	775 nm	1.9 s
	47 %	1180 nm	0.9 s
PTPB3	13 %	470 nm	0.4 s
	6 %	640 nm	2.0 s
	23 %	1200 nm	0.4 s

When kinetic results of PTPB3are compared with those of PTPB1, the switching times are shorter for the former one, which can be attributed to the increasing length of spacer unit which most probably led to improved ion diffusion and dopant insertion.

Based on electrochemical, spectroelectrochemical and kinetic results, it can be noted that these triphenylamine and benzotriazole based copolymers, escpecially PTPB1, can be used in the construction and the development of electrochromic devices and organic solar cells due to their promising properties.

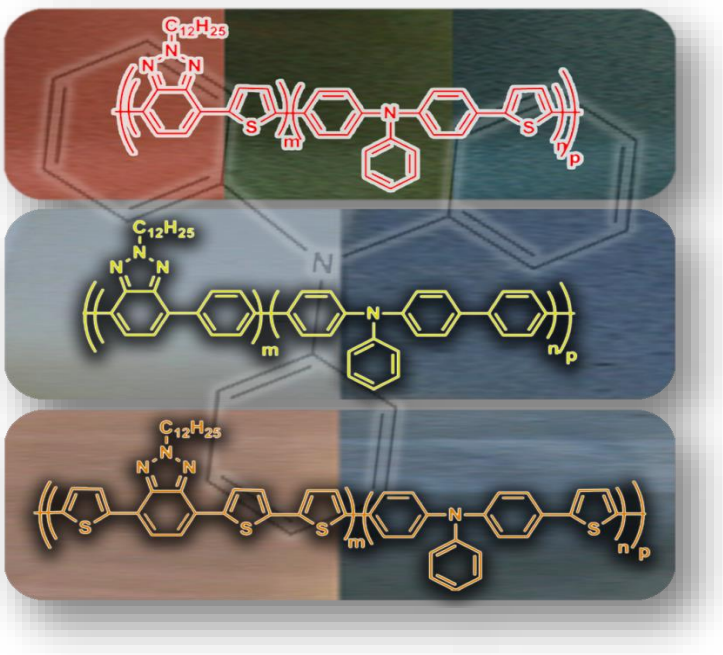

Scheme 3. 5. Schematic illustration of colors and structures for resulting polymers [61].

3.3. Construction and characterization of triazoloquinoxaline derivative P2 /PEDOT based dual type electrochromicdevice (ECD)

The synthesis and electrochemical characterization of P2 were summarized before (Chapter 3.1). Due to promising colors and electrochromic behaviors we decided to construct an electrochromic device with P2 and PEDOT.

3.3.1. The construction of an electrochromic device (ECD)

P2 and PEDOT werecoated electrochemically onto the ITO-coated glass slides to construct anelectrochromic device.Two polymer coated electrodes (with two different states) were arranged facing each other and separated by a gel electrolyte during construction [62,63]. The gel electrolyte was prepared with known procedures according to the literature [64]. Each process for the construction of the ECD was

summarized in Scheme 3.6. A schematic representation of the electrochromic device based on P2/ PTMA is shown in Scheme 3.7.

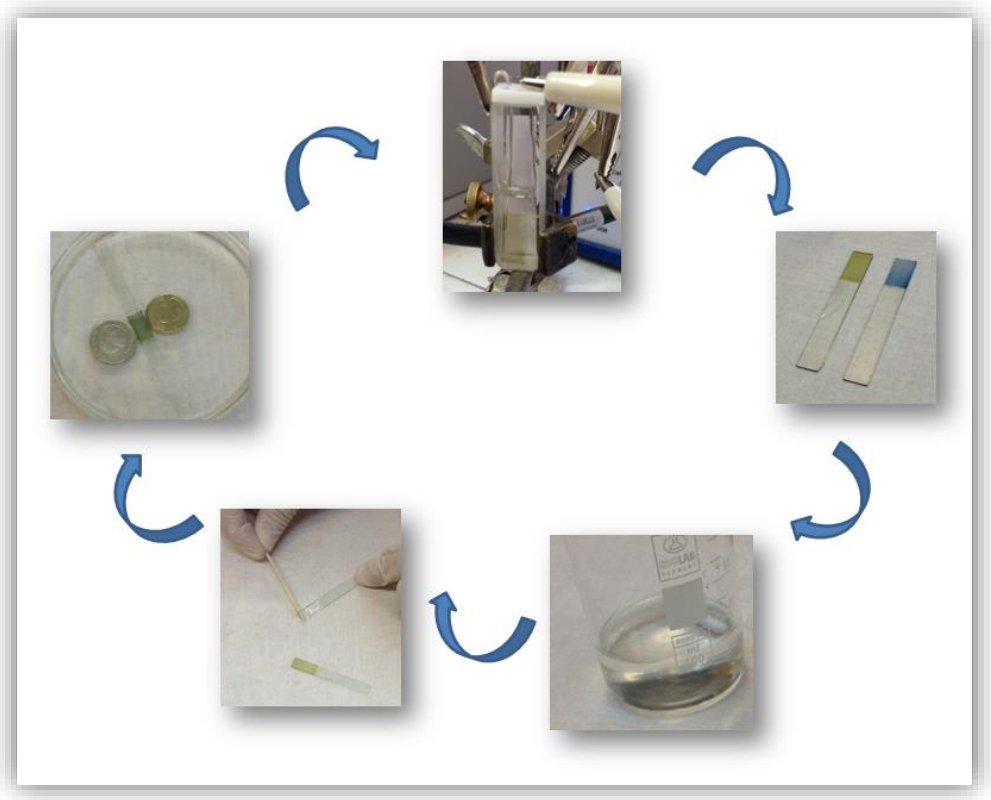

Scheme 3. 6. Schematic illustration for the electrochromic device construction.

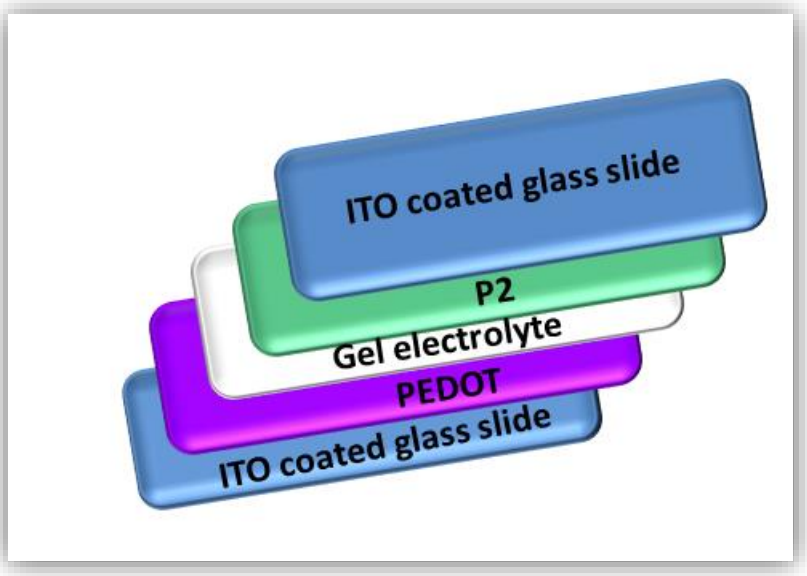

Scheme 3. 7. Schematic representation of the P2/PEDOT ECD.

3.3.2. Spectroelectrochemistry

After investigation of electrochemical and optical behaviors of P2, we fabricated a prototypesolid state electrochromic device in order to explore the electrochromic performance of polymer in ITO/P2/PEDOT/ITOdevice configuration.

The optoelectronic properties of the P2/PEDOT ECDwere investigated using a UV-Vis spectrophotometer. Duringspectroelectrochemical studies, incrementally increasing potentials were applied between -1.3 V and 1.3 V to record the electronic absorption spectra. Figure 3.14 illustrates the spectroelectrochemical studies of P2 based ECD between 1.3 V and -1.3 V. At -1.3 V PEDOT is in the oxidized state and has transmissive blue colorsothe green color was observed at that potential which is the neutral state color for P2.Then at 1.3 V P2 shows transmissive gray color and ECD illustrates the color of PEDOT as blue. In short, ECD is operating between green and blue. (Fig. 3.13)

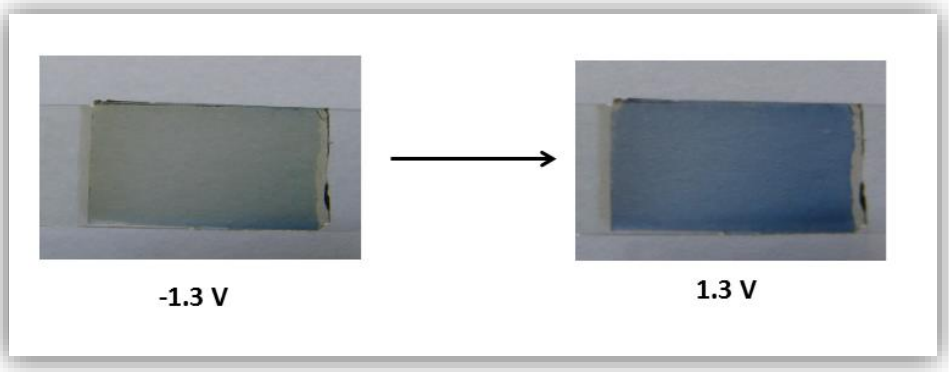

Figure 3. 13. Colors for P2/PEDOT based ECD at two extreme states.

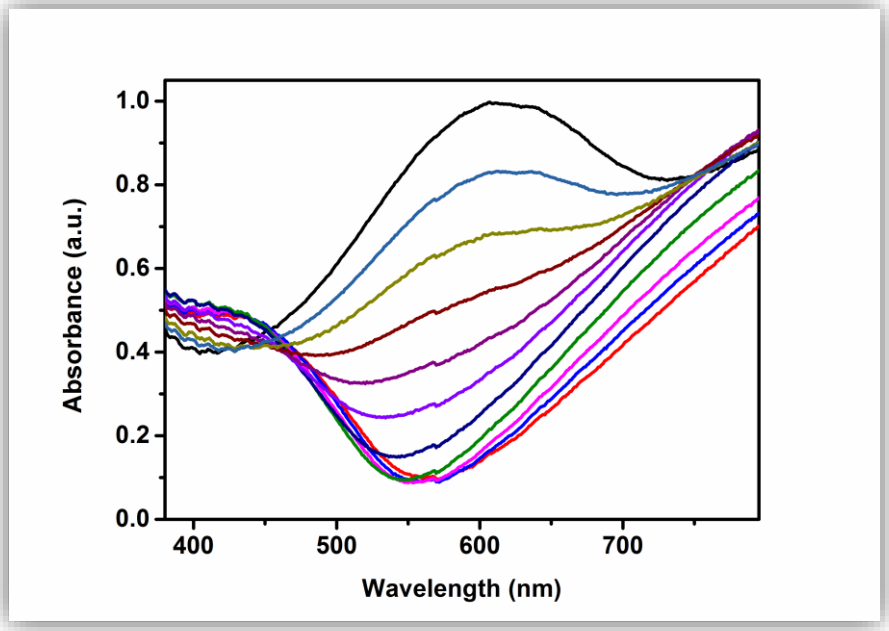

Figure 3. 14. Electronic absorption spectra of the P2/PEDOT ECDbetween +1.3 V and -1.3 V.

3.3.3. Kinetic studies

Kinetic studies were performed via sweeping the applied potentials between the two extreme states within 5 s time intervals and as a result of kinetic studies, optical contrast and switching times were calculated and reported in Table 3.5. While the

optical contrast could be defined as the change in percent transmittance between neutral and oxidized states, switching time is the time required for one full switch. For P2/PEDOT ECD optical contrast and swicthing times are calculated from Figure 3.15 as 15 % and 1 s, respectively.

Table 3. 5. Summary of optical and kinetic results for P2/PEDOT ECD.

	λ_{max} (nm)	Optical Contrast (T %)	Switching time (s)
P2/PEDOT ECD	610	15	1

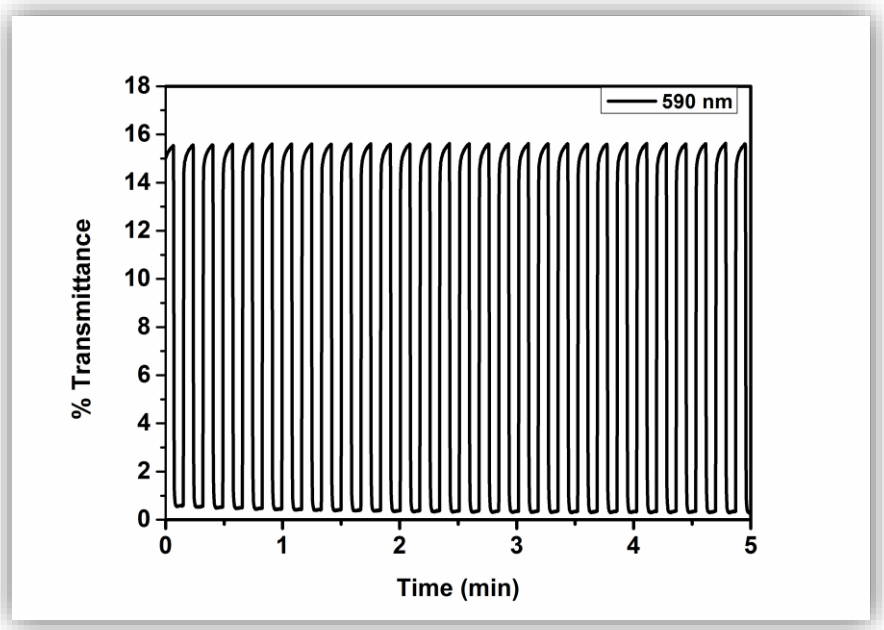

Figure 3. 15. Optical contrasts and switching times P2/PEDOT ECD at 590 nm.

3.3.4. Open Circuit Memory Studies for P2/PEDOT ECD

Open circuit memory experiments for ECDs were monitored as further characterizations to investigate and report the time at which the device maintains its

color under open circuit conditions [65,66]. During the optical memory experiments, 1 s pulse of +1.3 V or -1.3 V was applied to the ECD for each 200 s at 590 nm.Then for the 200 s, the device was kept under open-circuit conditions (without applying any potential) while simultaneously recording the percent transmittance changes at the corresponding wavelengths. The wavelength,590 nm was determined from the absorption maxima of spectroelectrochemical studies. As seen in Figure 3.16, P2 based ECD is very stable especially at -1.3 V showingno significant T% changeupon time. At 1.3 V after keeping devices under open circuit conditions for 200 s, T % values were decreased from 69% to 64% for P2 based ECD and the loss inT% is so low (7 %) that todetect them with naked eye is difficult.

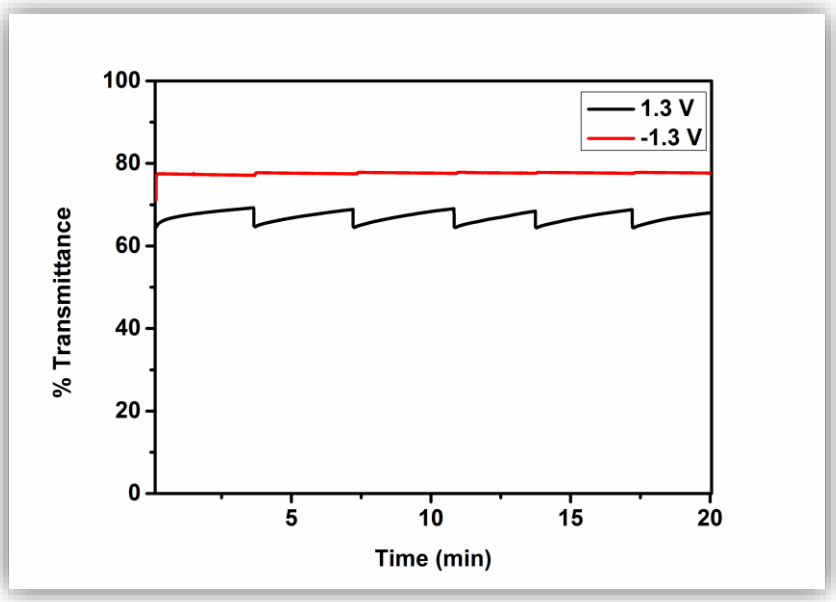

Figure 3. 16. Open circuit memory of P2/PEDOT ECD monitored by single wavelength absorption spectroscopy at +1.3V and -1.3V.

3.3.5. The stability of P2/PEDOT ECD

Finally for the characterization of ECD the stability experiments were performed. Stability of the P2/PEDOT ECD was investigated by the chronoamperometry technique while switching the device between two extreme states (-1.3 V and +1.3V) at every 5 seconds. In Fig. 3.17, the stability of the device initially and after 500 cycles was reported and it can be clearly stated that after 500 cycles the ECD retains its electrochromic performance without any significant electroactivity loss.

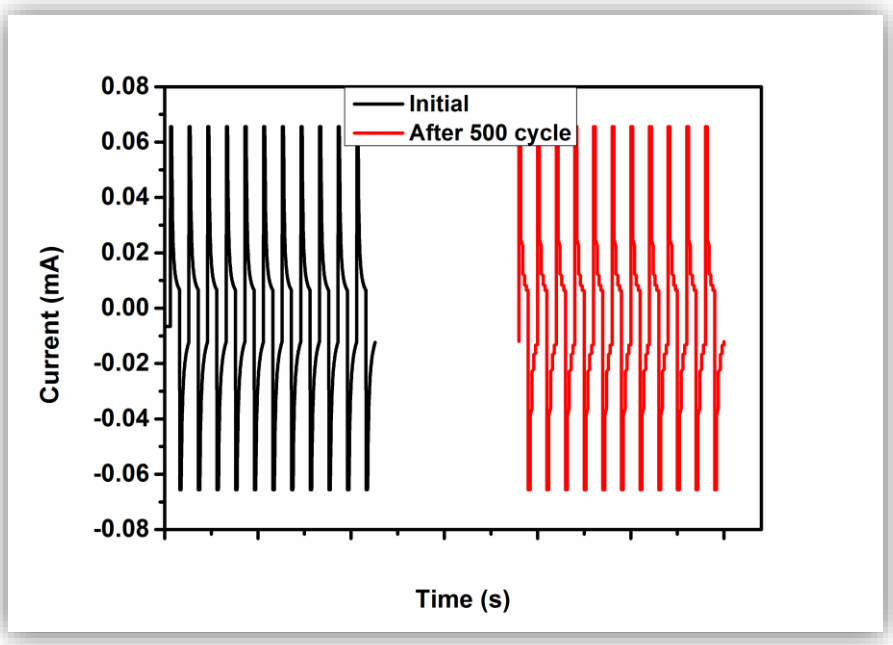

Figure 3. 17. Stability tests for P2/PEDOT ECD after 500 cycle.

3.4.Resynthesized benzotriazole and triphenylamine bearing random copolymers for electrochromic and organic photovoltaic applications

In this part, benzotriazole and triphenylamine bearing random copolymers were resynthesized in order to increase the amount of final product for different applications. In order to increase the yield experimental procedures were revised as depicted in Scheme 3.8. In addition, due to inreased molecular weigths of resulting

polymers electrochemical behaviors were also affected significantly. Results will be reported and explained in detail in this part.

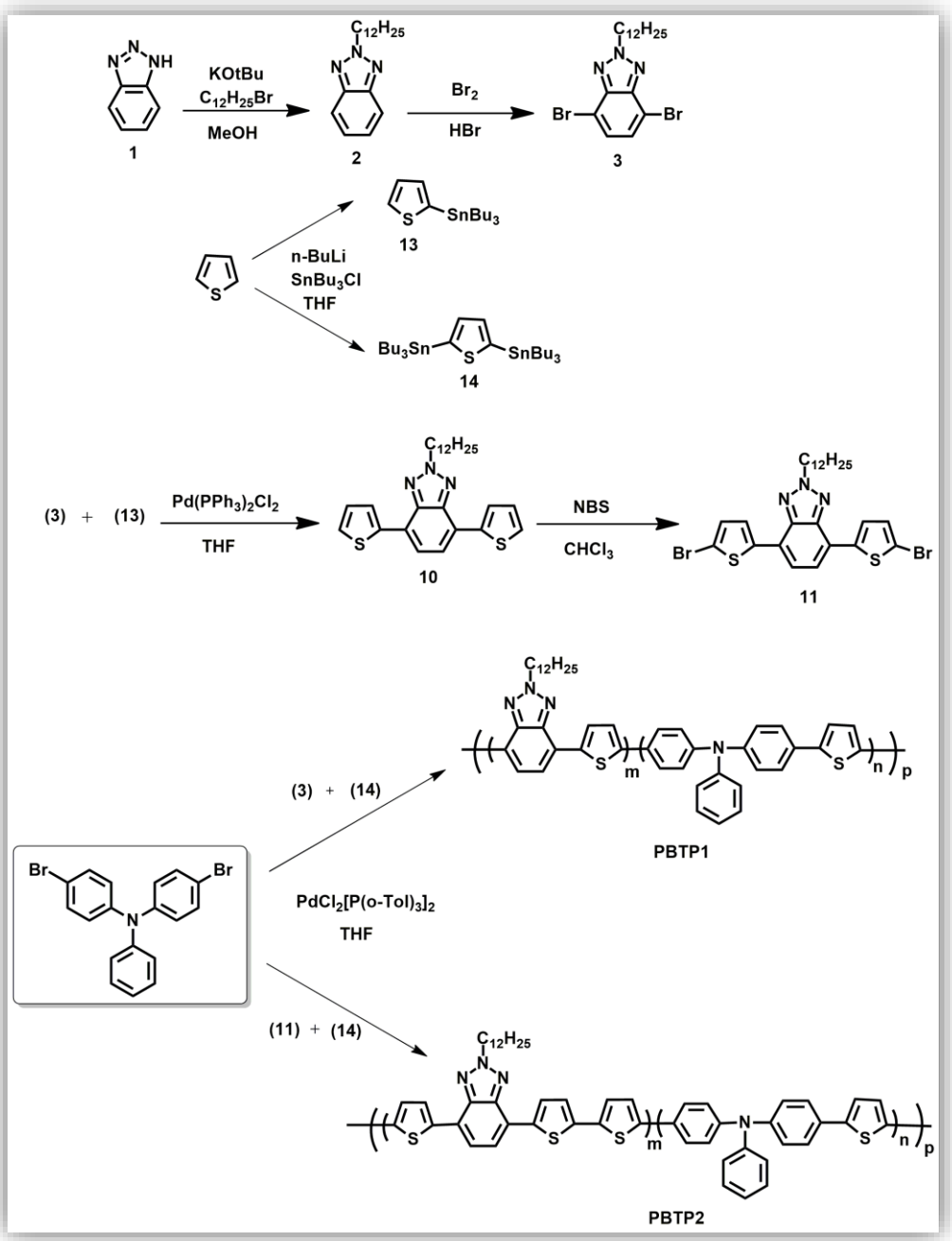

Scheme 3. 8. Synthetic route for the polymers.

3.4.1. Electrochemistry

The electrochemical behaviors of PBTP1 and PBTP2 were investigated with cyclic voltammetry technique. Cyclic voltammetry (CV) is a very useful method to record the electroactivity, oxidation potentials and doping behaviors of resulting polymers. In addition, HOMO/LUMO energy levels and band gap which were very crucial for applications, could be calculated with this technique. Both PBTP1 and PBTP2 were dissolved in $CHCl_3$ and coated on ITO coated glass slides via spray processing for electrochemical, spectroelectrochemical and kinetic studies. Cyclic voltammograms were carried out in 0.1 M of $TBAPF_6$ in acetonitrile (ACN) solution using three electrode system with silver wire and platinum wire which were used as pseudo reference electrode and counter electrode, respectively.

Single scan cyclic voltammograms for both PBTP1 and PBTP2 were illustrated in Figure 3.18 Both polymers have ambipolar character in other words, they have both p-type doping and n-type doping ability. Corresponding doping/dedoping potentials of PBTP1 and PBTP2 were observed at 1.04 V/ 0.54V and 0.90 V/ 0.70V, respectively. Both PBTP1 and PBTP2 have reversible redox couples during n-type doping process at -1.87 V/ -1.54 and -1.97 V/ -1.68 V.

These polymers were designed and synthesized in order to use them as donor molecules in organic solar cellshence, HOMO and LUMO energy levels are very important especially for that purpose. Energy levels were calculated from the onset of the oxidation of the p-doping state and the n-doping state as -5.43 eV /-3.20 eV for PBTP1 and -5.33 eV/ -3.02 eV for PBTP2. Corresponding electronic band gaps (E_g^{ec}) which are the difference between HOMO and LUMO were calculated as 2.23 eV and 2.31 eV and all electrochemical results were summarized in Table 3.6.

Table 3. 6. Summary of electrochemical properties of PBTP1 and PBTP2.

	$E_{p\text{-doping}}$ (V)	$E_{p\text{-dedoping}}$ (V)	$E_{n\text{-doping}}$ (V)	$E_{n\text{-dedoping}}$ (V)	HOMO (eV)	LUMO (ev)	E_g^{ec} (eV)
PBTP1	1.04	0.54	-1.87	-1.54	-5.43	-3.20	2.23
PBTP2	0.90	0.70	-1.97	-1.68	-5.33	-3.02	2.31

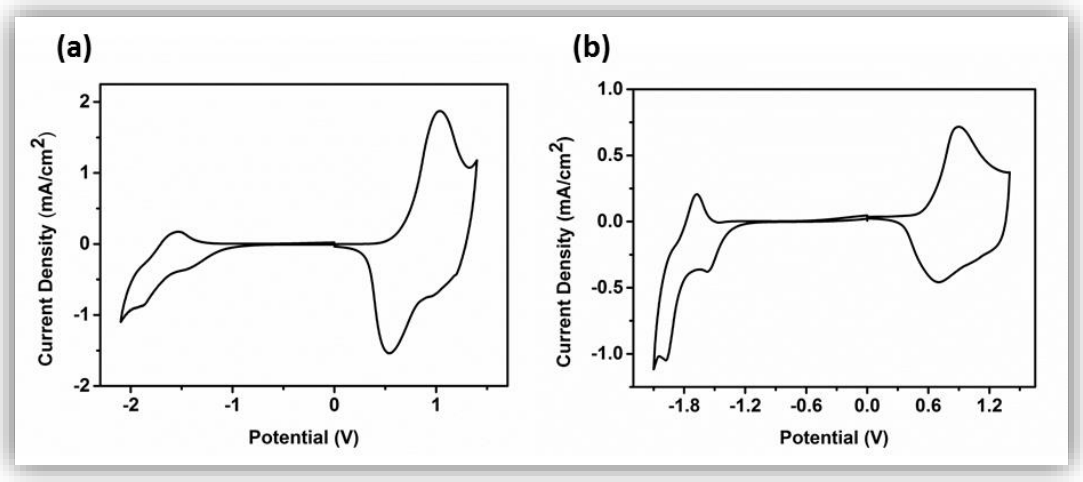

Figure 3. 18. Single scan cyclic voltammograms of (a) PBTP1 and (b) PBTP2 in a monomer free 0.1 M $TBAPF_6$/ACN solution.

When PBTP1 and PBTP2 were compared in terms of their oxidation potentials, differences can be explained with the π- bridges which affect the electron densities on polymer chains significantly. The number of thiophene unit for PBTP2 in the main chain is higher than that of PBTP1 so the electron density in the polymer backbone for the latter is higher which makes doping/ dedoping process easier at lower potentials.

The scan rate dependence of the doping/dedoping processes was explored via cyclic voltammetry with recording CVs at different scan rates. As seen in Figure 3.19, a linear dependence of current density to the scan rate was observed for both polymers which proves that the polymer films were well adhered and reversible doping/dedoping process is non-diffusion controlled.

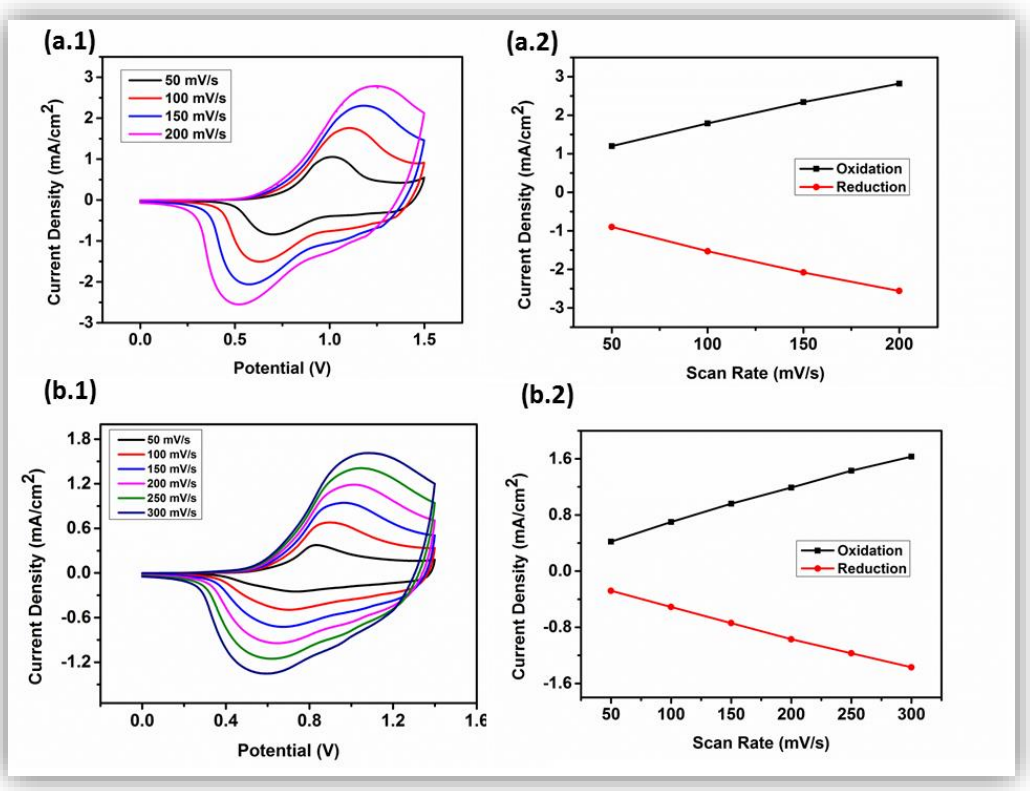

Figure 3. 19. Scan rate dependence of (a) PBTP1 and (b) PBTP2 films in a 0.1 M $TBAPF_6$ /ACN solution.

3.4.2. Spectroelectrochemistry

Spectroelectrochemical analyses were performed for both polymers in order to investigate the optical properties, formation of charge carriers via stepwise oxidation and calculate some crucial parameters as band gap. For spectroelectrochemical studies, both polymers were dissolved in $CHCl_3$ and spray coated onto ITO substrate. PBTP2 has lower solubility compared to that of PBTP1 so in order to acquire a homogeneous solution polymer solution was heated at 80 ^oC. Then, spectroelectrochemical studies were performedwith UV-Vis-NIR spectrophotometer in 0.1 M $TBAPF_6$/ACN solutions via incrementally increasing applied potential.

Before starting oxidation, constant potentials were applied to remove any trapped ions or charges to record true neutral state absorptions. Recording neutral state absorption is crucial to estimate the optical band gap correctly. Then, electronic absorption spectra were recorded while applying potential incrementally. During stepwise oxidation, new absorption bands namely polarons (radical cations) and bipolarons (bications) were appeared in NIR region while the neural state absorptions (λmax) were decreasing steadily. Polaron and bipolaron bands were observed at 780 nm/1300 nm for PBTP1 and at 700 nm/1100 nm for PBTP2.

As mentioned before absorption characteristics of polymers in the visible region and corresponding band gaps are important especially for organic solar cell applications. For this purpose λ_{max} and E_g^{op} valueswere calculated from Figure 3.20 and all data were depicted in Table 3.7. While λ_{max} values were recorded as 413/469 nm and 480 nm, the optical band gaps (E_g^{op}) were calculated as 1.88 eV and 1.85 eV for PBTP1 and PBTP2 (Table 3.7). As usual, optical band gaps were estimated from the onsets of lowest energy π-π* transitions.

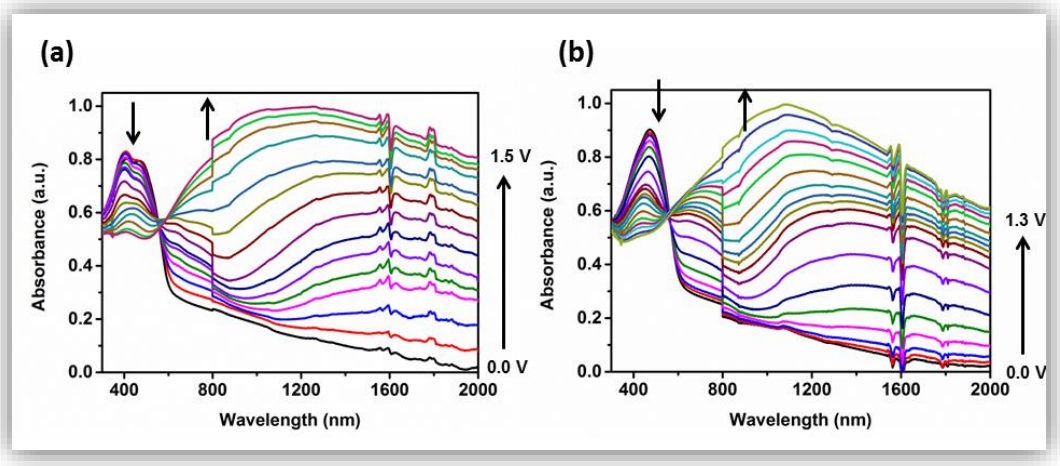

Figure 3. 20. Electronic absorption spectra of (a) PBTP1 and (b) PBTP2 in 0.1 M $TBAPF_6$/ACN solution.

Similar to the electrochemical behaviors, optical properties significantly affected by electron density on the polymer backbone. In addition, molecular weight and effective conjugation length are also crucial parameters. When PBTP1 and PBTP2 were compared in terms of their λ_{max} values, 11 nm red shift was observed for PBTP2. This red shift could be attributed to the changing π bridge from thiophene to the two thiophene. During molecular design, altough the expectation on π bridge effect is higher, this small shift could be explained with poor solubility of PBTP2 compared to that of PBTP1.

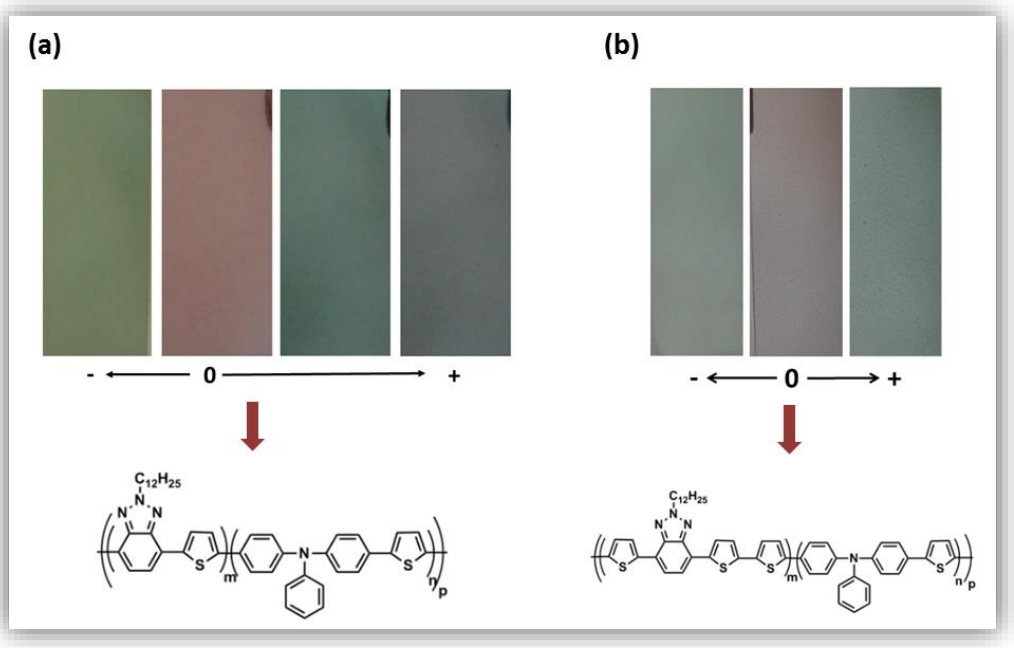

Figure 3. 21. Structures of the polymers and corresponding colors at their neutral and oxidized/reduced states.

Electrochromicity of polymers is another important parameter for conducting polymers since their colors in different states affect their applicability in different fields significantly such as; displays, mirrors, windows and sun-glasses. As seen in Figure 3.21, while PBTP1exhibits red color in the neutral state, it turns to gray in its oxidized state and green in the reduced states. In addition, PBTP1 has greenish blue color as the intermediate. Same experiments were also performed for the second polymer and PBTP2 shows red color in the neutral states with gray and greenish gray color at the oxidized and reduced states. (Figure 3.21)

Table 3. 7. Summary of spectroelectrochemical properties of PBTP1 andPBTP2.

	E_g^{ec} (eV)	λmax (nm)	E_g^{op} (eV)
PBTP1	2.23	413/469	1.88
PBTP2	2.31	480	1.85

3.4.3. Electrochromic contrast and switching studies

For electrochromic contrast and switching studies polymer films were prepared as described before on ITO electrodes. Experiments were performed via sweeping the applied potentials between its two extreme states (fully neutral and oxidized states) within 5 s time intervals. Similarly, monomer free 0.1 M $TBAPF_6$/ACN solution was used.

As a result of kinetic studies, optical contrast (the change in percent transmittance between neutral and oxidized states) and switching times (the time required for one full switch) were calculated and reported in Table 3.8 These parameters are important especially for electrochromic device applications. The wavelengths at which kinetic studies were performed were determined from the spectroelectrochemical studies as maximum absorbance values.

As illustrated in Table 3.8, PBTP1 showed 50 % transmittance change upon doping/dedoping processes at 1300 nm, 33% at 780 nm, and 17 % at 480 nm. Recorded optical contrast values for PBTP2 are 45 % at 1100 nm, 21% at 700 nm, and 22% at 475 nm. Switching times were calculated from Figure 3.22 as 1.8 s (1300 nm), 1.0 s (780 nm), and 0.7 s (480 nm) for PBTP1 and 1.7 s (1100 nm), 0.6 s (700 nm), and 0.5 s (475 nm) for PBTP2. The improved switching times and stability for PBTP2 compared to that of PBTP1 may be explained with the length of spacer unit

(thiophene vs. two thiophene) which most probably make doping/dedoping process easier.

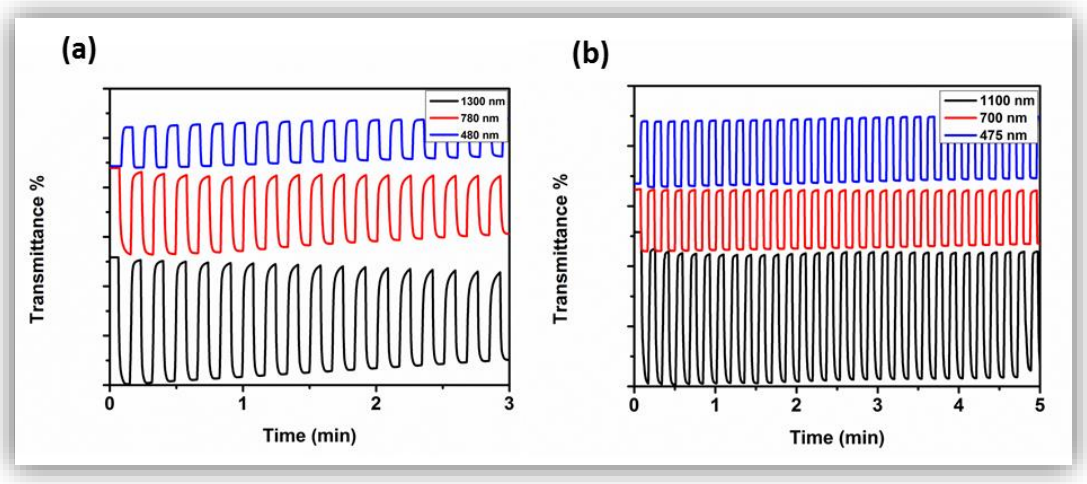

Figure 3. 22. Optical transmittance changes (a) for PBTP1 at 480 nm, 780 nm, 1300 nm and (b) for PBTP2 at 475 nm, 700 nm, 1100 nm in 0.1 M ACN/TBAPF$_6$ solution.

Table 3. 8. Summary of kinetic studies of PBTP1 and PBTP2.

	Wavelength (nm)	Optical Contrast (T %)	Switching Times (s)
PBTP1	1300	50	1.8
	780	33	1.0
	480	17	0.7
PBTP2	1100	45	1.7
	700	21	0.6
	475	22	0.5

3.4.4. Photovoltaic Properties

Performances of PSCs based on PBTP1 and PBTP2 were investigated with the device structure of ITO/PEDOT:PSS/Polymer(PBTP1/PBTP2):$PC_{71}BM$ /LiF/Al (Fig. 3.23).For organic solar cell device construction, $PC_{71}BM$ was used as the acceptor because of its stronger absorption in visible region compared to those of $PC_{61}BM$. In order to smooth the ITO electrode surface and increase the work function of ITO, PEDOT:PSS wascoated on an ITO electrode as hole transport layer.Energy levels of the respective materials were proposed in Figure 3.24.

Firstly proper solvents for both polymers were decided to construct efficient devices. While the PBTP1 - $PC_{71}BM$ blends were prepared in chlorobenzene (CB), the PBTP2 - $PC_{71}BM$ blends were prepared in 1,2-dichlorobenzene (DCB) due to poor solubility of PBTP2.This solubility difference could be attributed to their different molecular weights. Optimization studies of OSC were performed via exploring the effect of polymer:$PC_{71}BM$ ratios, additives, MeOH treatment and thermal annealing.

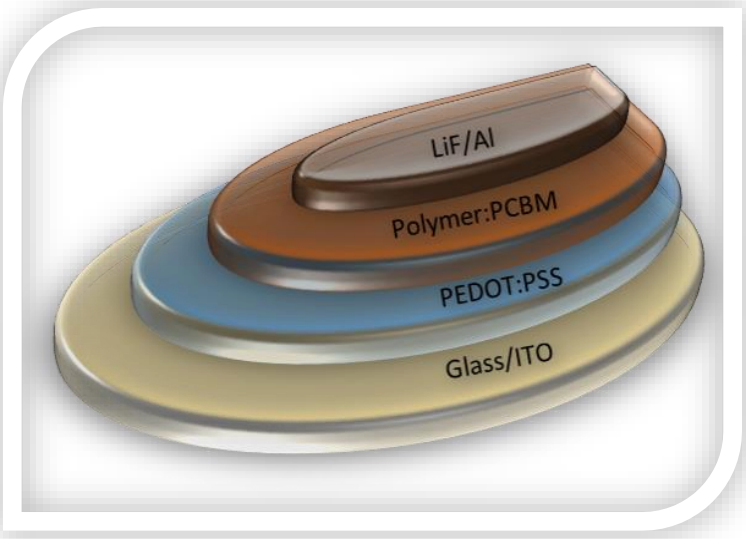

Figure 3. 23. Schematic representation of device configuration.

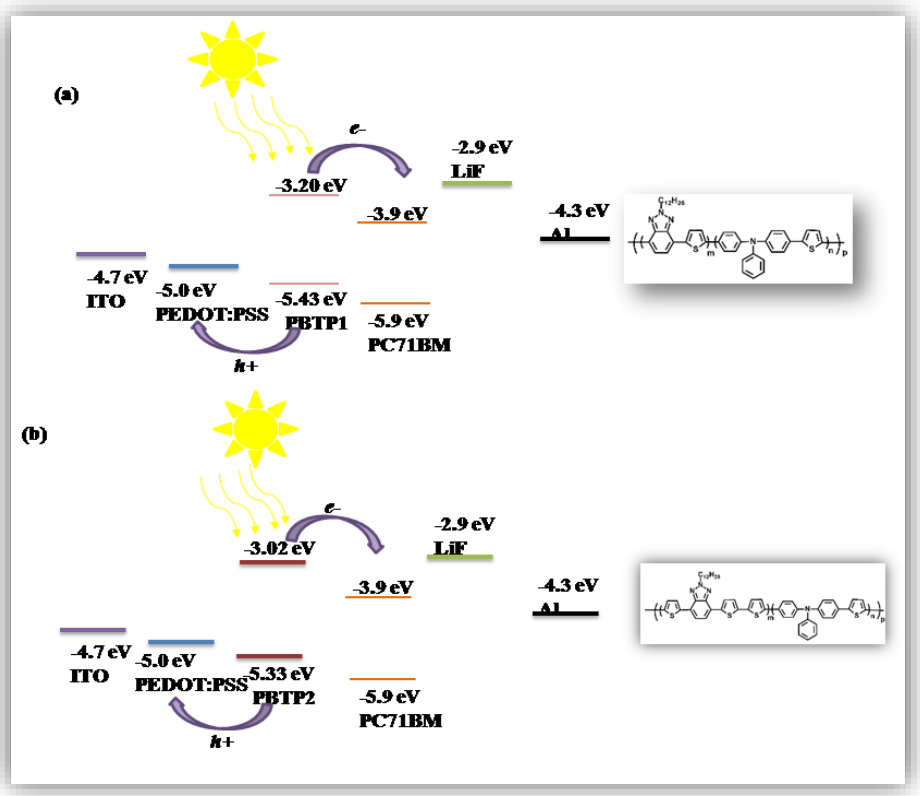

Figure 3. 24. Energy levels of polymers, ITO, PEDOT:PSS, PC71BM, LiF and Al .

After deciding on best solvents, the optimum weight ratios polymer to $PC_{71}BM$ were determined as 1:3 (PBTP1:PCBM) and 1:2 (PBTP2:PCBM). Photovoltaic parameters of the resulting devices which showed the highest performance and effect of additive usage/MeOH treatment are summarized in Table 3.9. Related I-V curves of the photovoltaic devices are depicted in Figure 3.25.

Before further optimization, the best device gave a PCE of 1.77 %, with V_{oc} of 0.620 V, Jsc of 6.65 mA cm^{-2}, and FF of 43% for PBTP1bearing device and PBTP2 based PSCs showed the highest photovoltaic performance of 1.48% with Voc of 0.64 V, Jsc of 6.10 mA $cm^{-2}$and FF (fill factor) of 38%.

In order to improve the photovoltaic performance and the morphology of the active layer, in literature annealing treatments, addition of an additive or methanol treatment can be carried widely[67-70].It is well known that “processing additives”

improve the morphology of the BHJ material which increases the performance of the resulting solar cells [71]. In addition, the underlying mechanism of the methanol treatment effect can be attributed to the modification of the interface between the PEDOT:PSS and the active layer which is the mixture of polymer and PCBM[72].

After additive processing (1,8-diiodooctane) and MeOH treatment, results for solar cells showed the highest photovoltaic performance as reported in Table 3.9. As seen, while treatments and additive processing improved PCE from 1.77 % to 2.72 % for PTPB1, PCE of PBTP2 based devices were enhanced from 1.48% to 3.65%.

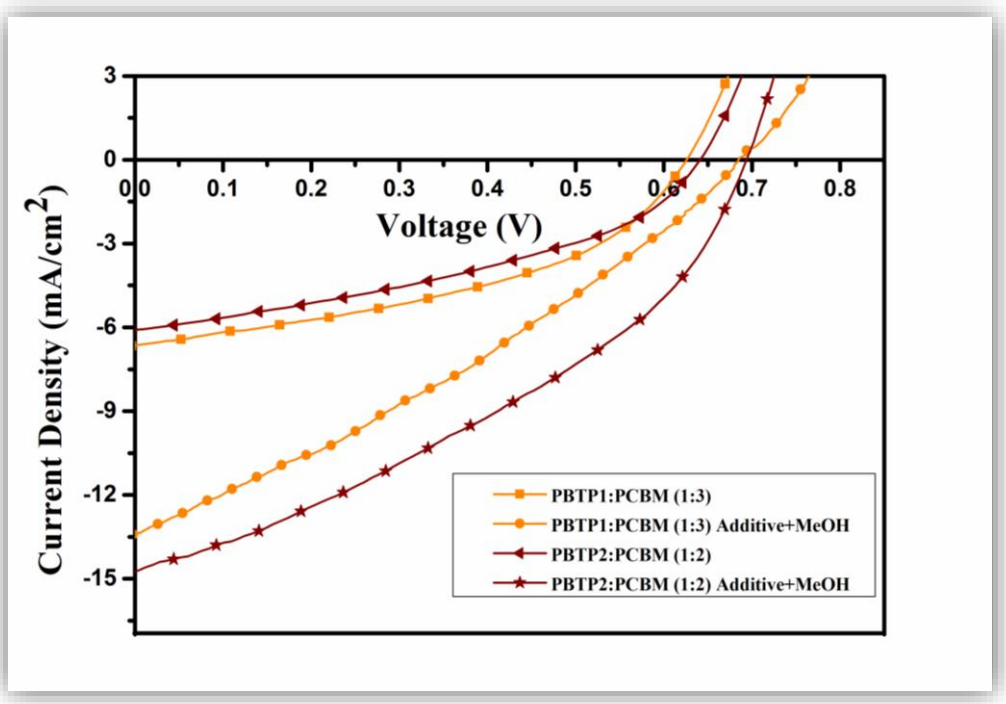

Figure 3. 25. J–V curves of bulk heterojunction OSCs based on PBTP1/PBTP2:$PC_{71}BM$.

Table 3. 9. Photovoltaic properties of bulk heterojunction OSCs based on PBTP1/PBTP2: $PC_{71}BM$.

Polymer	Polymer :$PC_{71}BM$ ratio	V_{oc} (V)	J_{sc} (mA/cm^2)	FF (%)	η (%)	Treatment
PBTP1	1:3	0.62	6.65	43	1.77	
PBTP1	1:3	0.60	9.99	37	2.21	Additive
PBTP1	1:3	0.68	13.36	30	2.72	Additive - MeOH
PBTP2	1:2	0.64	6.10	38	1.48	
PBTP2	1:2	0.69	14.73	36	3.65	Additive/MeOH

IPCE could be defined as the ratio of photocurrent to the incident photons, which are converted to carriers collected at the electrodes under short circuit conditions[73]. As illustarted in Figure 3.26, photocurrent response of both systems started from 350 nm and ended at 800 nm. The highest IPCE values of the devices reported as 28% for PBTP1 and 48% for PBTP2. Furthermore, both polymers as donor materials and PCBM made contribution to photon to electron conversion.

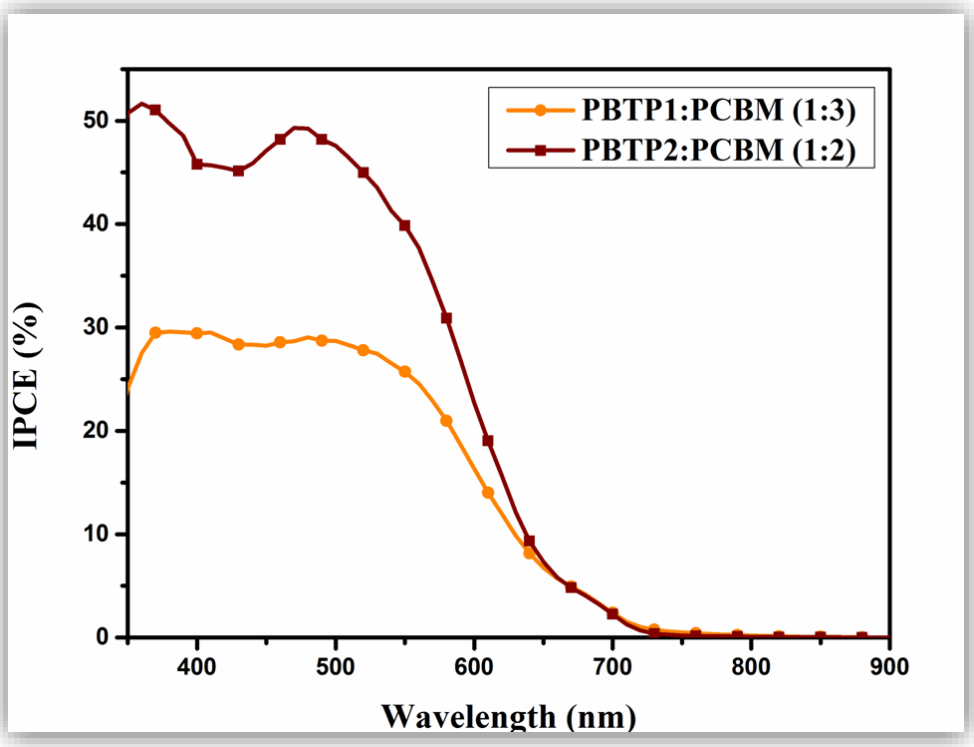

Figure 3. 26. IPCE curves of the best performance solar cells.

CHAPTER 4

CONCLUSION

Herein, it is aimed to design, synthesize and characterize novel donor-acceptor-donor type conducting polymers in order to use in the design of electrochromic devices and organic solar cells. Forthis purpose, mainly benzotriazole bearing polymers were designed. Firstly a novel acceptor unit triazzoloquinoxaline which is the combination of benzotriazole and quinoxaline units was synthesized. After synthesis of this new acceptor unit, it was coupled with donor units and electrochemical and spectroelectrochemical characterization were performed. Furthermore another important unit triphenylamine was inserted into the benzotriazole based polymers and affect of π bridge on electrochemical behaviors were also investigated via synthesizing benzotriazole and triphenylamine bearing random copolymers. Designed polymers are multifuntional and show promising results via applications. While triazoloquinoxaline derivatives were used for electrochromic device applications, triphenylamine bearing copolymers were used for organic solar cell applications as donor materials.

Three new donor–acceptor type monomers bearing combined benzotriazole and quinoxaline units as the acceptor and thiophene as the donor group were synthesized. Although both quinoxaline and benzotriazole derivatives were widely studied in the literature, their combination in one acceptor unit, in order to have a more electron deficient acceptor unit, was designed for the first time. After the characterization of the monomers, their polymers were electrochemically synthesized on ITO coated glass slides to investigate their electrochemical and optical properties. All polymers are both p- and n-dopable. Furthermore, themulticolored n-doped state for all polymers is a rare property that widens their use in several applications. Spectroelectrochemical studies illustrate the broad absorptions between 700 nm and

1000 nm which in return refer to low band gap polymers with about 1.00 eV. Another attractive character of the prepared polymers is their high optical contrast in the NIR region, especially for P1 which has 93% contrast at 2000 nm which makes it a promising candidate for NIR electrochromic applications.

Triphenylamine was utilized as another important donor unit to probe its effect on optical and electrochemical properties. Three new TPA and BTz comprising donor–acceptor–donor-type random copolymers were synthesized successfully. Their electrochemical and spectroelectrochemical characteristics were investigated by CV and spectroelectrochemistry. All polymers showed good solubility and high film quality. Changing π-bridges affect the oxidation potentials significantly due to their electron density on the polymer backbone. While PTPB2 and PTPB3 are only p-type dopable, PTPB1 has also n-type dopable characteristics. PTPB1 display red color in its neutral state and multichromic in different oxidized states. While PTPB2 is yellow and PTPB3 is orange in their neutral states, both show blue color in their oxidized states. Kinetic results illustrate that PTPB1 has shorter switching time, which can be explained by the increasing length of spacer unit which most probably leads to improved ion diffusion and dopant insertion. The role of TPA unit as a potential electron donating material and hole transporting material makes it a good choice for these structures.

Then P2(triazoloquinoxaline based polymer)/PEDOT based dual type electrochromic device (ECD) was constructed by taking advantage of P2polymer film where its electrochromic performance was investigated by cyclic voltammetry, chronoamperometry and UV-vis spectrophotometer techniques.P2/PEDOT ECD is operating between green (-1.3 V) and blue (1.3 V). The ECD exhibited good long-term stability with reasonable optical memory under atmospheric conditions. Altough optical contrast values are not so high for the resulting ECD, long term stability is promising at that operating potentials.

Finally triphenylamine and benzotriazole bearing random copolymers were resynthesized with improved synthesis and purification techniques. Resulting polymers PBTP1 and PBTP2 were characterized in terms of electrochemical and spectroelectrochemical behaviors and they were used as donor materials for organic solar cell applications. OSC fabrication of PBTP1 and PBTP2 were performed with conventional device configuration and optimization studies like usage of different polymer: PCBM blend ratio, annealing, solvent, methanol treatment, and additive were performed. After additive processing (1,8-diiodooctane) and MeOH treatment, PCE results were increased from 1.77 % to 2.72 % for PTPB1and from 1.48% to 3.65% for PTPB2.

REFERENCES

1. H. Letheby, J. Chem. Soc. 1862, 15, 161

2. G. Natta, G. Mazzanti, P. Corraddini, Atti. Acad. Naz. Lincei Rend.CI. Sci. Fis. Mat. Natur, 1958, 25, 3

3. H. Shirakawa, E. J. Louis, A. G. MacDiarmid, C. K. Chiang, A. J Heeger, J. Chem. Soc. Chem. Commun. 1977, 578

4. C. K. Chiang, Y. W. Park, A.J. Heeger, H. Shirakawa, E. J. Louis, A.G. MacDiarmid, Phys. Rev. Lett. 1977, 39, 1098

5. M.Dobbelin, R. Marcilla, C. Pozo-Gonzalo and D. Mecerreyes, J. Mater. Chem. 2010, 20, 7613–7622

6. A. Hadipour, B. Boer, J. Wildeman, F. B. Kooistra, J. C. Hummelen, M. G. R. Turbiez, M. M. Wienk, R. A. J. Janssen and P. W. M Blom, Adv. Funct. Mater. 2006, 16, 1897–1903

7. C. A. Zuniga, S. Barlow and S. R. Marder, Chem. Mater. 2011, 23, 658–681

8. M. Horie, L. A. Majewski, M. J. Fearn, C. Y. Yu, Y. Luo, A. Song, B. R. Saunders and M. L. Turner, J. Mater. Chem., 2010, 20, 4347–4355

9. F. Ekiz, F. Oguzkaya, M. Akin, S. Timur, C. Tanyeli and L. Toppare, J. Mater. Chem., 2011, 21, 12337–12343

10. L. Dami, Intelligent Macromolecules for Smart Devices From Materials Synthesis to Device Applications, Springer-Verlag London Limited, 2004

11. K. Shimamura, F.E. Karasz, J.A.Hirsch, J.C. Chien, Makromol. Chem. Rapid Commun. 1981, 2, 443.

12. J. L. Bredas, G. B Street, Acc. Chem. Res. 1985,18, 309

13. B. D. Malhotra, Handbook of Polymers in Electronics, United Kingdom, Rapra Technology Limited, 2002

14. J. L. Dai, Rev. Macromol. Chem. Phys., C39(2) (1999) 273–387.

15. A. G. Macdiarmid, Angew. Chem. Int. Ed., 40 (2001) 2581.

16. K. Müllen, J. R Reynolds, T. Masuda, Conjugated Polymers: A Practical Guide to Synthesis, Cambridge, GBR: Royal Society of Chemistry, 2013

17. F. A. Carey, R.J. Sudberg, Advanced Organic Chemistry, Part B: Reactions and Synthesis, New York, NY: Springer, 2001

18. K. Yoshino, S. Hayashi and R.Sugimoto, Japanese Journal of Applied Physics, part 2, 23, 1984, L899

19. L. B. Groenendaal, G. Zotti,P. H. Aubert, S. M. Waybright, J. R. Reynolds Adv. Mater., 2003, 15, 855.

20. J. Roncali, Chem. Rev., 1992, 92, 711.

21. M. E. G. Lyons, in Advances in Chemical Physics, Polymeric Systems, ed. I. Prigogine and S. A. Rice, John Wiley & Sons, New York, 1997, 94, 297

22. S. Hotta, T. Hosaka, W. Shimotsuma, Synth. Met.,1983, 6, 319.

23. N. S. Sariciftci, L. Smilowitz, , A. J. Heeger, F Wudl, Science ,1992,258, 1474

24. F. C. Krebs, Polymer Photovoltaics, Bellingham, Wash.:SPIE Press, 2008

25. A. Luque, S. Hegedus, Handbook of Photovoltaic Science and Engineering, Chichester, Wiley, 2003

26. H. Spanggaard, F. C. Krebs, Solar Energy Materials & Solar Cells 83 (2004) 125–146

27. R. Po, M. Maggini, N. Camoioni, J. Phys. Chem. C., 2010, 114, 695.

28. Y.-J. Cheng, S.-H. Yang, C.-S. Hsu, Chem. Rev. 2009, 109, 5868–5923

29. S. Gunes, H. Neugebauer, N. S. Sariciftci, Chem. Rev. 2007, 107, 1324-1338

30. V. A. Trukhanov, V. V. Bruevich, D.Y. Paraschuk, Sci. Rep. 2015, 5, 11478

31. M. Pagliaro, G. Palmisano, R. Ciriminna, 2008, Weinheim, Wiley-VCH

32. B. Qi, J. Wang,J. Mater. Chem. 2012, 22, 24315

33. C. J. Brabec, A. Cravino, D. Meissner, N. S. Sariciftci, T. Fromherz, M. T. Rispens, L. Sanchez, J. C. Hummelen, Adv. Funct. Mater. 2001, 11, 374.

34. A. J. Heeger, Adv. Mater.,2010, 1, 26.

35. X. Guo, N. Zhou, S. J. Lou, J. Smith, D. B. Tice, J. W. Hennek, R. P. Ortiz, J. T. L. Navarrete, S. Li , J. Strzalka, L. X. Chen, R. P. H. Chang, A. Facchetti, T. J. Marks, Nature Photonics 2013,7, 825.

36. C. W. Tang, Appl. Phys. Lett. 1986, 48, 183.

37. R. J. Mortimer, A. L. Dyer, J. R. Reynolds, Displays 2006, 27, 2.

38. D. R. Rosseinsky, R .J. Mortimer, Adv. Mater. 2001, 13, 783.

39. R.J. Mortimer, Electrochimica Acta 1999, 44, 2971.

40. W. T. Neo, Q. Ye, S.-J. Chuaac, J. Xu,J. Mater. Chem. C, 2016, DOI: 10.1039/c6tc01150k.

41. (a)P. R. Somani , S. Radhakrishnan, Mat .Chem. Phys. 2002, 77, 117.
(b) eetdnews.lbl.gov/nl05/eetd-nl05-1-window.html

42. Y.J. Cheng, S. H. Yang, C.S. Hsu, Chem. Rev. 2009, 109, 5868.

43. A. Iwan, D. Sek, Progress in Polymer Science, 2011, 36, 1277.

44. H. J. Yen, G. S. Liou, Polym. Chem. 2012, 3, 255.

45. M. Ouyang, G. Wang, C. Zhang, Electrochim. Acta, 2011, 56, 4645.

46. C. Xu, J. Zhao, C. Cui, M. Wang, Y. Kong, X. Zhang, J. of Electroanal. Chem. 2012, 682, 29.

47. G.L. Wu, G.J. Zhao, C. He, J. Zhang, Q.G. He, X.M. Chen, Y.F. Li, Sol. Energy Mater. Sol. Cells, 2009, 93, 108.

48. Y. Liu, Y. Xin, J. Li, G. Zhao, B. Ye, S. Xu, S. Cao, Reactive & Functional Polymers, 2007, 67, 253.

49. S. Beaupre, J. Dumas, M. Leclerc, Chem. Mater., 2006, 18, 4011.

50. S.-H. Hsiao, J.-C. Hsueh, J. of Electroanal. Chem., 2015, 758, 100.

51. A. Tanimoto, T. Yamamoto, Macromolecules, 2006, 39, 3546.

52. A. Tanimoto, T. Yamamoto, Adv. Synth. Catal., 2004,346, 1818.

53. A. Balan, D. Baran, G. Gunbas, A. Durmus, F. Ozyurt, L. Toppare, Chem. Commun., 2009, 6768.

54. A. Durmus, G. E. Gunbas, L. Toppare, Chem. Mater., 2007, 19, 6247–6251.

55. G. Gunbas, A. Durmus and L. Toppare, Adv. Funct. Mater., 2008, 18, 2026–2030.

56. S. Ozdemir, M. Sendur, G. Oktem, O. Dogan, L. Toppare, J. Mater. Chem., 2012, 22, 4687.

57. J. Hai, B. Zhao, F. Zhang, C.-Xiang Sheng, L. Yin, Y. Li, E. Zhu, L. Bian, H. Wu, W. Tang, Polymer, 2013, 54, 4930.

58. D. Baran, F. M. Pasker, S. Le Blanc, G. Schnakenburg, T. Ameri, S. Hoger, C. J. Brabec, J. Polym. Sci. Part A: Polym. Chem., 2013, 51, 987.

59. J. Hai , B. Zhao , E. Zhu , L. Bian , H. Wu ,W. Tang, Macromol. Chem. Phys. 2013, 214, 2473.

60. J. Hai, W. Yu, B. Zhao, Y. Li, L. Yin, E. Zhu, L. Bian, J. Zhang, H. Wu, W. Tang, Polym. Chem., 2014, 5, 1163.

61. S. O. Hacioglu, S. Toksabay, M. Sendur, L. Toppare, J. Polym. Sci. Part A: Polym. Chem,, 2014, 52, 537.

62. P. Camurlu, C. Gultekin, Sol. Energy Mater. Sol. Cells, 2012, 107, 142.

63. P. Camurlu, C. Gultekin, Z. Bicil, Electrochim. Acta, 2012, 61, 50.

64. I. Yagmur, M. Ak, A. Bayrakceken, Smart Mater. Struct., 2013, 22, 115022.

65. G. Wang, X. Fu, J. Huang, C. L. Wu, L. Wu, J. Deng, Q. Du and X. Zou, Electrochim. Acta, 2011, 56, 6352.

66. D.Yigit, S. O. Hacıoglu, M. Gullu, L. Toppare, New J. Chem., 2015, 39, 3371.

67. D. Gedefaw, M. Tessarolo, W. Zhuang, R. Kroon, E. Wang, M. Bolognesi, M. Seri, M. Muccini, M. R. Andersson, Polym. Chem., 2014, 5, 2083.

68. Y. Zhang, L. Gao, C. He, Q. Sun, Y. Li, Polym. Chem., 2013, 4, 1474.

69. B. Qu, D. Tian, Z. Cong, W. Wang, Z. An, C. Gao, Z. Gao,H. Yang, L. Zhang, L. Xiao, Z. Chen, Q. Gong, J. Phys.Chem. C, 2013, 117, 3272.

70. C. Du, W. Li, Y. Duan, C. Li, H. Dong, J. Zhu, W. Hub, Z. Bo, Polym. Chem., 2013, 4, 2773.

71. J. K. Lee, W. L. Ma, C. J. Brabec, J. Yuen, J. S. Moon, J. Y. Kim, K. Lee, G. C. Bazan, A. J. Heeger, J. Am. Chem. Soc., 2008, 130, 3619.

72. K. Zhang, Z. Hu, C. Duan, L. Ying, F Huang, Y. Cao, Nanotechnology, 2013, 24, 484003.

73. W.C.H, Choy, Organic solar cells. London: Springer, 2013.

APPENDIX A

NMR DATA

NMR spectra were recorded on a Bruker DPX 400.

Chemical shifts δ are reported in ppm relative to $CHCl_3$ (^1H: δ=7.27), $CDCl_3$ (^{13}C: δ=77.0) and CCl_4 (^{13}C: δ=96.4) as internal standards.

^1H and ^{13}C NMR spectra of products are given below.

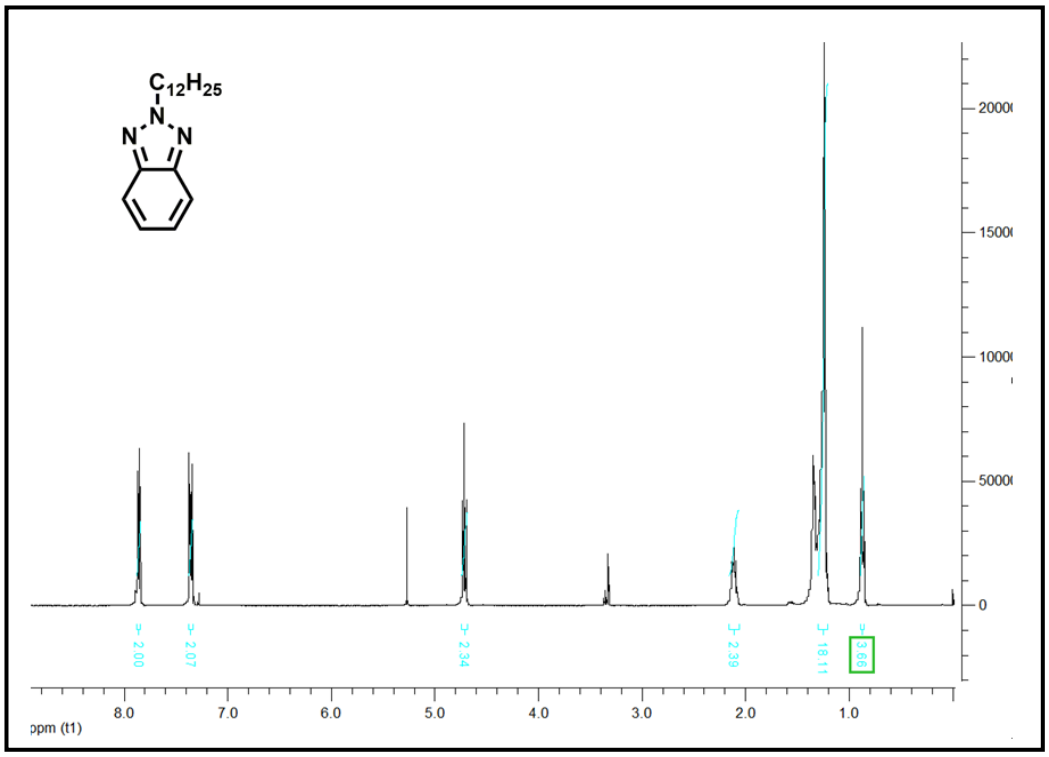

Figure A. 1. ^1H-NMR spectrum of 2-dodecyl-2H-benzo[d][1,2,3] triazole.

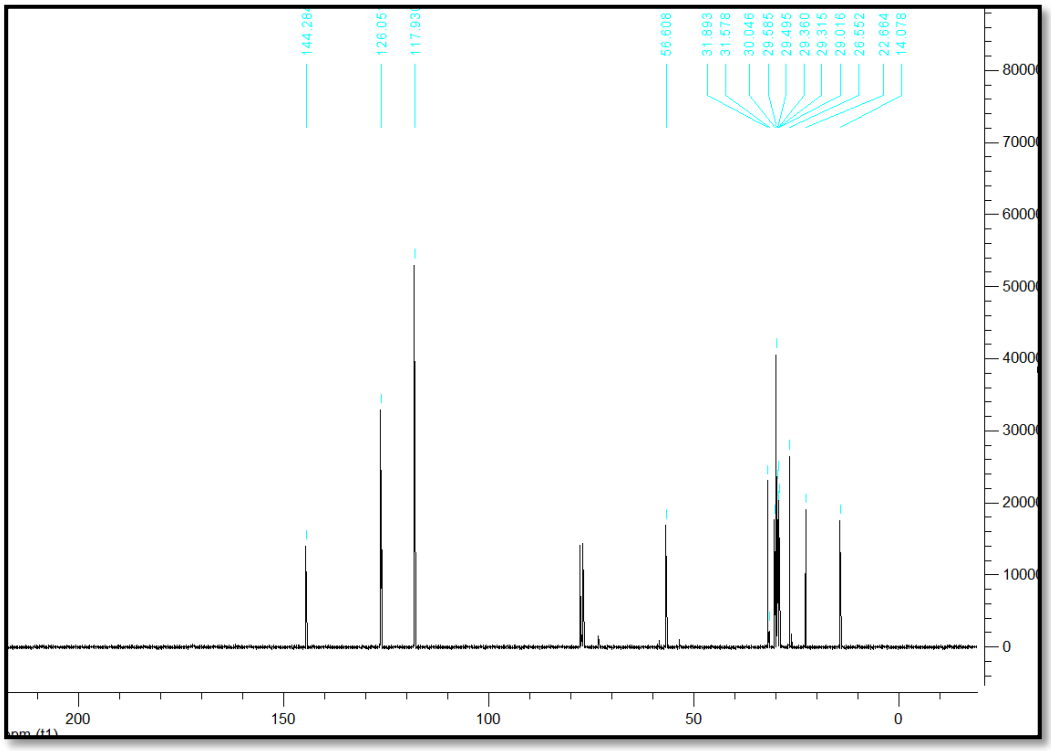

Figure A. 2. ^{13}C-NMR spectrum of 2-dodecyl-2H-benzo[d][1,2,3] triazole.

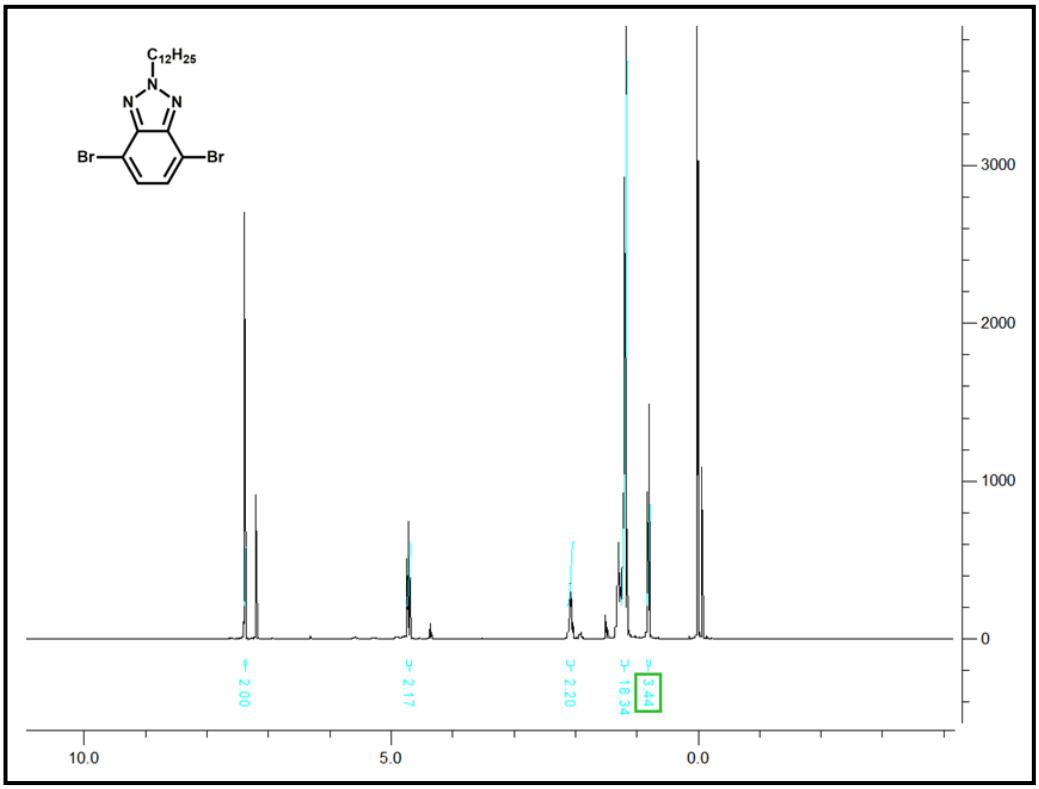

Figure A. 3. ^{1}H-NMR spectrum of 4,7-dibromo-2-dodecyl-2H-benzo[d][1,2,3]triazole.

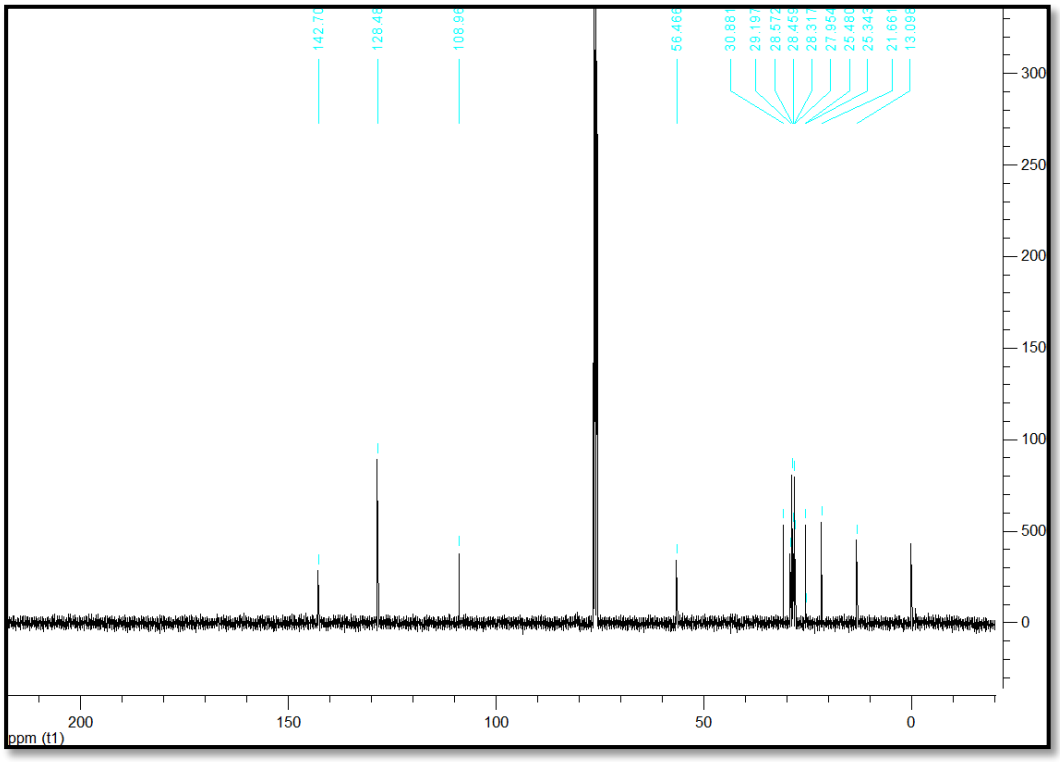

Figure A. 4. ^{13}C-NMR spectrum of 4,7-dibromo-2-dodecyl-2H-benzo[d][1,2,3]triazole.

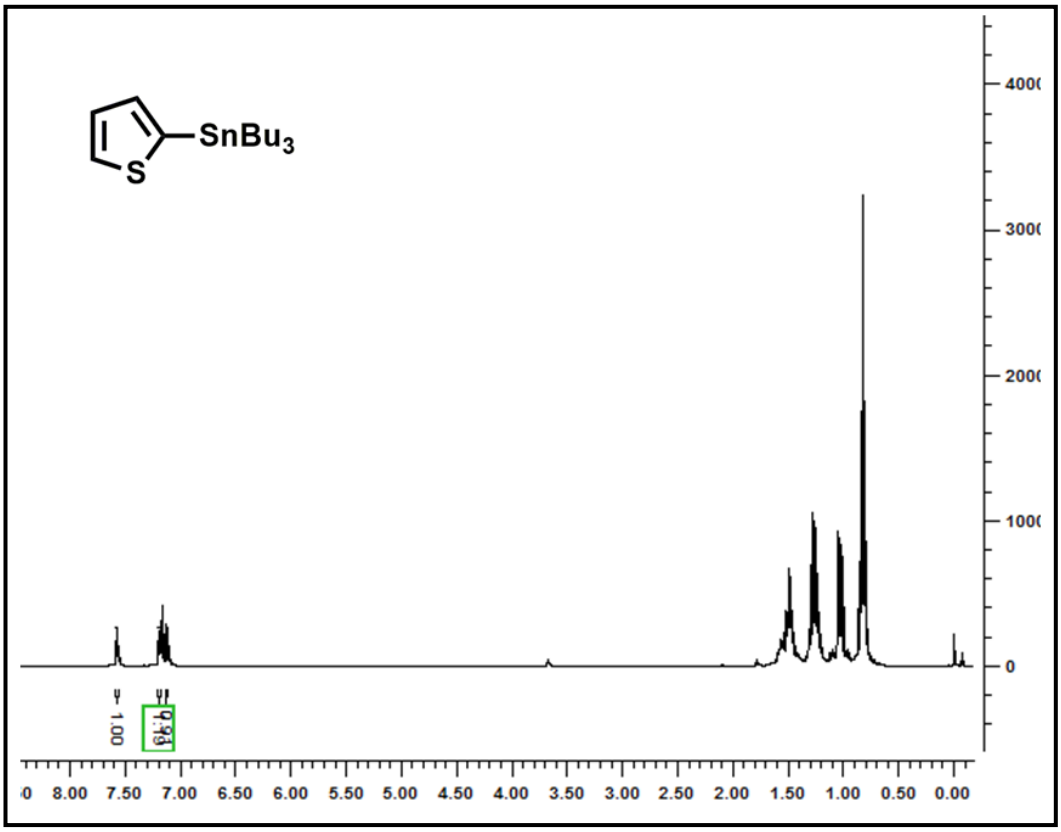

Figure A. 5. ^{1}H-NMR spectrum of tributyl(thiophen-2-yl)stannane.

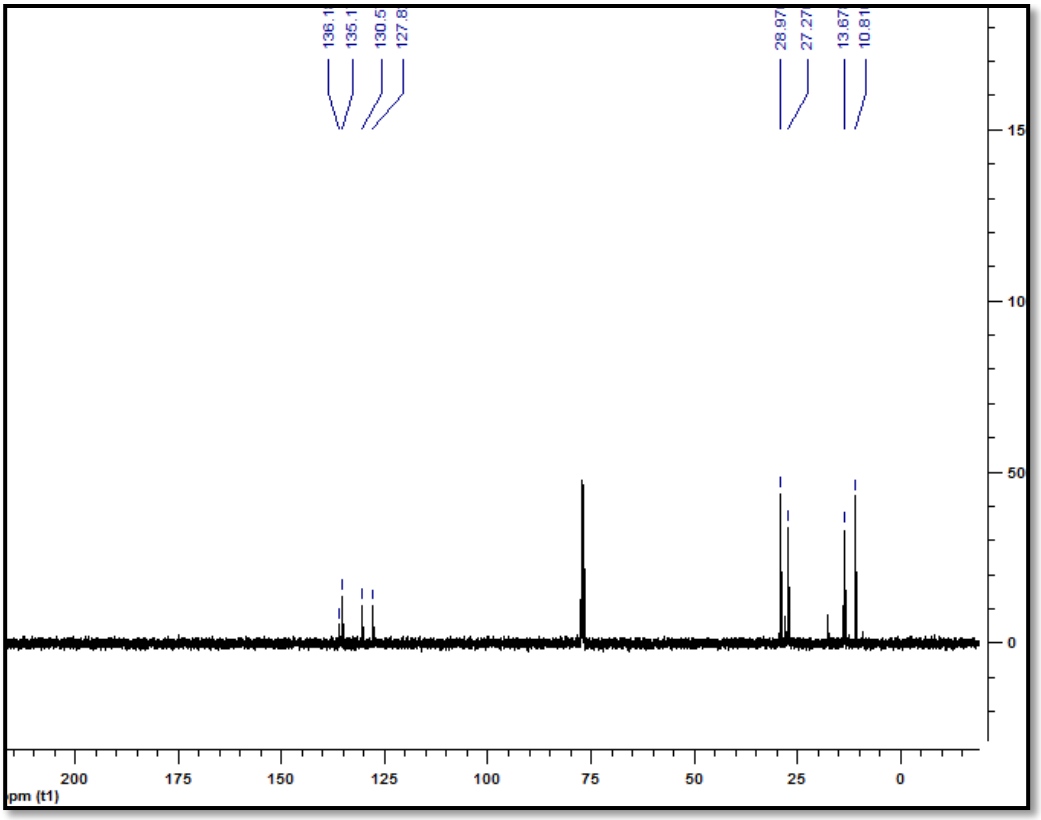

Figure A. 6. ^{13}C-NMR spectrum of tributyl(thiophen-2-yl)stannane.

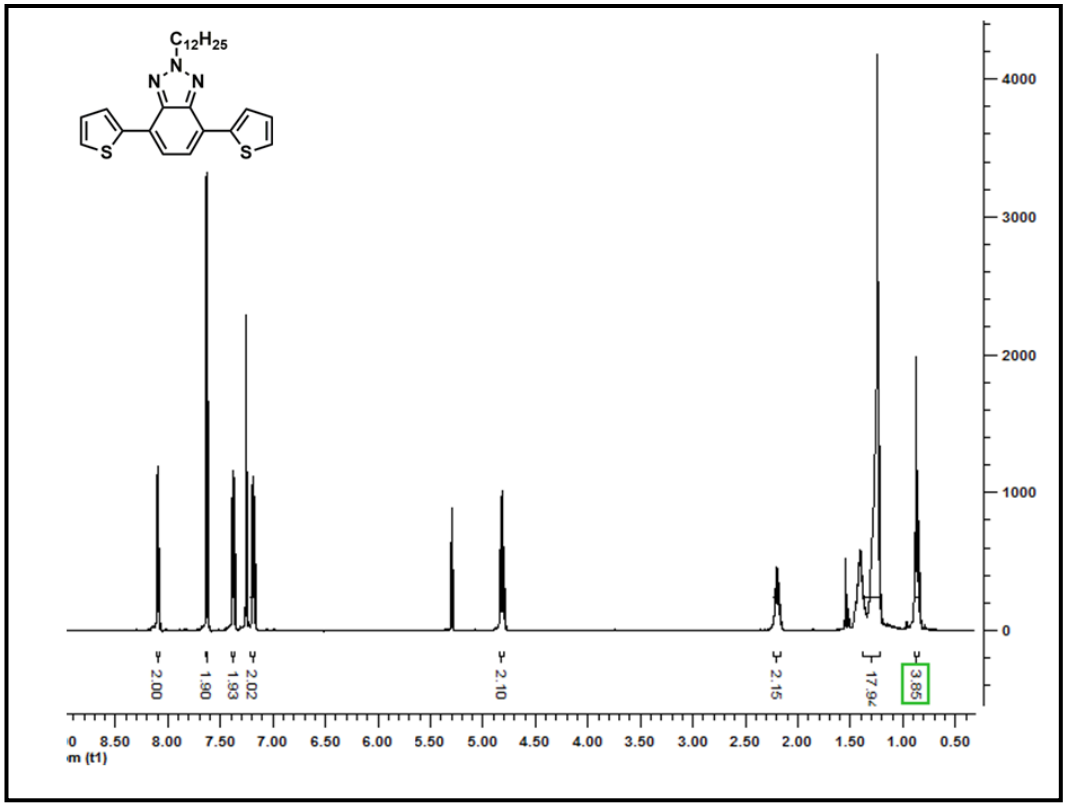

Figure A. 7. ^{1}H-NMR spectrum of 2-dodecyl-4,7-di(thiophen-2-yl)-2H-benzo[d][1,2,3]triazole.

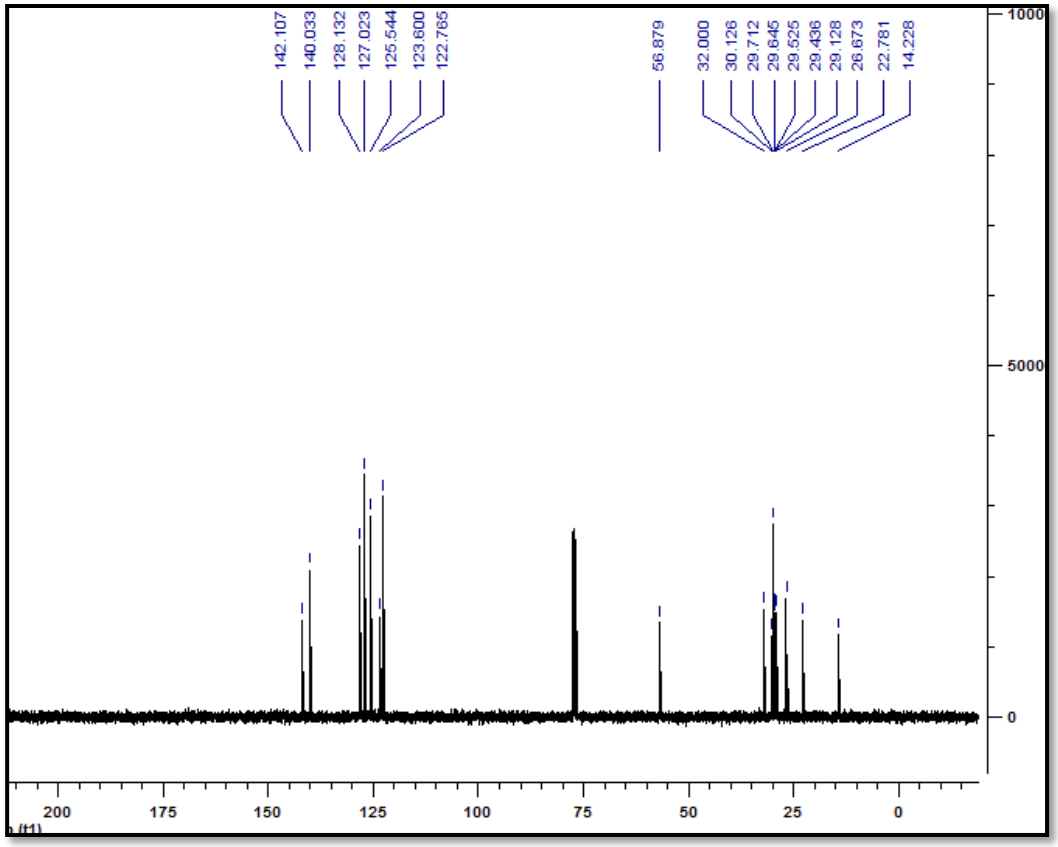

Figure A. 8. ^{13}C-NMR spectrum of 2-dodecyl-4,7-di(thiophen-2-yl)-2H-benzo[d][1,2,3]triazole.

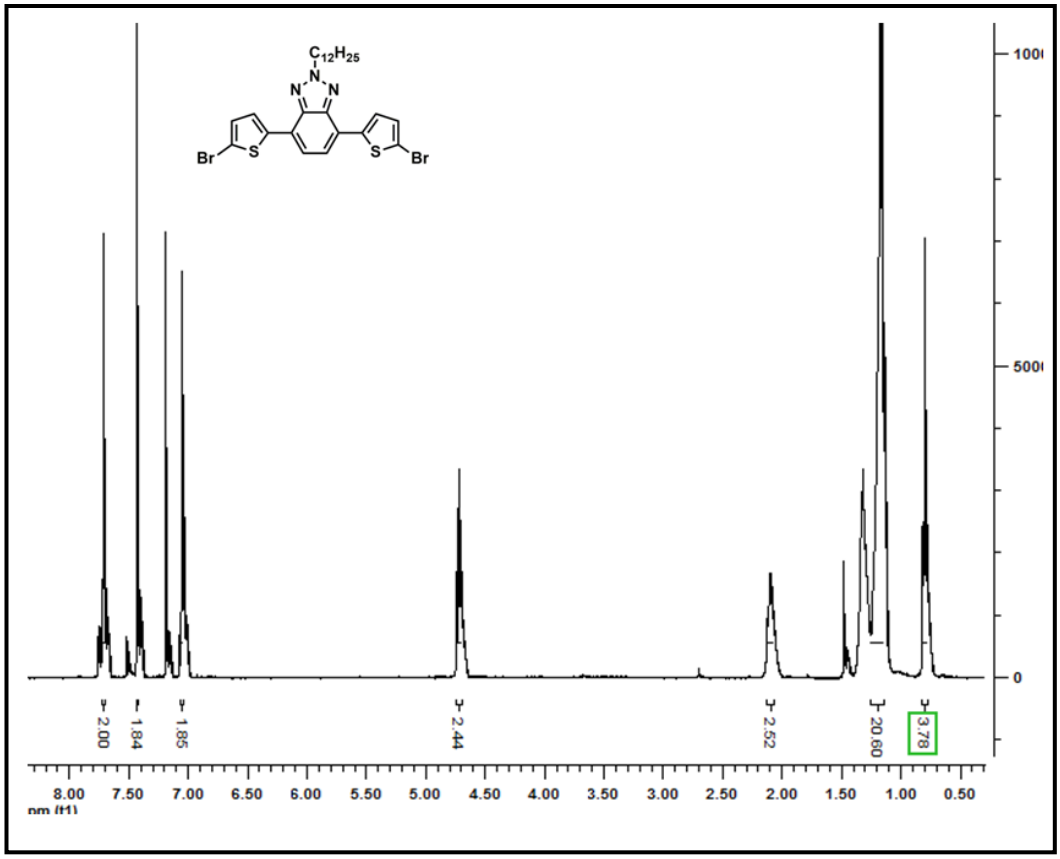

Figure A. 9. ^{1}H-NMR spectrum of 4,7-bis(5-bromothiophen-2-yl)-2-dodecyl-2Hbenzo[d][1,2,3]triazole.

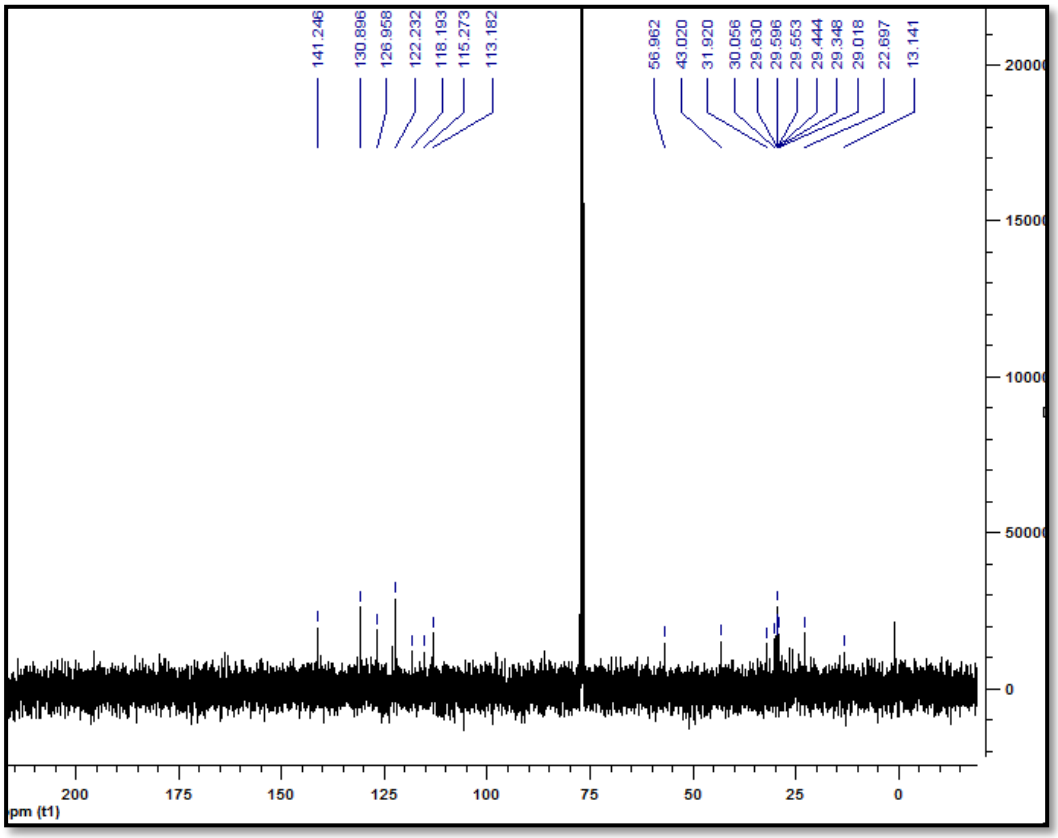

Figure A. 10. ^{13}C-NMR spectrum of 4,7-bis(5-bromothiophen-2-yl)-2-dodecyl-2Hbenzo[d][1,2,3]triazole.

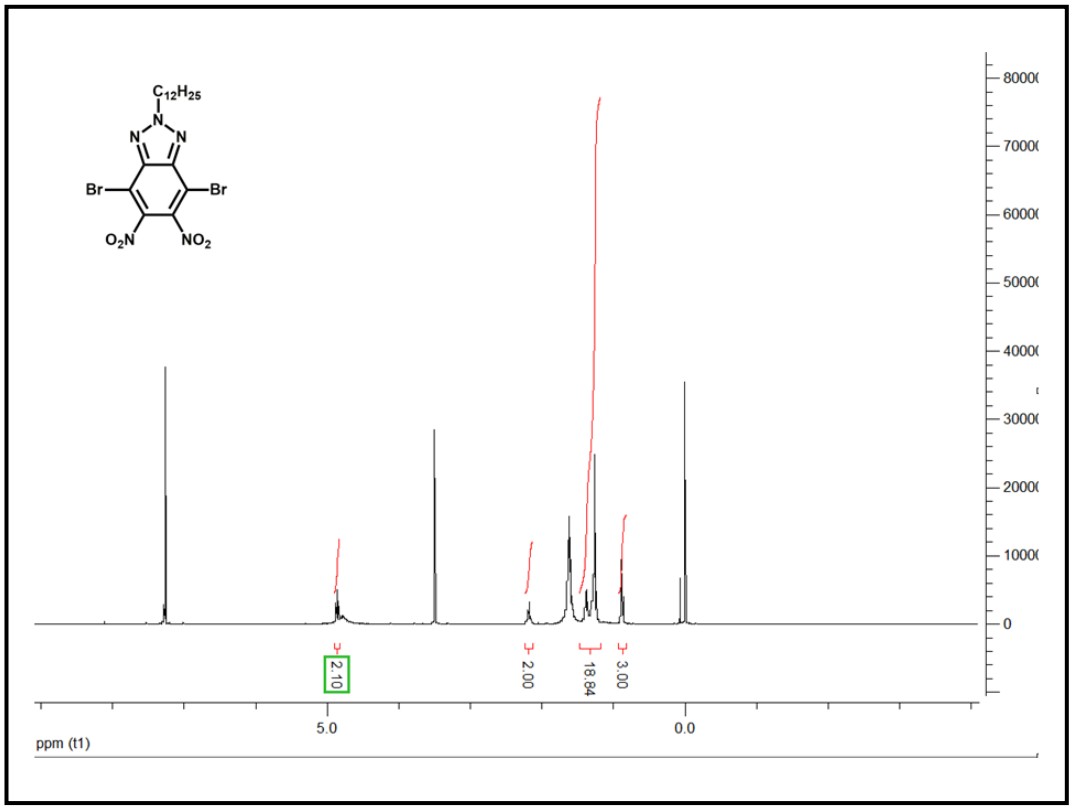

Figure A. 11. ^{1}H-NMR spectrum of 4,7-dibromo-2-dodecyl-5,6-dinitro-2H-benzo[d] [1,2,3]triazole.

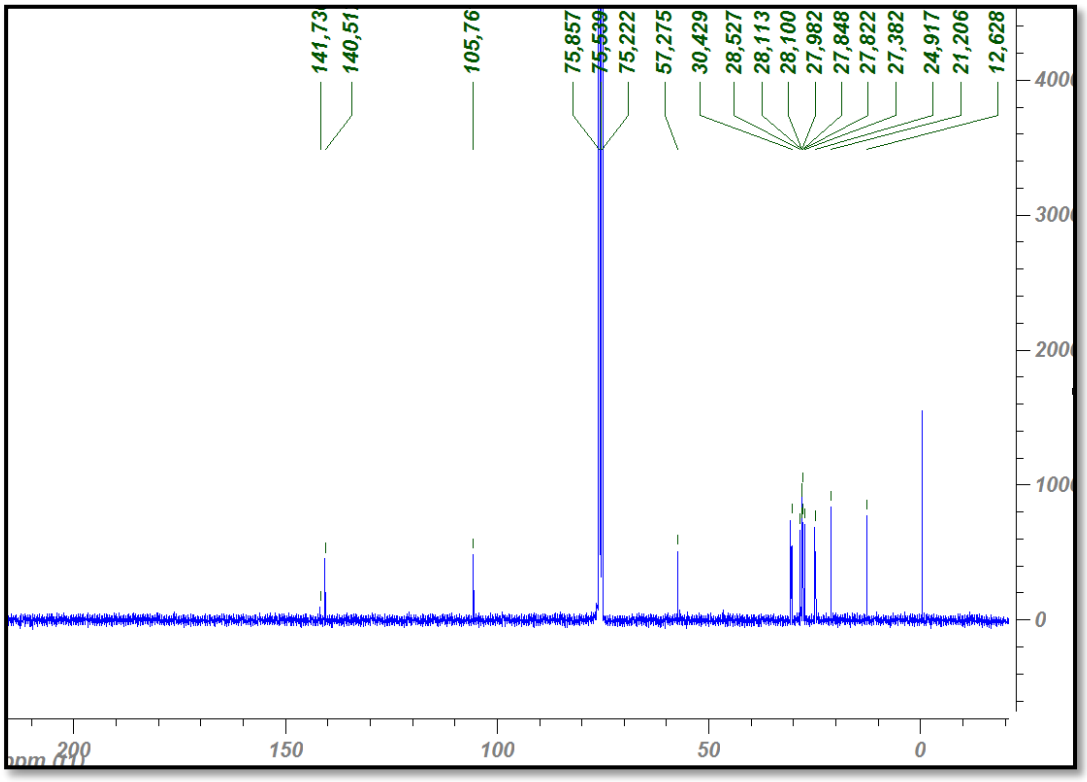

Figure A. 12. ^{13}C-NMR spectrum of 4,7-dibromo-2-dodecyl-5,6-dinitro-2H-benzo[d] [1,2,3]triazole.

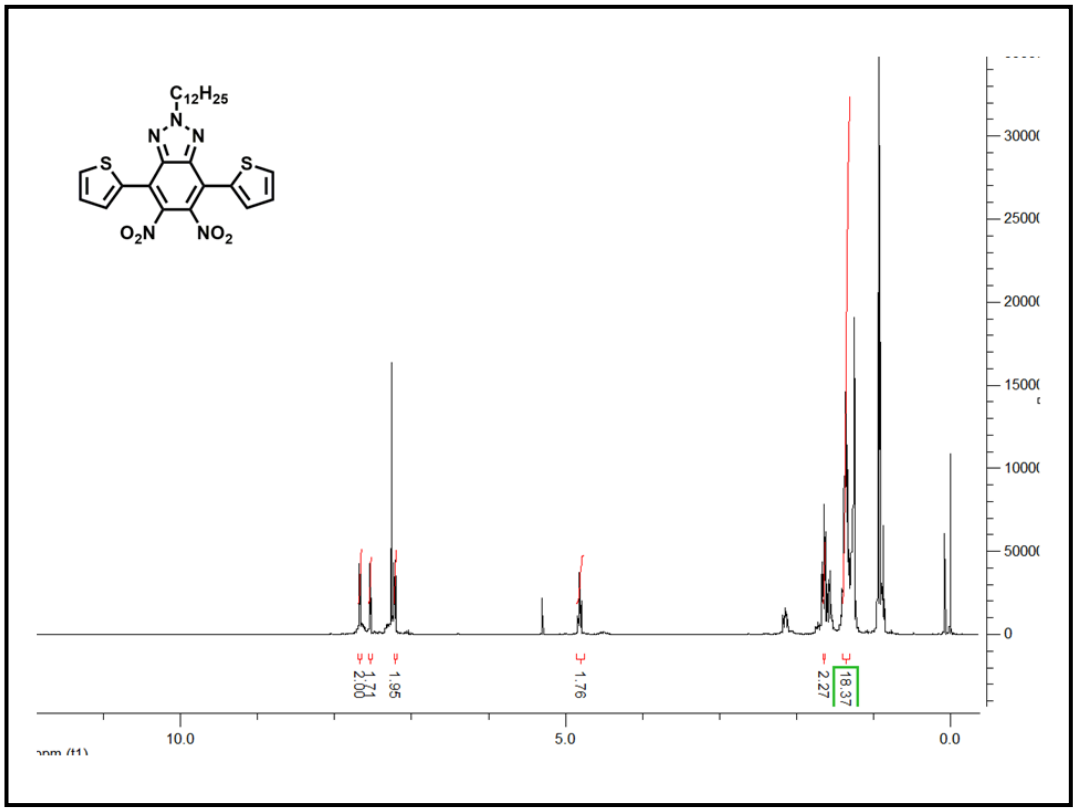

Figure A. 13. ^{1}H-NMR spectrum of 2-dodecyl-5,6-dinitro-4,7-di(thiophen-2-yl)-2Hbenzo[d][1,2,3]triazole.

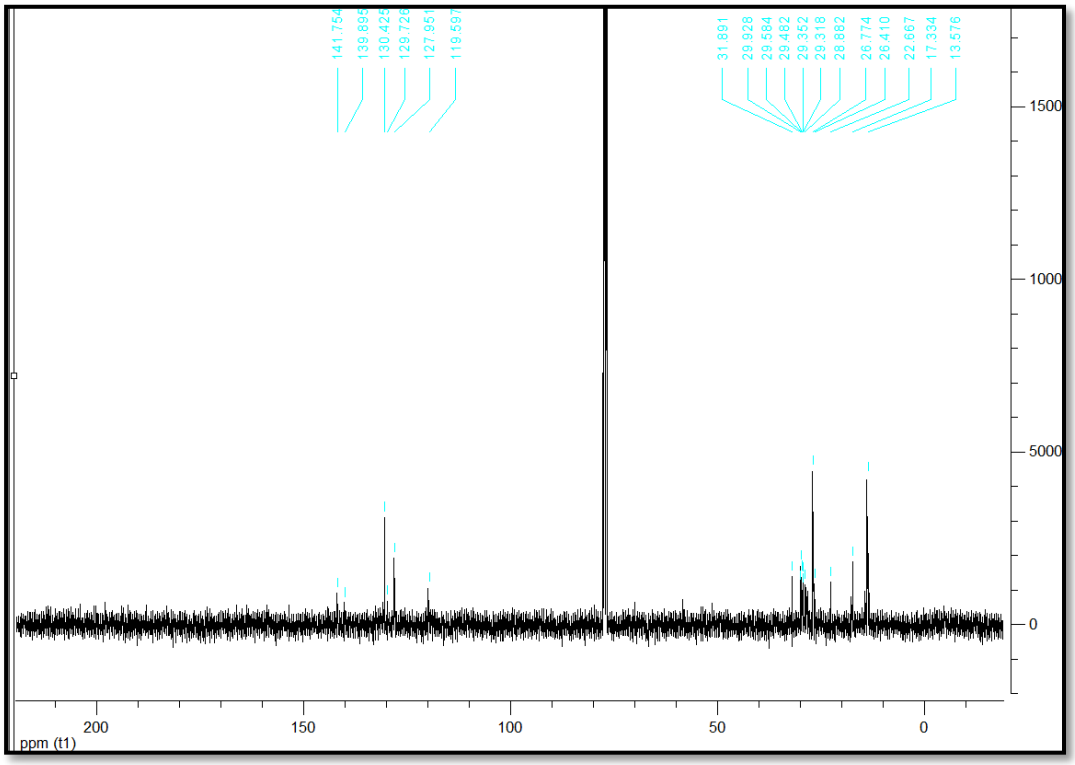

Figure A. 14. ^{13}C-NMR spectrum of 2-dodecyl-5,6-dinitro-4,7-di(thiophen-2-yl)-2Hbenzo[d][1,2,3]triazole.

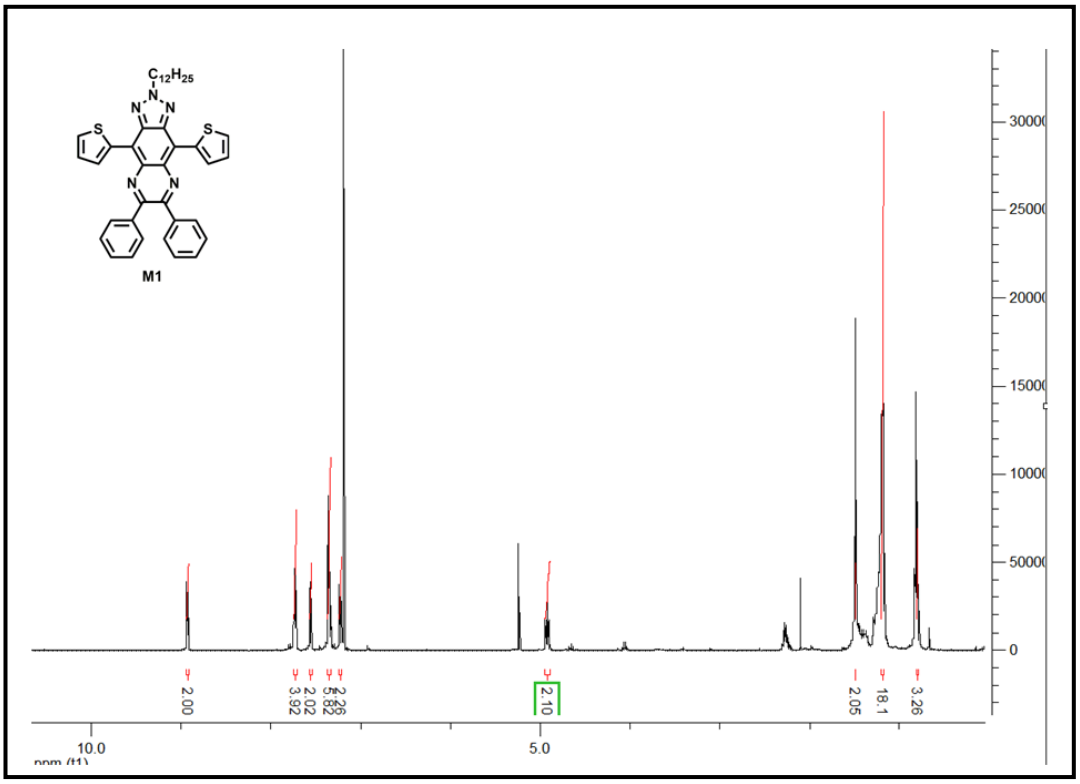

Figure A. 15. ^{1}H-NMR spectrum of 2-dodecyl-6,7-diphenyl-4,9-di(thiophen-2-yl)-2H- [1,2,3]triazolo[4,5-g]quinoxaline (M1).

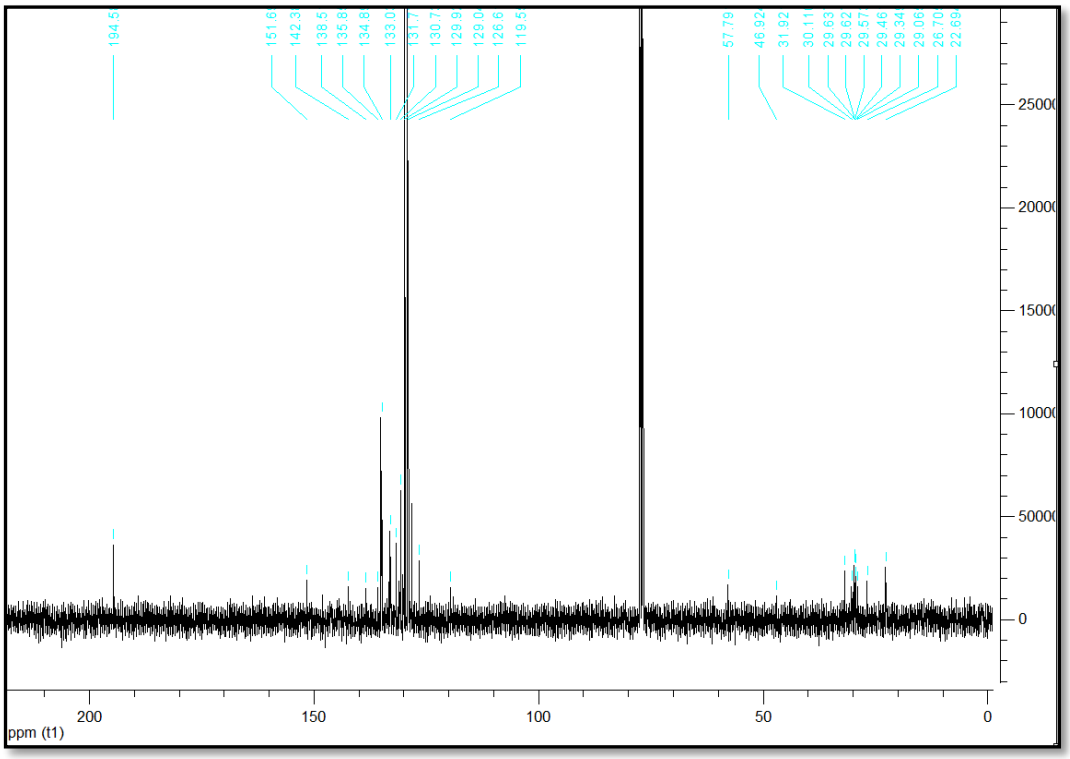

Figure A. 16. ^{13}C-NMR spectrum of 2-dodecyl-6,7-diphenyl-4,9-di(thiophen-2-yl)-2H-[1,2,3]triazolo[4,5-g]quinoxaline (M1).

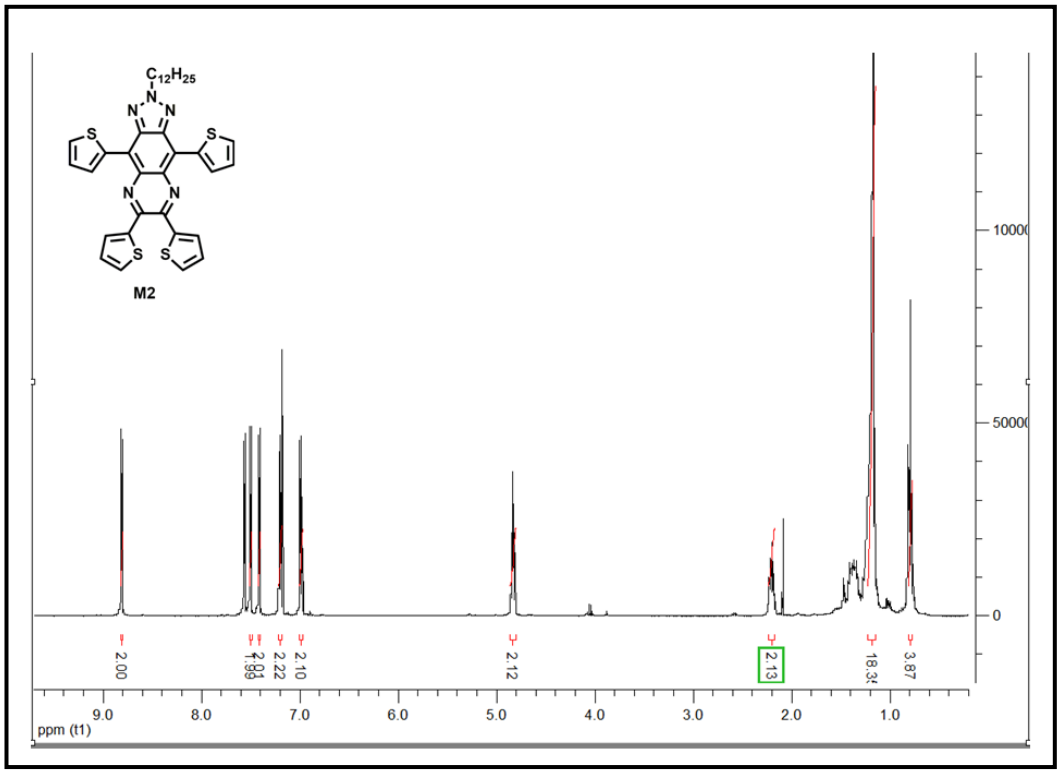

Figure A. 17. ^{1}H-NMR spectrum of 2-dodecyl-4,6,7,9-tetra(thiophen-2-yl)-2H-[1,2,3] triazolo[4,5-g]quinoxaline (M2).

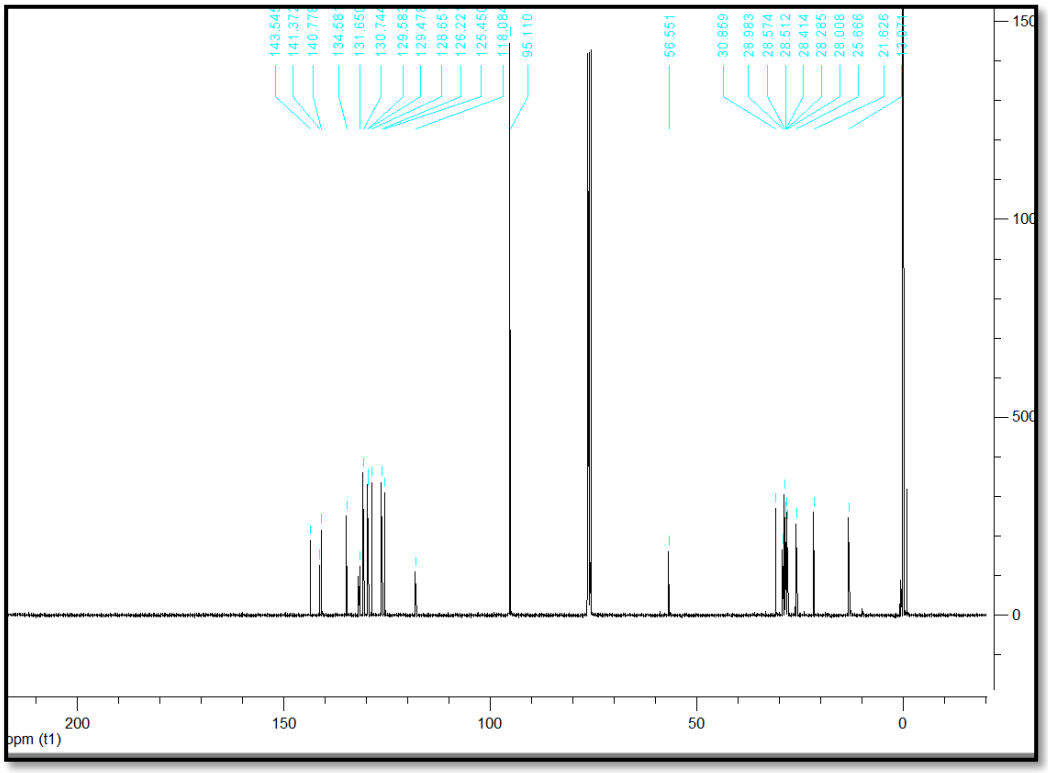

Figure A. 18. ^{13}C-NMR spectrum of 2-dodecyl-4,6,7,9-tetra(thiophen-2-yl)-2H-[1,2,3]triazolo[4,5-g]quinoxaline (M2).

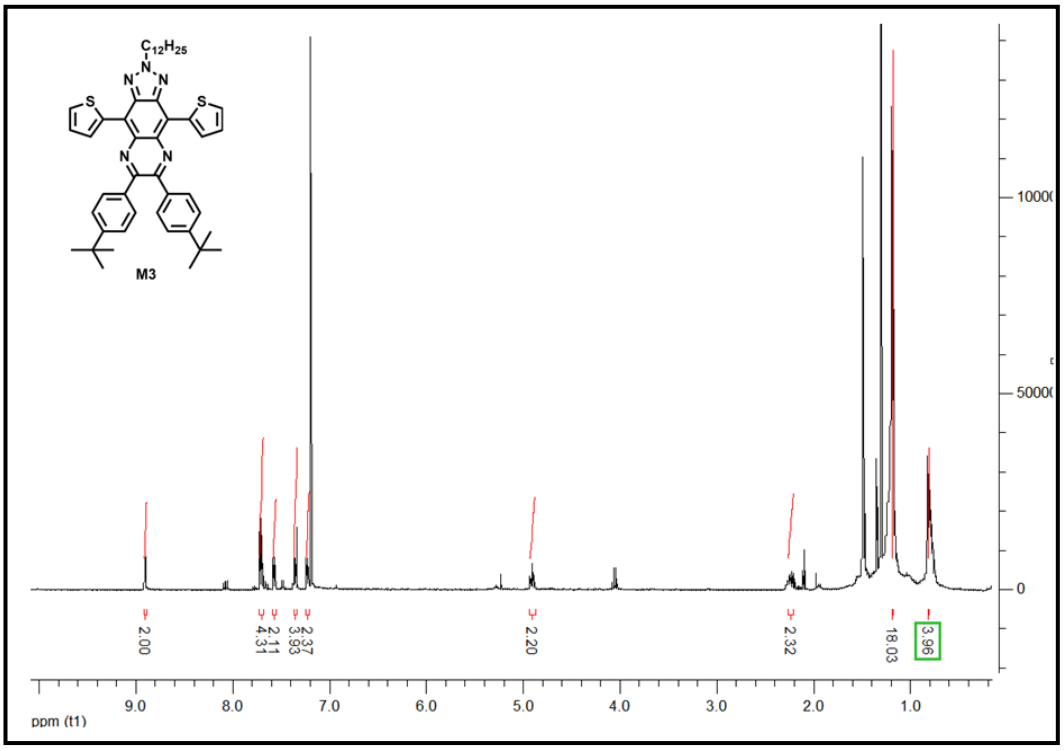

Figure A. 19. ^{1}H-NMR spectrum of 6,7-bis(4-tert-butylphenyl)-2-dodecyl-4,9-di(thiophen-2-yl)-2H-[1,2,3]triazolo[4,5-g]quinoxaline (M3).

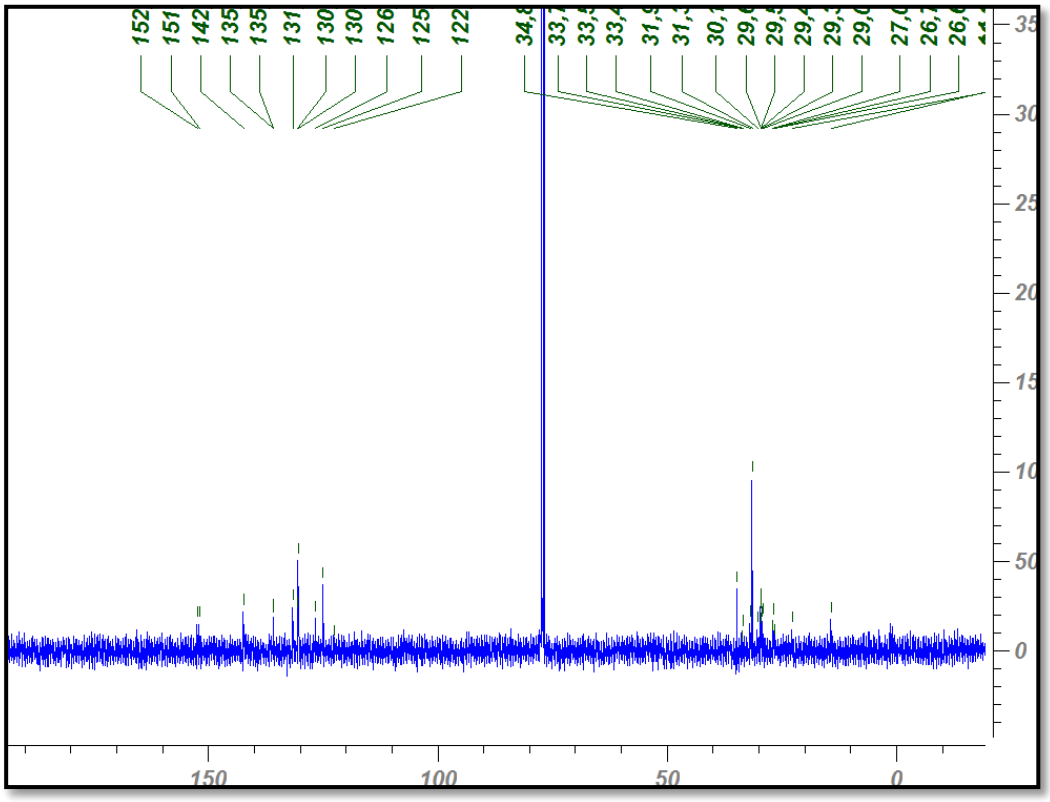

Figure A. 20. ^{13}C-NMR spectrum of 6,7-bis(4-tert-butylphenyl)-2-dodecyl-4,9-di(thiophen-2-yl)-2H-[1,2,3]triazolo[4,5-g]quinoxaline (M3).

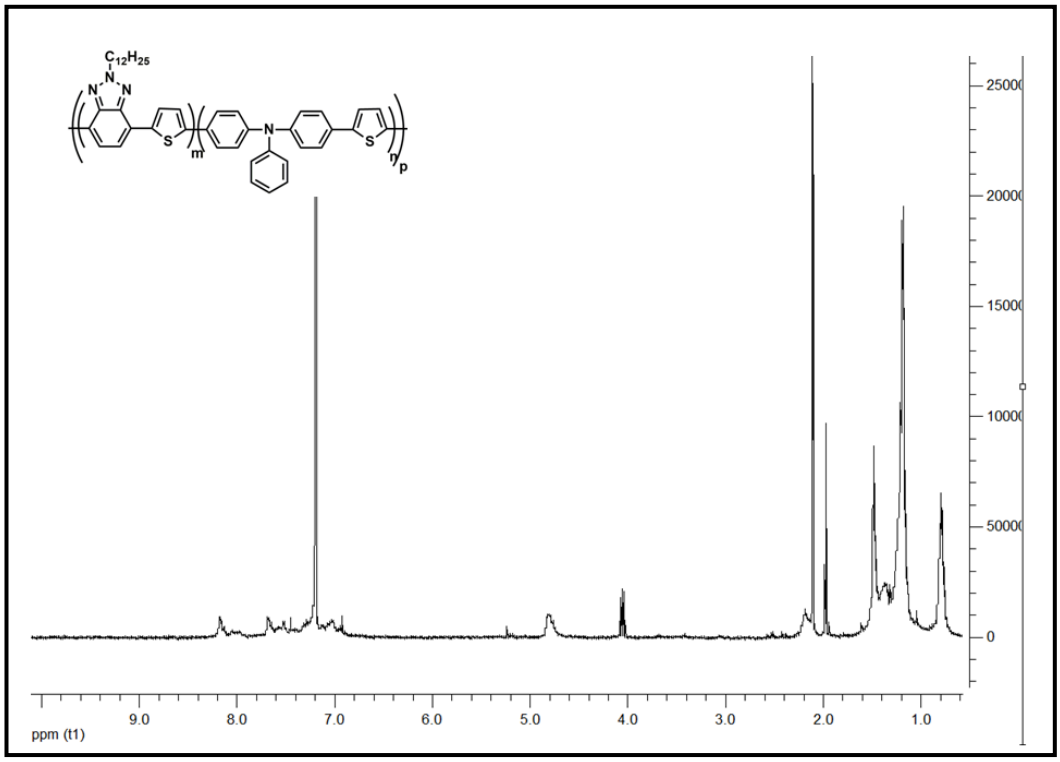

Figure A. 21. ^{1}H-NMR spectrum of poly4-(5-(2-dodecyl-7-methyl-2H-benzo[d][1,2,3]triazol-4-yl)thiophen-2-yl)-N-(4-(5-methylthiophen-2-yl)phenyl)-N-phenylaniline (PTPB1).

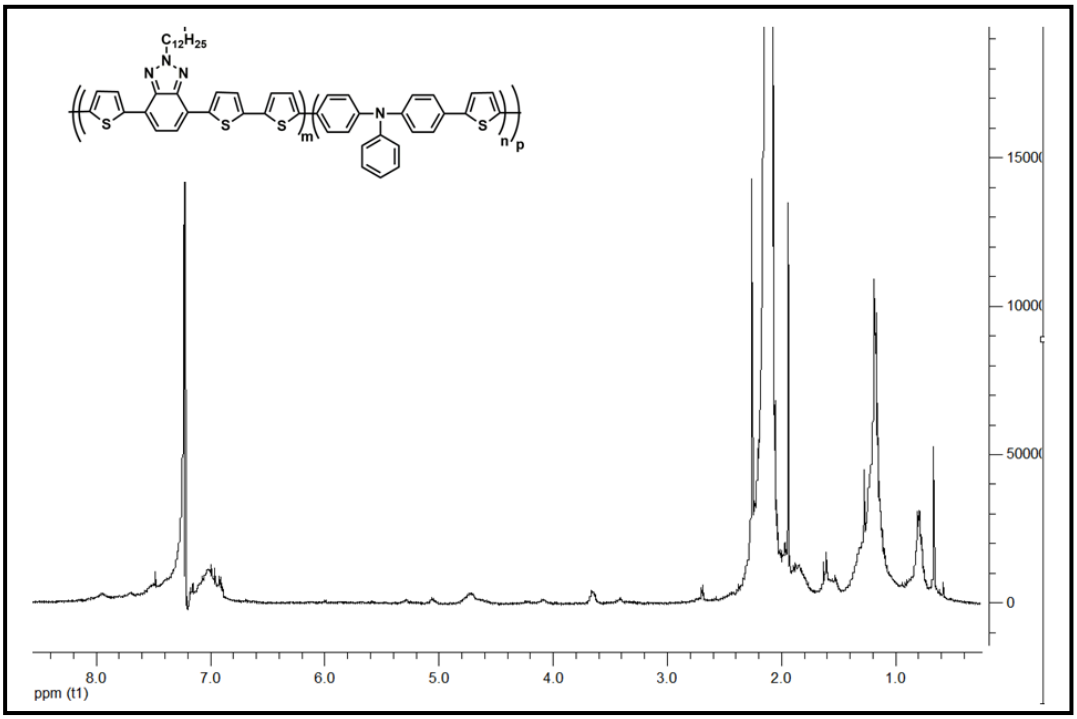

Figure A. 22. ^{1}H-NMR spectrum of poly4-(5'-(2-dodecyl-7-(5-methylthiophen-2-yl)-2H-benzo[d][1,2,3]triazol-4-yl)-[2,2'-bithiophen]-5-yl)-N-(4-(5-methylthiophen-2-yl)phenyl)-N-phenylaniline (PTPB3).

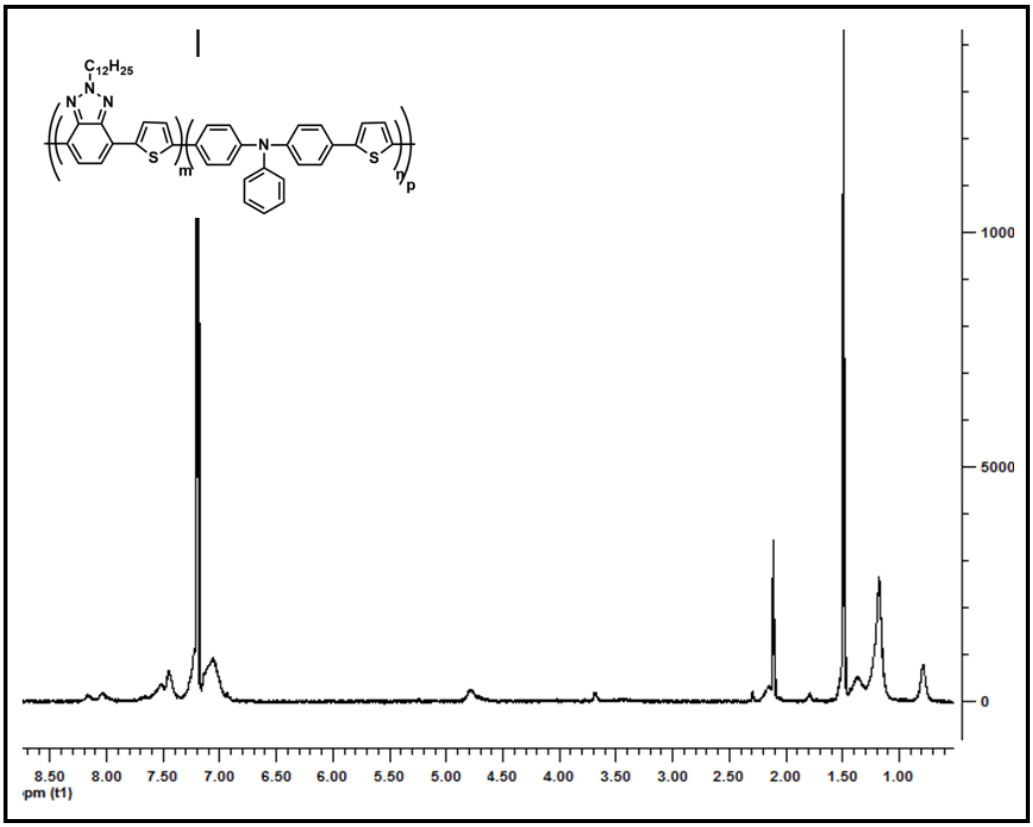

Figure A. 23. ^{1}H-NMR spectrum of resynthesized poly4-(5-(2-dodecyl-7-methyl-2H-benzo[d][1,2,3]triazol-4-yl)thiophen-2-yl)-N-(4-(5-methylthiophen-2-yl)phenyl)-N-phenylaniline (PBTP1).

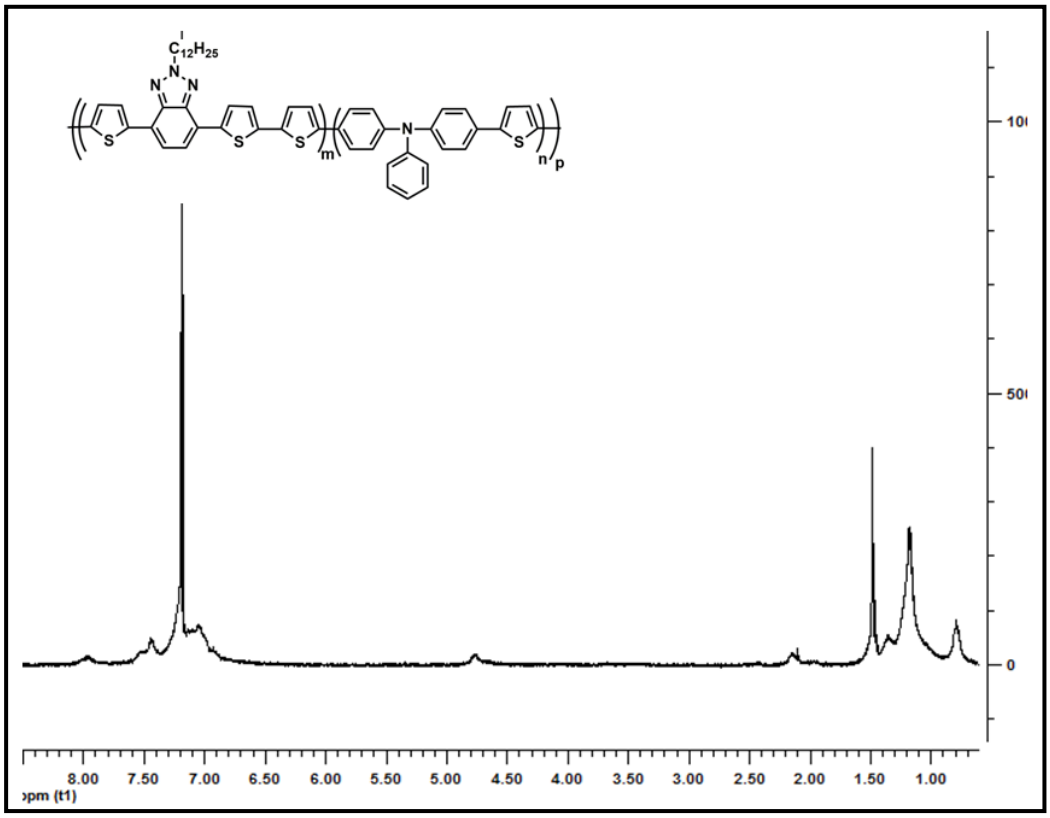

Figure A. 24. ^{1}H-NMR spectrum of resynthesized poly4-(5'-(2-dodecyl-7-(5-methylthiophen-2-yl)-2H-benzo[d][1,2,3]triazol-4-yl)-[2,2'-bithiophen]-5-yl)-N-(4-(5-methylthiophen-2-yl)phenyl)-N-phenylaniline (PBTP2).

CURRICULUM VITAE

PERSONAL INFORMATION

Surname, Name:	Özdemir Hacıoğlu, Şerife
Nationality:	Turkish
Phone:	+90 505 6575141
Date and Place of Birth:	19 Dec 1985
email:	serifeirem@gmail.com

EDUCATION AND TRAINING:

September 2010-present:	PhD Degree (expected date : September 2016) Middle East Technical University, Department of Chemistry 06800 Ankara Thesis Title: Syntheses Of New Multifunctional Donor Acceptor Type Polymers For Electrochromic and Organic Solar Cell Applications Supervisor: Prof. Dr. Levent TOPPARE Co-Supervisor: Prof. Dr. Özdemir DOĞAN CGPA: 3.93 / 4.00

Sep. 2008 – Sept. 2010 MSc Degree

Middle East Technical University, Department of Chemistry, 06800 Ankara

Thesis Title: Synthesis of a New Ferrocenyl Substituted Quinoxaline Derivative Monomers, Their Polymerization and Electrochemical Behavior

Supervisor: Prof. Dr. Özdemir DOĞAN

Co-Supervisor: Prof. Dr. Levent Toppare

CGPA: 3.71 / 4.00

Sept. 2003 – June. 2008 BSc Degree

Middle East Technical University, Department of Chemistry, 06800 Ankara

CGPA: 3.35/ 4.00

WORK EXPERIENCE:

2008-present: **Teaching Assistant**

Department of Chemistry, Middle East Technical University, 06800 Ankara/TURKEY

- Taught General Chemistry Laboratory for 7 semester
- Taught Physical Chemistry Laboratory for 5 semesters

2008–present: **Research Assistant**

Department of Chemistry, Middle East Technical University,

06800 Ankara/TURKEY

(Supervisor: Prof. Dr. Levent Toppare)

- Design, synthesis and electrochemical behaviors of π conjugated molecules for applications in a variety; biosensors, light harvesting systems, electrochromic devices and optoelectronic devices

2012-present **Laboratory Team Leader** – Electrochemical Analysis Laboratory in Toppare Research Group

Department of Chemistry, Middle East Technical University, 06800 Ankara/TURKEY

July 2007-August 2007 **Internship**

Şişecam Cam Elyaf Sanayii A.Ş. Gebze/Kocaeli

January 2007 **Internship**

Laboratory of Water, Refik Saydam Hıfzıssıhha Institute, Ankara.

2004-2006

Private Lesson

PUBLICATIONS:

1. A ferrocene functionalized multichromic p and n dopable donor–acceptor–donor type conjugated polymer, Serife Ozdemir, Abidin Balan, Derya Baran, Özdemir Dogan, Levent Toppare, Journal of Electroanalytical Chemistry (2010) 648, 184–189.

2. Green to highly transmissive switching multicolored electrochromes: Ferrocene pendant group effect on electrochromic properties, Serife Ozdemir, Abidin Balan, Derya Baran, Özdemir Dogan, Levent Toppare, React. & Function. Polym. (2011) 71, 168–174.

3. A promising combination of benzotriazole and quinoxaline units: A new acceptor moiety toward synthesis of multipurpose donor–acceptor type polymers, Serife Ozdemir, Merve Sendur, Gozde Oktem, Ozdemir Dogan, Levent Toppare, J. Mater. Chem., (2012) 22, 4687-4694.

4 Long wavelength photosensitizers in photoinitiated cationic polymerization: The effect of quinoxaline derivatives on photopolymerization, Bengisu Corakci, Serife O. Hacioglu, Levent Toppare , Umut Bulut, Polymer (2013) 54, 3182-3187.

5. The effect of para- and meta-substituted fluorine on optical behaviorof benzimidazole derivatives, Merve Ileri, Serife O. Hacioglu, Levent Toppare, Electrochim. Acta(2013) 109, 214– 220.

6. Structure–property relations in donor–acceptor–donor type benzimidazole containing conjugated polymers, Buket Zaifoglu, Serife O. Hacioglu, Naime A. Unlu, Ali Cirpan, Levent Toppare, J Mater Sci (2014) 49, 225–231

7. Development of a Novel Biosensor Based on a Conducting Polymer, Saniye Soylemez, Fulya Ekiz Kanik, Merve Ileri, Serife O. Hacioglu, Levent Toppare, Talanta, 118 (2014)84–89.

8. Synthesis and electrochromic properties of triphenylamine containing copolymers: Effect of π-bridge on electrochemical properties, Serife O. Hacioglu, Sinem Toksabay, Merve Sendur, Levent Toppare, J. Polym. Sci. Part A: Polym. Chem,. (2014) 52, 537–544

9. Development of an efficient ımmobilization matrix based on a conducting polymer and functionalized multiwall carbon nanotubes: synthesis and ıts application to ethanol biosensor, Saniye Soylemez, Fulya Ekiz Kanik, Sema Demirci Uzun, Serife O. Hacioglu, Levent Toppare, J. Mater. Chem. B, (2014)2, 511–521

10. Synthesis and electrochemical properties of perylene diimide (PDI) and benzotriazole (BTz) bearing conjugated polymers to investigate the effect of π-bridge on electrochemical properties, Sebnem Baysec, Naime Akbasoglu Unlu, Serife O. Hacioglu, Yasemin Arslan Udum, Ali Cirpan, Levent Toppare, J. Macromol. Sci. Part:A Pure Appl. Chem., (2014) Accepted)

11. Electrochemical manupilation of adhesion strength of polybenzoxazines on metal surfaces: from strong adhering to dismantling, Cansu Aydogan, Baris Kiskan, Serife O. Hacioglu, Levent Toppare, Yusuf Yagci, RSC Adv.(2014) 4, 27545-27551

12. Selenophene As A Bridge In Molecular Architecture Of Benzotriazole Containing Conjugated Copolymers To Gain Insight On Optical And Electrochemical Properties Of Polymers, Hande Unay, Naime Akbasoglu Unlu, Gonul Hizalan, Serife O. Hacioglu, Levent Toppare, Ali Cırpan, Phosphorus, Sulfur, and Silicon, (2015) 190:1294–1306,

13. A Novel Low Band Gap Benzimidazole Derivative and Its Copolymer with 3,4 ethylenedioxy thiophene for Electrochemical Studies, Saniye Soylemez, Serife O. Hacioglu , Sema Demirci Uzun, Levent Toppare, J. Electrochem. Soc. (2015)162 (1) H6-H14

14. Thieno[3,2-b]thiophene as π-bridge at Different Acceptor Systems for Electrochromic Applications, Sinem Toksabay, Serife O. Hacioglu, Naime A. Unlu, Ali Cirpan, Levent Toppare, Polymer (2014) 55, 3093-3099

15. A novel and effective surface design; conducting polymer/β-cyclodextrin host-guest system for cholesterol biosensor, Saniye Soylemez, Serife O. Hacioglu, Melis Kesik, Hande Unay, Ali Cirpan, Levent Toppare, ACS Applied Materials& Interfaces, 6 (2014) 18290−18300

16. Benzotriazole and benzodithiophene containing medium band-gap polymer for bulk heterojunction polymer solar cells applications, Hande Unay, Naime A. Unlu, Gonul Hizalan, Serife O. Hacioglu, Dilber Esra Yildiz, Levent Toppare, Ali Cirpan, J. Polym. Sci. Part A: Polym. Chem (2015) 53, 528–535

17. A novel Near-IR effective pyrene based donor acceptor electrochrome, Emre Sefer, Serife O. Hacioglu, Murat Tonga , Levent Toppare Ali Cirpan, Sermet Koyuncu, Macromol. Chem. Phys. (2015) 216, 829−836

18. Novel poly(2,5-dithienylpyrrole) (psns) derivatives functionalized with azobenzene, coumarine and fluorescein chromophore units: spectroelectrochemical properties and electrochromic device applications, Deniz Yigit, Serife O. Hacioglu, Levent Toppare, Mustafa Güllü, New J. Chem. (2015) 39, 3371-3379

19. Silafluorene-Based Polymers for Electrochromic and Polymer Solar Cell Applications, Ozan Erlik, Naime A. Unlu, Gonul Hizalan, Serife O. Hacioglu, Seda Comez, Esra D. Yildiz, Levent Toppare, Ali Cirpan, J. Polym. Sci. Part A: Polym. Chem. (2015) 53, 1541–1547

20. Syntheses and optical properties of perfluorophenyl containing benzimidazole derivatives: the effect of donor units, Merve Ilerı, Serıfe O. Hacıoglu, Alı Cırpan, Levent Toppare, Journal of Macromolecular Science, Part A: Pure and Applied Chemistry (2015) 52, 510–516

21. The effect of the different donor units on fluorescent conjugated polymers containing 2,1,3-benzooxadiazole as the acceptor unit, Seza Göker, Gonul Hizalan, Merve Ileri, Serife O. Hacioglu , Levent Toppare, Journal of Electroanal. Chem. (2015) 751, 80–89

22. Synthesis of a benzotriazole bearing alternating copolymer for organic photovoltaic applications, Cagla Istanbulluoglu, Seza Goker, Gonul Hizalan, Serife O. Hacioglu,Yasemin Arslan Udum, Esra D. Yildiz, Ali Cirpan, Levent Toppare, New J. Chem., 2015, 39, 6623—6630

23. Synthesis and spectroelectrochemical characterization of multicolored novel poly(3,6-dithienylcarbazole) derivatives containing azobenzene and coumarine chromophore units, Deniz Yiğit, Serife O. Hacioglu, Mustafa Güllü, Levent Toppare, Electrochim. Acta (2016) 196 , 140-152

24. Syntheses, electrochemical and spectroelectrochemical characterization of

benzothiadiazole and benzoselenadiazole based random copolymers,Seda Kutkan,Seza Goker, Serife O. Hacioglu,Levent Toppare, Journal of Macromolecular Science, Part A: Pure and Applied Chemistry (2016) 53, 475–483.

25.Syntheses and Electrochemical Characterization of Low Oxidation Potential Nitrogen Analogs of Pedot as Electrochromic Materials, Serife O. Hacioglu, Deniz Yigit, Emel Ermis, Saniye Soylemez, Mustafa G ullu, Levent Toppare,J. Electrochem. Soc. (2016) 163, E293-E299 .

26. A New, Solution Processable Blue to Transmissive Polymer with Superior Properties and its Use in High Performance Electrochromic Supercapacitors, Recep Yuksel, Emre Ataoglu, Janset Turan, Ece Alpugan, Serife Ozdemir Hacioglu, Levent Toppare, Ali Cirpan, Husnu Emrah Unalan, Gorkem Gunbas, J. Mater. Chem. C (2016) Submitted

INTERNATIONAL AND NATIONAL MEETINGS:

1.P-fam katalizörlüğünde azometin ilürlerin asimetrik 1,3-dipolar halkasal katilma tepkimeleri, Şerife Özdemir, Özdemir Doğan, XXIII. National Chemistry Congress 2009 (Poster Presentation)

1. Ferrosenil sübstite kinoksalin türevi monomerin sentezi, polimerizasyonu ve elektrokimyasal davranişlarinin incelenmesi,Şerife Özdemir, Abidin Balan, Derya Baran, Özdemir Doğan, Levent Toppare, XXIV. National Chemistry Congress 2010 (Poster Presentation)

2. A novel conducting polymer for biosensor applications,S. Soylemez, , F. Ekiz Kanik, M Ileri, S. Ozdemir Hacioglu, L. Toppare, Nanotech Conference & Expo 2013: An Interdisciplinary Integrative Forum on Nanotechnology, Microtechnology, Biotechnology and Cleantechnology, Washington, DC, United States, May 12-16, 2013 (2013), 1, 585-588 (Poster Presentation)

3. A promising combination of benzotriazole and quinoxaline units: a new acceptor moiety toward synthesis of multipurpose donor-acceptor type

polymers, Serife O. Hacioglu, 44th World Chemistry Congress İstanbul 2013 (Oral presentation)

4. Benzoselenadiazole and thienothiophene based monomer; electrochemical and spectroelectrochemical properties, Sinem Toksabay, Serife O. Hacioglu, Naime A. Unlu, Levent Toppare, 44th World Chemistry Congress (2013) (Poster Presentation)

6.Synthesis, electrochemical characterization, and applications of benzooxadiazole bearing low band gap conjugated polymer, Seza Goker, Gonul Hizalan, Serife O. Hacioglu, Levent Toppare, 247th ACS National Meeting & Exposition, Dallas, TX, United States, March 16-20 (2014) POLY-336 (Poster Presentation)

7. Benzoselenadiazole, dihydroquinoxaline and thienothiophene based monomer: Electrochemical and spectroelectrochemical properties, Sinem Toksabay, Naime A. Unlu, Serife O. Hacioglu, Levent Toppare,247th ACS National Meeting & Exposition, Dallas, TX, United States, March 16-20 (2014) POLY-330 (Poster Presentation)

8. Flor İçeren Benzimidazol Türevlerinin Sentezi ve Elektrokimyasal Davranışları, Merve Ileri, Serife O. Hacioglu, Levent Toppare, IV. Fiziksel Kimya Kongresi 5-8 Haziran Denizli (2014) (Poster Presentation)

9. Tiyeno[3,2-b]tiyofenin π- köprüsü olarak kullanildiği Donör-Akseptör (D-A) Tipi Konjüge Polimerlerin Elektrokromik ve Optoelektronik Uygulamalari, Naime A. Unlu, Serife O Hacioglu, Gonul Hizalan, Levent Toppare, Ali Cirpan, IV. Fiziksel Kimya Kongresi 5-8 Haziran Denizli (2014) (Poster Presentation)

10. Benzen ve Selenofen içeren Konjüge Alternatif Kopolimerin Sentezi, Elektrokimyasal ve Optik Çalışmaları, Hande Unay, Naime Unlu, Serife O. Hacioglu, Levent Toppare, Ali Cirpan, IV. Fiziksel Kimya Kongresi 5-8 Haziran Denizli (2014) (Poster Presentation)

11. Selenofen temelli benzookzadiazol içeren donör-akseptör tipi polimer sentezi ve optoelektronik özelliklerinin incelenmesi, Seza Göker , Gönül Hızalan, Serife

O. Hacioglu, Levent Toppare, IV. Fiziksel Kimya Kongresi 5-8 Haziran Denizli (2014) (Poster Presentation)

12.Işık saçan organik diyotlar için benzotriazol içeren konjuge polimerler, Cansel Temiz, Naime Akbasoglu Unlu, Sevki Can Cevher, Serife O. Hacioglu, Levent Toppare, Ali Cirpan, V. Polimer Bilim ve Teknoloji Kongresi 1-4 Eylül Tokat (2014)(Poster Presentation)

13.Organik güneş pilleri için bitişik thiazolo-thiazole halkasi içeren konjuge polimer, Ozge Azeri, Sevki Can Cevher, Serife O. Hacioglu, Ali Cirpan,V. Polimer Bilim ve Teknoloji Kongresi 1-4 Eylül Tokat (2014) (Poster Presentation)

14. Syntheses and optical properties of perfluorophenyl containing benzimidazole derivatives: the effect of donor units, Merve Ileri, Serıfe Özdemır Hacıoglu, Alı Çırpan, Levent Toppare,European Polymer Federation Congress Germany (2015)(Poster Presentation)

15. The effect of the different donor units on fluorescent conjugated polymers containing 2, 1, 3-benzooxadiazole as the acceptor unit, Seza Göker, Gönül Hızalan Özsoy, Merve İleri, Serıfe Özdemır Hacıoglu,Toppare Levent Toppare, European Polymer Federation Congress Germany(2015)(Poster Presentation)

16. Benzotriazole based alternating copolymer synthesis for organic photovoltaic applications, Çagla Istanbulluoglu, Seza Göker, Gönül Hızalan Özsoy, Serife Özdemir Hacıoglu, Yasemın Udum, Levent Toppare , SOLARTR-3 Ankara (2015)(Poster Presentation)

17. Silafluorene and thiophene bearing polymer for polymer solar cell applications,Gönül Hizalan Özsoy, Ozan Erlik, Naime Akbasoglu Ünlü, Serife Özdemir Hacioglu, Seda Çömez, Esra Yildiz Dilber, Levent Toppare , AliÇirpan,SOLARTR-3 Ankara (2015)(Poster Presentation)

18. Dibenzo[a,c]fenazin ve benzoditiyofen içeren d-a sistemine dayalı konjuge polimerin sentezi ve organik günes gözesi uygulamaları, Ece Aktas, Naime Akbasoglu Ünlü, Gönül Hizalan Özsoy, Serife Özdemir Hacioglu, Ali Çirpan, Levent Toppare, 5. Fiziksel Kimya Kongresi Ankara (2015) (Poster Presentation)

19. Organik günes pili uygulamaları için benzotriazol ve kuinokzalin yapıları içeren konjüge polimer. Cansel Temiz, Naime Akbasoglu Ünlü, Sevki Can Cevher, Serife

Özdemir Hacioglu, Levent Toppare, Ali Çirpan, 5. Fiziksel Kimya Kongresi Ankara (2015) (Poster Presentation)

20. Triazoloquinoxaline bearing copolymer for electrochromic and organic photovoltaic applications, Serife O. Hacioglu, Ece Aktas, Gonul Hizalan, Naime A. Unlu ,Ali Cirpana, Levent Toppare, EUPVSEC Munich Germany (2016) (Poster presentation)

21. The effect of the triphenylamine unit on electrochemical behaviors of benzotriazole bearing conjugated polymers, Serife O. Hacioglu, Sinem Toksabay, Merve Sendur, Levent Toppare, Macro 2016 World Polymer Congress Istanbul Turkey (2016) (Oral Presentation)

Academic Achievements

• 2005-2006 Spring Semester Honor Roll

• 2006-2007 Spring Semester Honor Roll

• 2006-2007 Fall Semester Honor Roll

• 2007-2008 Spring Semester High Honor Roll

• 2007-2008 Fall Semester High Honor Roll

Scholarship Program for PhD students, The Scientific and Technological Research Council of Turkey (TÜBİTAK 2211)

SCHOLARSHIP:

Scholarship Program for PhD students, The Scientific and Technological Research Council of Turkey (TÜBİTAK 2211)

PERSONAL SKILLS AND COMPETENCES

Language: Advanced English

Beginner German

COMPUTER SKILLS AND COMPETENCES

- MS Office Applications (Excel, Word, Powerpoint, etc.)
- Internet Tools
- ChemBioOffice 2010
- Origin program

TECHNICAL SKILLS

- Potentiostat/Galvanostat
- UV-Vis-NIR Spectrophotometer
- NMR
- Manipulating data obtained from the experiments and writing scientific papers

REFERENCES

1. Prof. Dr. Levent Toppare
   Middle East Technical University, Department of Chemistry
   Email: toppare@metu.edu.tr
   Tel: 0312 210 3251

2. Prof. Dr. Özdemir Doğan
   Middle East Technical University, Department of Chemistry
   Email: dogano@metu.edu.tr
   Tel: 0312 210 5134

3. Assoc. Prof. Dr. Ali Çırpan
   Middle East Technical University, Department of Chemistry
   Email: acirpan@metu.edu.tr
   Tel: 0312 210 51 03